Identification of the molecular basis of the lacrimo-auriculo-dento-digital syndrome (LADD)

Inaugural Dissertation

zur
Erlangung des Doktorgrades
Dr. nat. med.
der Medizinischen Fakultät
und
der Mathematisch-Naturwissenschaftlichen Fakultät
der Universität zu Köln

vorgelegt von

Dipl.-Biol. Edyta Rohmann
aus Arys (Polen)

Köln, 2007

Berichterstatter/Berichterstatterin: Prof. Dr. Rita Schmutzler……………………….
Prof. Dr. Thomas Wiehe……………………..

Tag der letzten mündlichen Prüfung: 27.02.2008…………………………………....

Contents

1. List of Papers…………………………………………………………………… 1

1.1 Main publications…………………………………………………………………… 1

1.2 Additional publications……………………………………………………………… 1

2. Abstract/Zusammenfassung…………………………………………………… 2

3. Introduction…………………………………………………………………….. 5

3.1 Fibroblast growth factors…………………………………………………………… 5

3.2 Fibroblast growth factor receptors………………………………………………… 6

3.3 FGF/FGFR signal transduction……………………………………………………. 8

3.4 Biological roles of FGF and FGFR isoforms………………………………………9

3.5 Human malformation syndromes due to defective FGF signalling……………….. 10

3.5.1 Craniosynostosis and skeletal dysplasia syndromes…………………………..10

3.5.2 Levy-Hollister/lacrimo-auriculo-dento-digital (LADD) syndrome………………12

4. Aims and major findings of this PhD thesis…………………………………… 13

4.1 Aims……………………………………………………………………………….... 13

4.2 Major findings……………………………………………………………………..... 13

5. Present investigations……………………………………………………………14

5.1 Mutations in different components of FGF signaling in LADD syndrome
(Rohmann et al., Nat Genet. (2006): Apr. 38 (4): 414-7)……………………………14

5.2 LADD syndrome is caused by reduced activity of the FGF10-FGF receptor 2
signaling pathway (Shams et al., Mol Cell Biol. (2007); 27: 6903-6912)………… 15

5.3 Structural basis for reduced FGFR2 activity in LADD syndrome: Implications
for FGFR autoinhibition and activation (Lew et al., Proc Natl Acad Sci USA.
(2007) Dec. 104 (50): 19802-19807)…………………………………………………17

6. Progress and concluding remarks……………………………………………… 20

6.1 Awards/Talks……………………………………………………………………… 21

7. Additional publications and activities during the PhD thesis…………………..22

7.1 Kaplan et al., Br J Ophthalmol. (2007): Oct 25; [Epub ahead of print]……………22

7.2 Pabst et al., Clin Res Cardiol. (2007): Sep 25; [Epub ahead of print]……………23

7.3 Kalay et al., Human Mutat. (2006): 27(7), 633-639…………………………………24

7.4 Li et al., Thorax. (2006): 61, 273-274………………………………………………...26

8. References…………………………………………………………………………27

9. Publications

10. Appendix: Acknowledgements and Curriculum Vitae

1. List of publications

This PhD thesis is based on the following publications:

1.1 Main publications

Rohmann E, Brunner H, Kayserili K, Uyguner O, Nürnberg G, Lew E, Dobbie A, Eswarakumar V, Uzumcu A, Ulubil-Emeroglu M, Leroy J, Li Y, Becker C, Lehnerdt K, Cremers C, Yüksel-Apak M, Nürnberg P, Kubisch C, Schlessinger J, Bokhoven H, Wollnik B; Mutations in different components of FGF signaling in LADD syndrome; Nat Genet. (2006): Apr. 38 (4): 414-7

Shams I, Rohmann E, Eswarakumar VP, Lew E, Yuzawa S, Wollnik B, Schlessinger J, Irit L; LADD syndrome is caused by reduced activity of the FGF10-FGF receptor 2 signaling pathway; Mol Cell Biol. (2007); 27: 6903-6912.

Lew E, Bae JH, Rohmann E, Wollnik B, and Schlessinger J; Structural basis for reduced FGFR2 activity in LADD syndrome: Implications for FGFR Autoinhibition and Activation; Proc Natl Acad Sci U S A. (2007): Dec. 104 (50): 19802-19807

1.2 Additional publications

Kaplan Y, Vargel I, Kansu T, Akin B, Rohmann E, Kamaci S, Uz E, Ozcelik T, Wollnik B, Akarsu NA: Skewed X-inactivation in an X-linked Nystagmus Family Resulted From a Novel, p.R229G, Missense Mutation in the FRMD7 Gene. Br J Ophthalmol. (2007): Oct 25; [Epub ahead of print]

Pabst S, Wollnik B, Rohmann E, Hintz Y, Grohé C: A novel stop mutation truncating critical regions of the cardiac transcription factor NKX2.5 in a large family with autosomal-dominant inherited congenital heart disease. Clin Res Cardiol. (2007): Sep 25; [Epub ahead of print]

Kalay E, Li Y, Uzumcu A, Uyguner O, Collin R, Caylan R, Ulubil-Emeroglu M, Kersten F, Hafiz G, van Wijk E, Kayserili H, Rohmann E, Wagenstaller J, Hoefsloot L, Strom T, Nürnberg G, Baserer N, Hollander A, Cremers F, Cremers C, Becker C, Brunner H, Nürnberg P, Karaguzel A, Basaran S, Kubisch C, Kremer H, Wollnik B ; Mutations in the lipoma HMGIC fusion partner-like 5 (LHFPL5) Gene Cause Autosomal Recessive Nonsyndromic Hearing Loss ; Human Mutat. (2006): 27(7), 633-639

Li Y, Wollnik B, Pabst S, Lennarz M, Rohmann E, Gillissen A, Vetter H, Grohe C ; BTNL2 gene variant and sarcoidosis ; Thorax. (2006): 61, 273-274

2. Abstract

Lacrimo-auriculo-dento-digital (LADD) syndrome, also known as Levy-Hollister syndrome, is a rare autosomal dominant developmental disorder, mainly characterized by abnormalities of the lacrimal system and salivary glands, ears and hearing, teeth and distal limb development. Besides these cardinal features, facial dysmorphism and malformations of the kidney and the respiratory system have been reported. In this study, the *LADD1* locus was mapped to chromosome 10q26 by genome wide linkage analysis using the Affymetrix GeneChip 10K array in three large LADD families. In all three LADD families and in one sporadic case, heterozygous missense mutations were found in exon 16 of the gene encoding the fibroblast-growth-factor-receptor 2 (*FGFR2*). After exclusion of the *FGFR2* locus by haplotype analysis in two additional LADD families, one missense mutation was identified in *FGFR3* and one mutation was found in the fibroblast-growth-factor 10 (FGF10), a known ligand of FGFR2 [Rohmann et al., 2006]. The functional properties of FGF10 LADD and FGFR2 LADD mutants were analyzed and compared to the activities of their normal counterparts. Protein expression in BL21 cells and binding studies showed that each of the three analyzed FGF10 mutations demonstrated severely impaired activity by different mechanisms. Transient and stable expression studies exhibited that the FGFR2 mutations possess a reduced autophosphorylation and a weaker tyrosine kinase activity. Mutations also lead to diminished phosphorylation activity in FGFR2-mediated substrates (e. g. FRS2 and Shc) and to a decreased downstream signaling pathway, as shown by MAPK activity. While tested FGF10 LADD mutations caused haploinsufficiency, the FGFR2 LADD mutants could exert a dominant-negative effect on normal FGFR2 protein [Shams and Rohmann et al., 2007]. An *in vitro* kinase assay and crystallization of both, FGFR2 WT and the p.A628T missense mutation in the catalytic part of the tyrosine kinase domain, demonstrated that the A628T LADD mutation disrupts the catalytic activity due to conformational changes, leading to LADD syndrome. In addition, the newly described crystal structure of FGFR2 in comparison to FGFR1 revealed that the FGFR2 utilizes a less stringent mode of autoinhibition [Lew, Bae and Rohmann et al., 2007].

2. Zusammenfassung

Das Lakrimo-aurikulo-dento-digitale (LADD) Syndrom, auch als Levy-Hollister Syndrom bekannt, ist eine seltene autosomal-dominante angeborene Erkrankung, die hauptsächlich durch Fehlbildungen und Störungen der Tränen- sowie der Speicheldrüsen, der Ohren und des Hörvermögens, der Zähne und der Entwicklung distaler Extremitäten gekennzeichnet ist. Außerdem sind Gesichtsdysmorphien, Fehlbildungen der Nieren und des respiratorischen Systems beschrieben. Der *LADD1*-Locus wurde durch eine genomweite Kopplungsanalyse mit dem *Affymetrix GeneChip 10K Array* in drei großen LADD-Familien auf Chromosom 10q26 kartiert. In allen drei LADD-Familien und in einem sporadischen Fall wurden heterozygote Mutationen in Exon 16 des Gens, welches den Fibroblasten Wachstumsfaktor-Rezeptor 2 (*FGFR2*) kodiert, identifiziert. Nachdem in zwei zusätzlichen Familien der *LADD1-Locus* durch Haplotypanalyse ausgeschlossen wurde, konnte eine kausale Mutation in *FGFR3* und eine weitere Mutation in *FGF10*, einem bekannten FGFR2-Liganden, identifiziert werden [Rohmann et al., 2006]. Die funktionellen Eigenschaften der FGF10-LADD- und der FGFR2-LADD-Mutanten wurden analysiert und mit den Aktivitäten des normalen Wildtyp(WT)-Repezptors verglichen. Durch Proteinexpression in BL21 Zellen und Bindungsstudien konnte gezeigt werden, dass die drei analysierten FGF10-Mutationen eine stark beeinträchtigende Aktivität aufweisen, die durch verschiedene Mechanismen verursacht wird. Transiente und stabile Expressionsstudien zeigten, dass die FGFR2-LADD-Mutanten eine reduzierte Autophosphorylierung und eine verringerte Tyrosinkinaseaktivität des Rezeptors besitzen. Des Weiteren konnte eine stark abgeschwächte Phosphorylierung von FGFR2-vermittelten Substraten, wie FRS2 und Shc, als auch eine herabgesetzte nachgeschaltete Signalweiterleitung (was durch die reduzierte MAPK-Aktivität gezeigt wurde) beobachtet werden. Während die getesteten FGF10-LADD-Mutationen Haploinsuffizienz bedingen, zeigen die FGFR2-LADD-Mutationen wahrscheinlich einen dominant-negativen Effekt auf das normale FGFR2-Protein [Shams und Rohmann et al., 2007]. Zur weiteren Charakterisierung wurde eine *in vitro* Kinaseuntersuchung und eine Kristallisation des FGFR2-WTs und der A628T-LADD-Mutation, die in dem katalytischen Teil der Tyrosinkinasedomäne von FGFR2 lokalisiert ist, durchgeführt. Die Ergebnisse zeigten, dass die p.A628T-LADD-Mutation die katalytische Aktivität auf Grund von Konformationsänderungen zerstört und hierdurch die Rezeptoraktivität herabsetzt. Außerdem hat die neu beschriebene

Kristallstruktur von FGFR2-WT im Vergleich zu FGFR1 hervorgebracht, dass FGFR2 einen weniger stringenten Mechanismus der Autoinhibition benutzt [Lew, Bae and Rohmann et al., 2007].

3. Introduction

3.1 Fibroblast growth factors

Fibroblast growth factors (FGFs) belong to a large family of highly conserved polypeptide growth factors that are found in organisms from nematodes to humans. FGFs mediate a variety of cellular responses during embryonic development and in the adult organism. During embryonic development, FGFs regulate the communication between mesenchym and epithelium and are essential for the development of tissues and organs. FGFs play a critical role in embryonic morphogenesis by regulating cell proliferation, differentiation and migration. In the adult organism, FGFs play a crucial role in the control of the nervous system, tissue repair, wound healing, tumor angiogenesis, cholesterol metabolism and serum phosphate regulation (Eswarakumar et al., 2005, Yamashita, 2005, Yu et al., 2000).

In humans, 22 *FGF* genes have been identified with known chromosomal location. They are found scattered throughout the genome and can be subdivided into seven families, each consisting of 2-4 members. The members of a subfamily share increased sequence similarity and biochemical and developmental properties. Most of the *FGF* genes consist of three coding exons. FGFs have a conserved ~120-amino acid residue core, with 30-60% amino acid identity (Itoh and Ornitz, 2004). Some of these highly conserved regions are responsible for the interaction with their receptors (fibroblast growth factor receptors (FGFRs); see 3.2).

Most FGFs (FGF 3-8, 10, 15, 17-19, and 21-23) have amino-terminal signal peptides and are readily secreted from cells. Subsets of FGFs lack an obvious amino-terminal peptide. FGF 9, 16 and 20 are secreted due to an N-terminal hydrophobic sequence (Miyamoto et al., 1993, Miyake et al., 1998, Ohmachi et al., 2000). FGF1 and FGF2 are not secreted, but can be released from damaged cells or independently through the endoplasmic-reticulum-golgi pathway (Miyakawa et al., 1999). FGF 11-14 are thought to remain intracellular and act in a receptor independent manner. Therefore, they are also called FHFs (fibroblast growth factor homologous factors), which have a high similarity in sequence and structure to the FGFs, but show different biochemical and functional properties (Schoorlemmer and Goldfarb, 2001, Goldfarb, 2005).

Initial structural studies on FGF1 and FGF2 identified 12 antiparallel β strands in the conserved core region of the protein. The regions between the β strands 1 and as well as between the β strands 10 and 12 form a coherent surface, which contains several basic amino-acid residues that mediate binding to negatively charged heparin or heparan sulfate proteoglycan (HSPG). These interactions stabilize FGFs towards thermal denaturation and proteolysis and may severely limit their diffusion and release into the interstitial space (Flaumenhaft et al., 1990). Due to the binding to heparan sulfates, FGFs are located on the cell surface and are therefore available for their targets. Furthermore, heparin or HSPG are required by FGFs, which act as ligands, to effectively activate specific FGFRs (Yayon et al., 1991). Thereby, heparin and HSPG cause specific conformation changes within the ligand that increase affinity to bind the receptor, thus lead to efficient activation and further signal transduction. The FGF-FGFR signaling system is highly conserved throughout the metazoan evolution (see 3.3).

3.2 Fibroblast growth factor receptors

The fibroblast growth factor receptors (FGFRs) belong to the family of the receptor tyrosine kinases (RTKs) and trigger the transduction of FGF mediated signals into the cells. RTKs are transmembrane glycoproteins and activate numerous signaling pathways within cells leading to cell proliferation, differentiation, migration, or metabolic changes (Schlessinger and Ullrich, 1992).

RTKs consist of an extracellular portion that binds polypeptide ligands, a transmembrane helix, and a cytoplasmic portion that possesses tyrosine kinase catalytic activity. Tyrosine kinases (TKs) catalyze the transmission of the terminal phosphate from ATP (adenosintriphosphate) to the hydroxyl group of a tyrosine side chain in a protein. The vast majority of RTKs exist as single polypeptide chain and are monomeric in the absence of a ligand. Dimerization upon ligand binding causes the transfer of the extracellular signal to the cytoplasm by phosphorylating tyrosine residues in the activation loop within the kinase domain on the receptors (autophosphorylation) and subsequently on downstream signaling proteins (Hubbard and Till, 2000). The autophosphorylation increases the catalytic activity within the kinase domain and leads to a positive feedback. Hence, the phosphorylated tyrosines mediate the possible binding of substrates to the cytoplasmic domain.

Four functional *FGFR* genes (*FGFR1-4*) have been identified in humans (Itoh and Ornitz, 2004). The FGFRs consist of a single polypeptide chain and have a molecular weight of 100-150 kDa. The extracellular domain of FGFRs comprises an N-terminal signal peptide and a region containing three immunoglobulin (Ig)-like domains (D1-D3). Each of the Ig-like domains is stabilized by disulfide bonds formed by cysteines. FGFRs possess a contiguous stretch of acidic residues in the linker region between D1 and D2 which is termed ´acid box`. D2 contains a conserved positively charged region to bind heparin (Schlessinger et. al., 2000). D2 and D3 are responsible for ligand binding, whereas D1 and the ´acid box` account for the autoinhibition. Moreover, the FGFRs comprise a single transmembrane helix and a cytoplasmic region. The cytoplasmic domain is subdivided into a juxtamembrane domain and a tyrosine kinase domain. The catalytic TK domain of a receptor consists of an ATP-binding site, a catalytic and an activation loop. Specific tyrosines of the activation loop produce cis- and trans-autophosphorylations to ensure further signal transduction (see 3.3).

An important hallmark of the FGFR1-3 is that a variety of FGFR isoforms are generated by alternative splicing (Eswarakumar et al., 2005). The N-terminal half of the third Ig-like domain (D3) is always encoded by the same exon and the C-terminal half of D3 is encoded by alternatively spliced exons. For example, it has been shown that exon 7 of the *FGFR2* gene encodes for the N-terminal half of D3 (designated ´a`), while exon 8 and 9 alternatively encode for the C-terminal half of D3 and are thus designated as ´b` and ´c` isoforms of FGFR, respectively. The generated isoforms show different ligand-binding specificities and affinities. While FGFR2b can bind FGF7 and FGF10, but not FGF2, the FGFR2c isoform binds FGF2 and FGF18, but not FGF7 and FGF10 (Eswarakumar et. al., 2005). Furthermore, these alternative splicing events occur in a tissue specific fashion, resulting in mesenchymal ´c` and epithelial ´b` isoforms (Mohammadi et al., 2005). Importantly, the tissue expression patterns of the FGFs are opposite to their receptors and result in the creation of a paracrine signaling loop between mesemchym and epithelium that is fundamental for human development.

3.3 FGF/FGFR signal transduction

The interaction of FGF, FGFR and heparan sulfate proteoglycan (HSPG) is responsible for the activation of intracellular signal transduction.

Two fundamentally different crystallographic models have been proposed to explain, at the molecular level, how HSPG/heparin enables FGF and FGFR to assemble into a functional dimer on the cell surface (Mohammadi et al., 2005). In the symmetric two-end model, heparin promotes dimerization of two FGF-FGFR complexes by stabilizing bivalent interactions of the ligand and receptor through primary and secondary sites and by stabilizing direct receptor-receptor contacts. In the asymmetric model, there are no protein-protein contacts between the two FGF-FGFR complexes, which are bridged solely by heparin (Ibrahimi et al., 2005). In general the symmetric model is more widely accepted.

Upon ligand binding, receptor dimers are formed and their intrinsic tyrosine kinase is activated leading to trans-phosphorylation of multiple tyrosine residues on the receptor. These residues then serve as docking sites for the recruitment of SH2 (src homology-2) or PTB (phosphotyrosine binding) domains of adaptors, docking proteins or signaling enzymes (Dailey et al., 2005). Signaling complexes are assembled and recruited to the activated receptors resulting in a cascade of phosphorylation events (Schlessinger, 2000). The best understood signal transduction pathways concomitantly activated by FGFs are the RAS-MAP kinase pathway, which includes ERK1/2, p38 and JNK kinases; the P-I-3 kinase-AKT pathway, and the PLCγ pathway (see Figure 1). The activation of the RAS-MAP kinase pathway has been observed in all cell types, while the activities of other signal transduction pathways vary depending on the cell type. Key components of the FGF signaling are the docking protein FRS2 (FGF-receptor substrate 2) and the signaling enzyme PLCγ (phospholipase Cγ). Most of these phosphorylation transduction pathways target transcription factors within the nucleus, thereby affecting gene expression, cell proliferation and differentiation (see Figure 1).

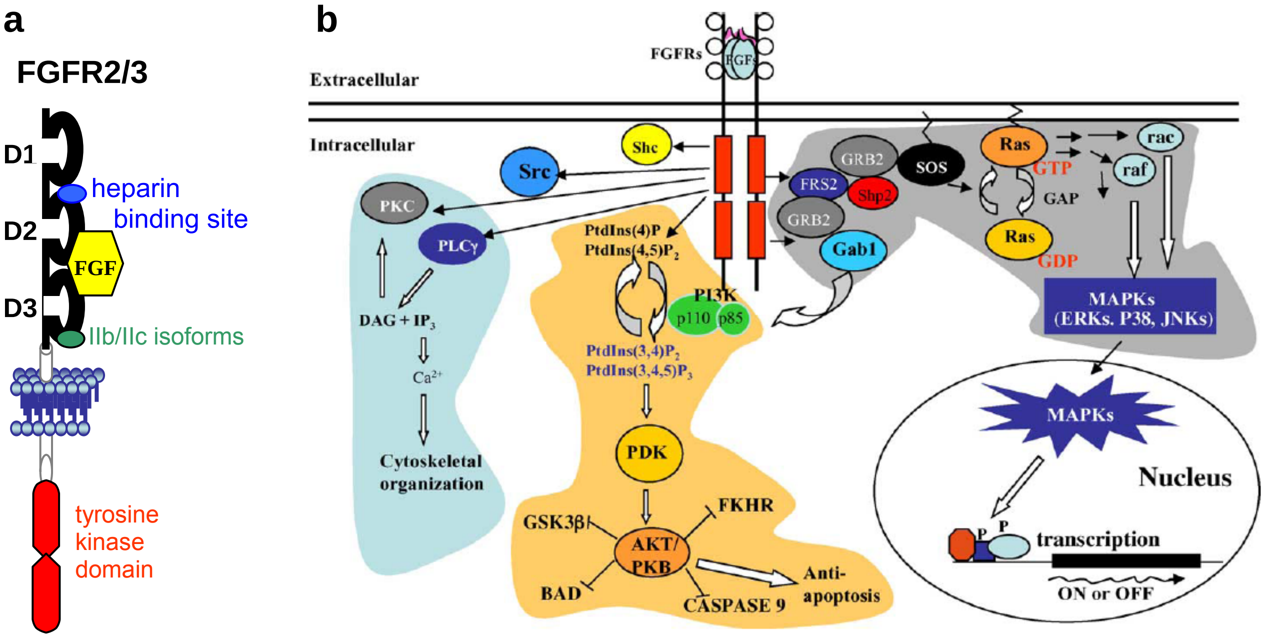
a
FGFR2/3
D1
heparin binding site
D2
FGF
D3
IIb/IIc isoforms
tyrosine kinase domain
b
FGFRs
FGF
Extracellular
Intracellular
Shc
Src
PKC
PLCγ
DAG + IP3
Ca2+
Cytoskeletal organization
PtdIns(4)P
PtdIns(4,5)P2
PI3K
p110
p85
PtdIns(3,4)P2
PtdIns(3,4,5)P3
PDK
GSK3β
FKHR
AKT/PKB
BAD
CASPASE 9
Anti-apoptosis
GRB2
FRS2
Shp2
GRB2
Gab1
SOS
Ras
GTP
GAP
Ras
GDP
rac
raf
MAPKs (ERKs, P38, JNKs)
MAPKs
Nucleus
P
P
transcription
ON or OFF

Figure 1: a) Scheme of the FGFR2/3 structure. b) FGF signaling transduction pathways. Activated FGFRs (red rectangles) stimulate PLCγ pathway (blue highlight), the P-I-3 kinase-AKT/PKB pathway (yellow highlight), and the FRS2-Ras-MAP kinase pathway (grey highlight). The activated MAP kinases (ERKs, p38, or JNKs) are translocated to the nucleus where they phosphorylate (P) transcription factors, thereby regulating target genes (Dailey et al., 2005).

3.4 Biological roles of FGF and FGFR isoforms

The biological roles of more than half of the 22 known mammalian FGFs and all known FGFRs have been investigated by targeting their genes by homologues recombination. These studies showed that certain members of the FGF family have very specialized biological roles resulting in a highly specific phenotype (i.e. Angora mutant of FGF5 -/- mice), while the loss of other FGFs can be compensated by related members of the FGF family resulting in no obvious phenotypes (no obvious defect in FGF1 -/- mice) (Eswarakumar et al., 2005). A mean part of the mutant FGF mice models were lethal at different developmental stages, for instance caused by inner cell mass proliferation (FGF4 -/- mice) or delayed ossification and increased chondrocyte proliferation (FGF18 -/- mice). A major part of the mutant FGF mice models were viable but showed alterations in, e. g. muscle regeneration (FGF6 -/- mice), neuronal, skeletal and skin phenotype (FGF2 -/- mice) or midline cerebral development (FGF17 -/- mice).

Targeted disruption of each FGFR and the corresponding isoforms (´b` and ´c`) generated different phenotypes. The FGFR1 -/- mice were lethal as a result of defects in cell migration through the primitive streak, which was also observed in FGFR1c -/- mice. However, the FGFR1b -/- mice showed no obvious phenotype. The FGFR2 -/- and FGFR2b -/- mice were both lethal. While the FGFR2 -/- mice died due of defects in the placenta at E10.5, the FGFR2b -/- mice died immediately after birth because of severe impairment in the development of the lung, limbs, and other tissues. In contrast, the FGFR2c -/- mice were viable and resulted in impairment of skull and bone development. Targeted disruption of the FGFR3 gene resulted in bone overgrowth and no obvious phenotype was observed in FGFR4 -/- mice (Eswarakumar et al., 2005).

The interaction of Fgf10 with Fgfr2b is essential for bud formation during development. Fgf10 is expressed in the mesoderm during organogenesis and diffuses to its receptor Fgfr2b, which is located in adjacent cells originated from the endoderm and ectoderm. Activation of the receptor initiates the bud formation (Orr-Urtreger et al., 1993). Numerous mice models showed that a disruption of Fgf10-Fgfr2b signaling causes severe malformations and dysfunction in many organs and was, therefore, embryonically lethal. *Fgfr2b*$^{-/-}$ zygotes died shortly after implantation due to defects of the trophoblast (Arman et al., 1998). Further experiments showed that Fgfr2b is fundamentally required for limb outgrowth and branching lung morphogenesis and that a disturbed function of Fgfr2b leads to agenesis of multiple organs. *FGF10*$^{-/-}$ mice showed a similar phenotype. The mice died during birth because of the absence of the lung and showed no initiation of the bud formation. Besides, several other mice models of *Fgf10* and *Fgfr2b* identified the lack of different other organs and also a formation of cleft palate. Additional affected organs are the pituitary gland, thyroid gland, salivary gland, lacrimal gland, inner ear, teeth, pancreas, kidney, thymus, skin and hair follicle.

3.5 Human malformation syndromes due to defective FGF signaling

3.5.1 Craniosynostosis and skeletal dysplasia syndromes

Mutations in FGFR1-3 were identified in a variety of craniosynostosis syndromes. Craniosynostosis, the premature fusion of one or more cranial sutures, occurs with a prevalence of 1 in 2500 births and is the hallmark of over 100 distinct syndromes, including Apert syndrome (AS) (Wilkie et al., 1995, Anderson et al., 1998), Pfeiffer syndrome (PS) (Jabs et al., 1994, Muenke et al., 1994, Rutland et al., 1995), Crouzon syndrome (CS) (Reardon et al., 1994, Steinberger et al., 1998) and Jackson-Weiss syndrome (Jabs et al., 1994, Sabatino et al., 2004). Hallmarks of craniosynostosis include abnormally shaped skull, often associated with increased

intracranial pressure, mental retardation, developmental delay, seizures, and blindness caused by constrictions of the growing brain (Eswarakumar et al., 2006).
AS is characterized by a markedly fore-shortened skull base and severe midfacial retrusion with hypertelorism. It is mostly associated with coronal sutural synostosis and a widely unossified median sagittal diastema in place of metopic and sagittal sutures. In contrast, the related CS, PS and Jackson-Weiss syndromes display more variable and overlapping craniofacial anomalies. AS is often accompanied by severe syndactyly of hands and feet, whereas traditionally, limb pathology in PS is moderate and not evident in CS. PS patients show broad fingers and feet. Jackson-Weiss syndrome is characterized by brachy- and acrocephaly.

The inheritance of the mentioned syndromes is autosomal dominant and caused mainly by *gain-of-function* mutations in *FGFR1-3*. The majority of the known mutations have been found in the extracellular domain of the receptor and resulted in constitutive receptor activation. In *FGFR2*, mutations occur mostly in the regions between D2 and D3, within D3 or between D3 and the transmembrane domain and can therefore manifest in both mesenchymal \`c´ and epithelial \`b´ splice isoforms of *FGFR2*. A ligand independent receptor dimerization and signal transduction occurs due to the mutations. If one of two highly conserved cysteines in D3 or adjacent amino acids are changed, the residual cysteine forms a disulfide bridge with a cysteine of the second receptor molecule. The same is true for mutations found in the transmembrane domain. Amino acid changes lead to the formation of hydrogen bonds between two receptor molecules and therefore cause activation of the receptor independent of ligand binding. Exceptions were found for AS mutations. Here, the mutations activate the receptor only in the presence of a ligand due to changed binding specificity of the receptor. Just a few mutations responsible for syndromic craniosynostosis were found in the tyrosine kinase domain of FGFR1-3, which also led to constitutive activation of the receptor. In addition, mutations in *FGFR3* cause different forms of dwarfism, like achondroplasia, hypochondroplasia and thanatophoric dysplasia type I and II. Mutations responsible for hypochondroplasia and thanatophoric dysplasia type II are located within the catalytic tyrosine kinase domain. These mutations are also *gain-of-function* mutations leading to ligand independent receptor activation (Eswarakumar et al., 2005). The mutations generate conformational changes in the TK domain of the monomeric receptor leading to autophosphorylation of tyrosines. Hence, receptor dimerization for activation or signal transduction is not necessary. Because activated FGFR3 is needed for inhibition of chondrocyte proliferation, dysfunction herein leads to dwarfism. In 2006, a novel tall stature syndrome (CATSHL, **ca**mptodactyly, **t**all **s**tature, **h**earing **l**oss) was described, caused by a putative *loss-of-function* mutation in *FGFR3* (Toydemir et al., 2006).

3.5.2 Levy-Hollister/lacrimo-auriculo-dento-digital (LADD) syndrome

The Levy-Hollister syndrome, also known as LADD syndrome, was first described in 1967 by W.J. Levy and in 1973 by D.W. Hollister (Levy, 1967; Hollister, 1973). LADD syndrome is a rare autosomal dominant disorder, which is characterized by distinctive malformations of several organ systems. LADD syndrome mainly affects the lacriamal glands and ducts, external and inner ears, salivary glands and ducts, teeth and digital development. The lacrimal system is affected by hypoplasia, atresia and aplasia of the nasolacrimal ducts and puncta leading to frequent conjunctivitis. Auricular symptoms include ear malformations such as cup-shaped, small and low-set ears, as well as sensorineural, conductive or mixed-type hearing loss. Hypoplasia or aplasia of the parotid and submandibular glands leads to xerostomia and early-onset caries. Teeth malformations are characterized by microdontia and hypodontia. The digital system most often involves the thumbs, ranging from total aplasia to hypoplastic, digitalized, triphalangeal, and duplicated thumbs. Mild syndactylies of fingers and lower limb anomalies are less frequent. Additional features of LADD syndrome include renal abnormalities (Bamforth and Kaurah, 1992), lung hypoplasia, cleft lip/palate (Ramirez and Lammer, 2004), facial dysmorphisms, and long QT syndrome (Fierek, 2003).

At the time this PhD study was initiated, the etiology of the LADD syndrome was unknown.

4. Aims and major findings of this PhD thesis

4.1 Aims

The aim of the study performed in this PhD thesis was to identify the genes underlying autosomal dominantly inherited LADD syndrome and to understand the pathophysiological mechanisms leading to the developmental anomalies present in LADD syndrome.

Genome wide linkage analysis in large LADD families were performed to identify linked genomic regions and positional as well as candidate gene approaches were intended to identify disease causing genes. In order to understand the molecular mechanisms of LADD syndrome mutations, a combination of biochemical assays of purified mutant proteins, functional analysis in transiently and stably transfected cells and structural analysis of a mutant crystal was utilized.

4.2 Major findings

(1) Mapping of the first LADD locus to 10q26

(2) Identification of three causative LADD genes and mutations in *FGFR2/3* and in *FGF10* responsible for LADD syndrome

(3) Screening of additional LADD patients and families showing the mutational spectrum of LADD mutations. Establishment of quantitative gene copy analysis and identification of large deletions and a duplication of *FGF10*. Determination of breakpoints using high density tiling arrays covering the FGF10 region

(4) First case of autosomal recessively inherited LADD syndrome and functional analysis of the identified homozygous mutation in stably transfected L6 myoblasts

(5) Molecular analyses identified TWIST1 and TP73L mutations as causative in LADD-like phenotypes

(6) Detection of reduced tyrosine kinase activity of FGFR2 underlying the pathogenesis of LADD syndrome in 4 patients with *FGFR2* mutations

(7) Combination of biochemical studies and structural analysis of p.A628T-FGFR2 mutant crystal showed alteration of the catalytic pocket of the tyrosine kinase domain leading to impaired substrate coordination

5. Present investigations

5.1 Mutations in different components of FGF signaling in LADD syndrome (Rohmann et al., Nat Genet. (2006): Apr. 38 (4): 414-7)

The autosomal dominant lacrimo-auriculo-dento-digital (LADD) syndrome is a multiple congenital anomaly mainly characterized by lacrimal duct aplasia, malformed ears and deafness, small teeth, and digital anomalies. To identify the genetic cause of the LADD syndrome, we initially genotyped three large LADD families using the Affymetrix GeneChip 10K array and mapped the LADD1 locus to chromosome 10q26 to a 6.2 Mb critical region between markers *D10S1693* and *D10S1723*. The gene encoding the fibroblast-growth-factor-receptor 2 (*FGFR2*) was regarded to be an excellent positional and functional candidate gene because: (i) a mouse model carrying a dominant interfering *Fgfr2b* mutant presents with limb and digit malformations; (ii) submandibular gland morphogenesis is regulated by Fgfr2b; and (iii) haploinsufficiency of the known FGFR2b ligand, FGF10, causes lacrimal and salivary gland abnormalities in humans and mice.

We sequenced the entire coding and non-coding exons of *FGFR2* and identified heterozygous missense mutations in exon 16 in all three LADD families and in one sporadic case. Two families carried the c.1942G>T transition predicting the substitution of the highly conserved alanine at position 648 by threonine (p.A648T). The third family showed a 3-bp deletion, c.1947-1949delAGA, leading to a substitution of the highly conserved arginine to serine at position 649 and to the deletion of the neighboring aspartic acid (p.R649Sdel650D). In the sporadic case a *de novo* mutation, c.1882G>A (p.A628T), was identified. In two additional LADD families the *FGFR2* locus was excluded by haplotype analysis. To identify further causative genes, *FGFR1*, *FGFR3*, and *FGFR4*, as well as two known FGFR2 ligands, *FGF8* and *FGF10*, were tested as functional candidate genes. In one family the causative missense mutation c.317G>T in exon 1 of *FGF10* was detected, which is predicted to change the conserved amino acid cysteine at position 106 to phenylalanine (p.C106F). In the other family a missense mutation in *FGFR3* was found. The c.1537G>A transition results in the amino acid substitution p.D513N within the conserved tyrosine kinase domain. We confirmed further that the mutations, which cosegregated with the disease, were present neither in unaffected family members nor in 200 ethnically matched control individuals.

Notably, all LADD mutations identified in *FGFR2/3* are located within the tyrosine kinase domains of the receptors within loops that have an important regulatory function in the control of receptor activity. 3D-modeling of the identified mutations suggested that – in contrast to described FGFR2/3 *gain-of-function* mutations in syndromic craniosynostosis and skeletal dysplasia syndromes - LADD syndrome might be caused by diminished FGF-signaling due to tyrosine kinase impairment. Therefore, reduced functional activity of FGFR2/3 seemed to be a plausible mechanism underlying the molecular basis of LADD syndrome.

Own contributions:
At first I evaluated and interpreted the Affymetrix GeneChip 10K Array data and carried out haplotype analysis in the pedigrees. Subsequently, I identified *FGFR2* as the causative gene in the linked region. Furthermore, I established test assays for additional candidate genes, such as *FGFR3* and *FGF10*, analyzed patients and families and identified causative mutations. Finally, I analyzed and construed the results and set up the segregation of the mutations within each family and performed the control studies either by enzyme restriction assays or direct sequencing.

5.2 LADD syndrome is caused by reduced activity of the FGF10-FGF receptor 2 signaling pathway (Shams et al., Mol Cell Biol. (2007); 27: 6903-6912)

The next aim was to determine the molecular mechanisms of the previously identified LADD mutations. In this paper, we described the functional effects of FGF10 (I156R, C106F and K137X) and FGFR2 LADD mutants (A628T, A648T and R649S) in comparison to the properties of their normal counterparts. In addition, we generated a kinase-defective (KD) mutant (K508A) and a Pfeiffer syndrome *gain-of-function* FGFR2b (K641R) mutant as controls for the functional analysis.

Protein expression of the FGF10 LADD mutations and binding studies in L6 cells stably expressing FGFR2b showed that the mutants were unable to stimulate tyrosine autophosphorylation of the receptor or tyrosine phosphorylation of the downstream signaling molecules FRS2 and Shc. Furthermore, no MAPK stimulation was detected. Additionally, ligand displacement assays with radiolabeled FGF10, limited proteolysis analyses and intrinsic fluorescence measurements demonstrated that each of the three FGF10 mutants affected the FGF10 activity by a different mechanism. The initially identified p.C106F mutant showed reduced protein stability responsible for its disturbed biological function, which was indicated by the formation of low-molecular-weight degradation products and also by increased changes of the fluorescence spectrum. Moreover, stimulation of L6 cells stably expressing FGFR2b with or without heparin and with the p.C106F mutant showed a protective effect for the MAPK stimulation when treated with heparin. The subsequently described p.I156R mutation presented a drastically reduced receptor binding capacity indicated by a higher 50% inhibitory concentration of ^{125}I-labeled FGF10 bound to FGFR2b in L6 cells. Modeling based on the X-ray crystal structure of FGF10 depicted that Ile156 is located in a region forming contact with FGFR2b and that the amino acid change to arginine leads to the disruption of critical electrostatic interactions essential for binding between FGF10 and FGFR2b. In contrast, p.Cys106 is located on the surface of FGF10 and the amino acid change to the larger phenylalanine is suggested to form a bulky region causing instability of the mutant protein. Finally, the p.K137X mutant exhibited no expression in different experimental conditions assuming a rapid degradation.

FGFR2 mutants were characterized using transient expression in HEK293 cells and stable expression in L6 cells. Western-blot analysis demonstrated that the FGFR2 LADD mutants possess different degrees of tyrosine autophosphorylation. The p.R649Sdel650D mutant had the highest residual TK activity, whereas p.A628T had the lowest. Further, we demonstrated that the three mutants failed to stimulate tyrosine phosphorylation of two well-characterized FGFR substrates, FRS2 and Shc, and also of the MAPK pathway. Combining the findings of the co-expression studies of FGFR2 WT and LADD mutants and with known mouse data suggested that LADD mutants might exert a dominant-negative effect on normal FGFR2 protein.

We concluded that FGF10 LADD mutants cause haploinsufficiency of FGF10. Moreover, we concluded that FGFR2 LADD mutants cause a strongly attenuated intrinsic tyrosine kinase activity leading to impaired tyrosine phosphorylation of critical substrates and cell signaling. Since all LADD mutations are clustered in the catalytic domain of FGFR2, these mutations are not isoform specific. Furthermore, we described the importance of exact doses of receptor signaling in mediating biological responses.

Own contributions:
Initially, I generated different mutant constructs of FGF10 and FGFR2 by site directed mutagenesis and expressed human FGF10 WT and FGF10 LADD mutants in *E. coli* using the bacterial expression vector pET11c. In addition, I generated the cloning strategy for the human FGFR2b WT construct using the retroviral pBABE/neo expression vector for stable L6 cell line transfection. For the transient transfection of FGFR2b WT in HEK293 cells, I used the pcDNA-3 expression vector. Furthermore, I transformed FGF10 WT and FGF10 LADD mutants in BL21(DE3)pLysS *E. coli* strains and purified the recombinant proteins by fast-perfomance liquid chromatography. Consequently, I determined the protein purity by SDS-PAGE analysis and performed the binding studies between the purified FGF10 WT/LADD mutants and the FGFR2b in L6 cells. Additionally, I conducted the transfection experiments of FGFR2b WT and FGFR2b LADD mutants in L6 cells and assembled the immunoprecipitation (IP) assays and applied the IP products of all performed experiments on SDS-PAGE followed by Western Blot analysis.

5.3 Structural basis for reduced FGFR2 activity in LADD syndrome: Implications for FGFR autoinhibition and activation (Lew et al., Proc Natl Acad Sci U S A. (2007) Dec. 104 (50): 19802-19807)

After demonstrating that FGFR2 mutations responsible for LADD syndrome cause a decreased tyrosine kinase phosphorylation and a reduced ligand-induced recruitment of downstream signaling molecules (Shams and Rohmann et al., 2007), we wanted to investigate how these point mutations located in highly conserved regions of the kinase domain lead to partial inactivation or loss of function phenotype. For this purpose, we biochemically analyzed the kinetics of tyrosine phosphorylation and in addition generated crystals of FGFR2 WT and the identified *de novo* missense mutation p.A628T, which is located in the catalytic part of the tyrosine kinase domain of FGFR2.

Purification of the intact kinase domains of FGFR2 WT and p.A628T-FGFR2 mutant exhibited that both proteins are monomers with similar elution profiles. Therefore, we suggested that the p.A628T-FGFR2 mutant remains intact and possesses a surface charge in concordance with that of the FGFR2 WT. Applying an *in vitro* kinase assay, we observed a fully phosphorylated (5P, 5 phosphorylations sites) FGFR2 WT kinase after 45 min at 4 ˚C and after 10 min at RT. In contrast, the mutant failed to undergo autophosphorylation at 4 ˚C and showed incomplete tyrosine phosphorylation at RT. These results proved that the p.A628T-FGFR2 mutant directly compromises the intrinsic catalytic activity of FGFR2 kinase, which is in agreement with the decreased tyrosine phosphorylation of ectopically expressed p.A628T-FGFR2 mutant in transfected L6 cells (Shams and Rohmann et al., 2007). In addition, we performed the *in vitro* kinase assay for FGFR1 WT in comparison to FGFR2 WT. We detected that FGFR2 WT was modestly more catalytically active than FGFR1 WT, indicated by a faster emergence of the full phosphorylated (5P) FGFR2 WT, concluding that the kinase of FGFR2 WT is less autoinhibited than the one of FGFR1.

The crystal structures of several receptor tyrosine kinases (RTKs), like FGFR1 and IRK (Insulin receptor kinase), are known. We compared those with the generated FGFR2 WT and p.A628T-FGFR2 mutant crystal. The crystals illustrated a very similar structure between the inactive crystals of FGFR2 WT and p.A628T-FGFR2 mutant. Both crystal structures in the inactive state appeared accessible at the nucleotide-binding site as well as at the substrate-binding pocket. These observations were quite in contrast to the crystal structure of FGFR1, although FGFR1 and FGFR2 share >90% sequence identity. Viewed closely, the conformation of the C-terminal lobe was nearly identical, whereas the N-terminal lobe of FGFR2 relative to FGFR1 revealed a rotation, which is reminiscent of an active state. Instead, the crystal structure of FGFR2 in the inactive state had a stronger similarity to the structure of active IRK (IRK-3P) leading to the conformation that FGFR2 kinase is less autoinhibited than FGFR1. Further fluorescence titration experiments of the p.A628T-FGFR2 crystal with an ATP analog demonstrated that the mutant does not affect ATP binding and confirmed that the p.A628T-FGFR2 mutant is responsible for disruption of the catalytic pocket.

In conclusion, the structure definitely depicted that the p.A628T-FGFR2 LADD mutation alters the conformation of key residues in the catalytic pocket, which impairs the ability of the tyrosine kinase to coordinate its substrate and, finally, causes partial inactivation, as seen in LADD syndrome mutations. Furthermore, we demonstrated that FGFR2 utilizes a less stringent mode of autoinhibition than FGFR1 and that the mechanism of autoinhibition is dependent on alteration of the conformational dynamics.

Own contributions:

Initially, I performed bacterial expression of a construct containing residues 461-768 of the human FGFR2. For the protein crystallization, I integrated a TEV enzymatic cleavage site by PCR and produced the single point mutation, p.A628T, by site directed mutagenesis. Moreover, I set up the bacterial expression of p.A628T-FGFR2 LADD mutant and purified the protein using French Press and a Ni-NTA-His resin. Subsequently, I analyzed the phosphorylation states of the purified proteins of FGFR2 WT and p.A628T-FGFR2 via an *in vitro* kinase assay and visualized the results by native gel electrophoresis.

6. Progress and concluding remarks

During my PhD thesis further genetic analysis was done in familial and sporadic LADD patients and several novel mutations were identified: ***FGF10*****:** p.E145X, IVS1+3delA; ***FGFR2*****:** p.R488G, p.E710-L712dupELF. Autosomal recessive inheritance was found for the first time in one family, which was caused by the homozygous p.R579W in the TK domain of FGFR2. Both parents were carriers and clinically not affected. Using newly established quantitative assays, such as multiplex ligation-dependent probe amplification (MLPA) and quantitative Taqman analysis, one large deletion and two duplications of *FGF10* were identified. These large structural anomalies were further investigated by fine-tiling array comparative genomic hybridization (CGH) and the exact breakpoints of a 12.15 kb deletion affecting exons 2 and 3 of *FGF10* in a large LADD family were defined. A junction fragment could be amplified confirming the deletion. In two other patients, duplications of different sizes were found, one of them determined as a 2.2 Mb duplication including the complete *FGF10* gene.

Additional candidate genes were tested in patients negative for LADD mutations to identify novel LADD genes. In one sporadic patient who presented overlapping features with LADD syndrome, a *de novo* deletion of the complete *TWIST1* gene on chromosome 7p21.2 was found by MLPA. Screening of the *TP73L* gene (p63 protein) in our cohort with possible diagnosis of LADD identified the heterozygous p.R298Q, which is a hot-spot mutation for the acro-dermato-ungual-lacrimal-tooth (ADULT) syndrome and was described in 3 out of 4 ADULT syndrome patients. The p.R279H mutation in *TP73L* (previously described in patients with ectrodactyly, ectodermal dysplasia and cleft lip/palate (EEC) syndrome) was found in a patient diagnosed with LADD but presenting an EEC-syndrome-like phenotype upon re-examination.

Within the present PhD thesis, I identified the molecular basis of the congenital LADD syndrome and determined the pathophysiological mechanisms underlying different LADD genes and mutations. The identified mutations in *FGF10* caused haploinsufficiency of FGF10 leading to a *loss-of-function* phenotype in LADD syndrome. The mutations identified in *FGFR2* caused a strongly attenuated intrinsic tyrosine kinase activity due to conformational changes and resulted in an impaired signal transduction in the cascade of the FGF-FGFR signaling pathway, finally resulting in LADD syndrome. LADD patients with mutations in FGF10 or FGFR2 present no specific phenotypic differences. Furthermore, LADD syndrome exists with a wide range of phenotypic variability of symptoms, even within one family carrying the identical mutation. This impedes genotype-phenotype correlations. The heterogeneity of the LADD syndrome and the absence of known LADD mutations in some of our patients, led us to the suggestion of further genes to be involved in the pathogenesis of LADD syndrome.Therefore, I performed further genetic analysis and could identify mutations in genes already described for syndromes with overlapping clinical features in LADD-like syndromes. These results display nicely the overlap of clinical phenotypes between p63-associated disorders and LADD syndrome. Future functional analysis of the FGFR3-LADD mutation might provide additional insights into impaired FGF signaling causing LADD syndrome.

6.1 Awards/Talks

Participant and young scientist representative of the University of Cologne at the Meeting of Nobel Laureates in Medicine/ Physiology in Lindau, 2007

Medical faculty prize 2006 for the best individual publication of the University of Cologne will be given for the Nature Genetics publication.

Rohmann E., Lax I., Lew E.D., Eswarakumar V.P., Brunner H.G., Li Y., Kayserili H., Schlessinger J., Wollnik B. Oral Presentation: LADD syndrome is caused by mutations that reduce the tyrosine kinase activity of FGFR2. 18th Annual Meeting of the German Society of Human Genetics March 7 –10, 2007, Bonn.

Rohmann E., Lax I., Lew E.D., Eswarakumar V.P., Brunner H.G., Li Y., Kayserili H., Schlessinger J., Wollnik B. Oral Presentation: LADD syndrome is caused by mutations that reduce the tyrosine kinase activity of FGFR2. 56th Annual Meeting of The American Society of Human Genetics, October 9 –13, 2006, New Orleans.

Wollnik B., Brunner H.G., Kayserili H., Uyguner O., Nürnberg G., Lew E.D., Dobbie A., Eswarakumar V.P., Uzumcu A., Ulubil-Emeroglu M., Leroy J.G., Li Y., Becker C., Lehnerdt K., Cremers C.W., Yuksel-Apak M., Nürnberg P., Kubisch C., Schlessinger J., van Bokhoven H., Rohmann E. Oral Presentation: Mutations in different components of FGF-signaling in LADD syndrome. 17th Annual Meeting of the German Society of Human Genetics, March 8 –11, 2006, Heidelberg.

Wollnik B., Brunner H.G., Kayserili H., Uyguner O., Nürnberg G., Lew E.D., Dobbie A., Eswarakumar V.P., Uzumcu A., Ulubil-Emeroglu M., Leroy J.G., Li Y., Becker C., Lehnerdt K., Cremers C.W., Yuksel-Apak M., Nürnberg P., Kubisch C., Schlessinger J., van Bokhoven H., Rohmann E. Oral Presentation: Mutations in different components of FGF-signalling in LADD syndrome. 38th European Human Genetics Conference, May 9 –12, 2006, Amsterdam.

7. Additional publications and activities during the PhD thesis

7.1 Kaplan Y, Vargel I, Kansu T, Akin B, Rohmann E, Kamaci S, Uz E, Ozcelik T, Wollnik B, Akarsu NA: Skewed X-inactivation in an X-linked Nystagmus Family Resulted From a Novel, p.R229G, Missense Mutation in the FRMD7 Gene. Br J Ophthalmol. (2007): Oct 25; [Epub ahead of print]

Congenital motor nystagmus (NYS) is a genetically heterogeneous disorder and is characterized by ocular oscillatory movement caused by a motor instability that can manifest with or without afferent visual system dysfunction. Autosomal dominant, recessive and X linked inheritance are described, whereby the X linked inheritance is the most common form of NYS (NYS1). To date, two loci on the Xq26-q27 and on Xp11.4 have been reported for X-linked dominant NYS. Recently, for the former loci mutations in the *FRMD7* (FERM domain-containing 7) gene have been reported as a molecular cause in Xq26-linked families. This gene shows restricted expression pattern in the human embryonic brain and developing neural retina, but minor knowledge exists about the function of *FRMD7*.

We investigated a large NYS1 pedigree, including 162 individuals from six generations of South-Eastern Turkish decent. The two most prominent findings in this family were nystagmus, obesity, and/or type 2 diabetes. The penetrance of the NYS1 phenotype in females was estimated to be approximately 36% for this family. We mapped the disease locus to chromosome Xq26-q27 by genetic linkage analysis. Subsequently, we identified a novel missense mutation in the gene *FRMD7* by direct sequencing. The c.686C>G mutation in exon 8 leads to the substitution of a conserved arginine by a gylcine (p.R229G) in the functionally important FERM-C domain of the protein. We performed X-chromosome inactivation analysis by enzymatic predigestion of DNA with a methylation-sensitive enzyme, followed by PCR of the polymorphic CAG repeat of the androgen receptor gene. We demonstrated that skewed X-inactivation was significantly increased in affected females compared to unaffected females in this family. Besides, we observed the first homozygote female case of the NYS phenotype, but no obvious phenotypic differences to heterozygote females was detected.

In conclusion, we identified a novel missense mutation in the *FRMD7* gene responsible for NYS1 and we demonstrated skewed X inactivation, which influences the manifestations of the disease in X linked females.

Own contributions:

I designed the primers of the *FRMD7* gene by using genome databases and established the test conditions for PCR amplification and sequencing. Furthermore, I evaluated the sequencing results by using database analysis and performed the control studies of 120 control individuals by establishing a restriction enzyme digestion assay.

7.2 Pabst S, Wollnik B, Rohmann E, Hintz Y, Grohé C: A novel stop mutation truncating critical regions of the cardiac transcription factor NKX2.5 in a large family with autosomal-dominant inherited congenital heart disease. Clin Res Cardiol. (2007): Sep 25; [Epub ahead of print]

Congenital cardiovascular diseases (CCVD) are the most common developmental anomalies, and are diagnosed in 1% of newborns. Atrial septal defect (ASD) is the most often inherited CCVD and is characterized by an abnormality of the upper chambers of the heart (atria) where the wall between the right and left atria does not close completely. In sporadic patients and families presenting association of ASD with atrioventricular AV conduction block and other CCVDs heterozygous mutations in the cardiac transcription factor *NKX2-5* were identified. Also, mice models carrying homozygote deletion of *NKX2-5* are lethal due to impaired cardiac looping. Heterozygosity results in hypoplasia of the atrioventricular conduction system in mice.

We described a family affected by an autosomal dominantly inherited AV conduction block associated with ASD and CCVD. For the reasons described above, we screened the *NKX2-5* gene by direct sequencing. We identified a novel heterozygous nonsense mutation c.325G>T (p.E109X) in exon 1 of the cardiac transcription factor in this family. The mutation is predicted to truncate the protein after 109 amino acids, which results either in an truncated protein lacking all known domains that are necessary for its functionality or in rapid degradation of the mutated mRNA due to nonsense-mediated mRNA decay (NMD).

We concluded that the described AV associated with ASD and CCVD in this family is caused by the novel nonsense mutation in the *NKX2-5* gene and that the pathophysiological mechanism is triggered by loss of function leading to haploinsufficiency of NKX2-5. In general, the phenotype of patients with defects in *NKX2-5* mutations shows high variability, even within the same family. Therefore, no genotype-phenotype correlation could be established yet. Molecular screening of candidate genes, as done in the present study, is helpful for the identification of high risk family members and important for accurate and early therapy.

Own contributions:

First of all, I considered *NKX2-5* as a highly relevant candidate gene for the disorder in the family and designed the primers of the *NKX2-5* gene for PCR amplification and established the test assays for the PCR conditions as well as for the sequencing reactions. In addition, I performed the control studies of 50 control individuals also by direct sequencing and analyzed all sequencing results by using database analysis.

7.3 Kalay E, Li Y, Uzumcu A, Uyguner O, Collin R, Caylan R, Ulubil-Emeroglu M, Kersten F, Hafiz G, van Wijk E, Kayserili H, Rohmann E, Wagenstaller J, Hoefsloot L, Strom T, Nürnberg G, Baserer N, Hollander A, Cremers F, Cremers C, Becker C, Brunner H, Nürnberg P, Karaguzel A, Basaran S, Kubisch C, Kremer H, Wollnik B ; Mutations in the lipoma HMGIC fusion partner-like 5 (LHFPL5) Gene Cause Autosomal Recessive Nonsyndromic Hearing Loss ; Human Mutat. (2006): 27(7), 633-639

Autosomal recessive nonsyndromic hearing loss (ARNSHL) is the most common hereditary form of deafness and accounts for >70% of cases. Until now, more than 70 loci for ARNSHL (*DFNB*) and 23 of the corresponding genes have been identified.

We investigated two large Turkish consanguineous families (DF44 and TR77) diagnosed with isolated hearing loss. After exclusion of common genes known to be responsible for hearing loss by sequencing and haplotype analysis, we performed genome wide linkage analysis and homozygosity mapping using the Affymetrix GeneChip Human Mapping 10K Array. We mapped the disease causing locus to chromosome 6p21.3-21.1 in both families. Further fine-mapping with microsatellite markers and inclusion of additional family members minimized the critical region to an 8.4-Mb interval between the markers *D6S1629* and *D6S400* in the family DF44 and to a 7.5-Mb interval between the markers *D6S1583* and *D6S1575* in the family TR77. In both families the critical region partially overlaps with the recently described DFNB66 locus and excluded at the same time the locus DFNB53, in which the gene

COL11A2 is known to cause autosomal recessive deafness. Further analysis of the critical region led to the investigation of the lipoma HMGIC fusion partner-like 5 (*LHFPL5*) gene. Due to the fact that the recently described mouse model carrying homozygous mutation in Lhfpl5 showed deafness and vestibular dysfunction (*hscy*, "hurry-scurry" mouse), *LHFPL5* seemed to be a highly relevant positional candidate gene. In family DF44, we found a homozygous one-base pair deletion (p.Glu216ArgfsX26) and in family TR77 we identified a homozygous transition (p.Thr165Met) in *LHFPL5* by direct sequencing. We screened further index patients from 96 Turkish ARNSHL families and 90 Dutch ARNSHL patients and identified the one-base pair deletion (p.Glu216ArgfsX26) in one additional Turkish family. In addition, we found a heterozygous putative mutation (p.Arg176Leu) in a Dutch patient, but could not find a second mutation in *LHFPL5*. We continued the molecular analysis and sequenced the *LHFPL5* homologs *LHFPL3* and *LHFPL4* for 78 index patients from Turkish ARNSHL families, but we identified no disease-associated mutation.

In conclusion, we found a novel deafness gene, *LHFPL5*, responsible for ARNSHL in humans without vestibular dysfunction, which is in contrast to the "hurry-scurry" mouse with vestibular dysfunction. We suggested that *loss-of-function* of LHFPL5 causes the phenotype in the investigated families. Moreover, we showed evidence from haplotpye analysis that the identified one-base pair deletion was originated by a shared founder in the two investigated Turkish families.

Own contributions:

For this project, I established the test conditions for the sequencing reactions to perform the control studies for the identified mutations in control DNAs from 170 unrelated individuals of Turkish origin and over 90 Caucasian individuals from The Netherlands.

7.4 Li Y, Wollnik B, Pabst S, Lennarz M, Rohmann E, Gillissen A, Vetter H, Grohe C ; BTNL2 gene variant and sarcoidosis ; Thorax. (2006): 61, 273-274

Sarcoidiosis is an immune system disorder characterized by non-caseating granulomas (small inflammatory nodules), which primarily affects the lungs and lymph node. The clinical course is presented by the acute and chronic type, whereby the latter can lead to lung fibrosis. The pathogenesis of the disease is still unknown, but a genetic predisposition to develop the disease is assumed due to investigations of familial clustering and relatives with increased risk of sacroidosis.

We confirmed a recently described significant association between sarcoidosis and a frequent single nucleotide polymorphism (SNP) in the *BTNL2* gene, rs2076530, by using a case-control association study including 210 patients with sarcoidosis and 202 controls. By applying the quantitative Taqman technique, we observed that A allele carriers of rs2076530 have a more than twofold increased risk of developing sarcoidosis compared with GG homozygotes. In addition, we showed that susceptibility is preferential towards the chronic form of sarcoidosis.

Own contributions:
I supported the design of the oligonucleotides and the probe for testing the SNP rs2076530. Furthermore, I supported the establishment of the Taqman technique to perform the SNP analysis.

8. References

Anderson, J., Burns, H. D., Enriquez-Harris, P., Wilkie, A. O. and Heath, J. K., 1998. Apert syndrome mutations in fibroblast growth factor receptor 2 exhibit increased affinity for FGF ligand. Hum Mol Genet. 7, 1475-1483.

Arman, E., Haffner-Krausz, R., Chen, Y., Heath, J. K. and Lonai, P., 1998. Targeted disruption of fibroblast growth factor (FGF) receptor 2 suggests a role for FGF signaling in pregastrulation mammalian development. Proc Natl Acad Sci U S A. 95, 5082-5087.

Bamforth, J. S. and Kaurah, P., 1992. Lacrimo-auriculo-dento-digital syndrome: evidence for lower limb involvement and severe congenital renal anomalies. Am J Med Genet. 43, 932-937.

Daily, L., Ambrosetti, D., Mansukhani, A., Bsilico, C., 2005. Mechanisms underlying responses of FGF signalling. Cytokine Growth Factor Rev. 16, 233-247.

Eswarakumar, V. P., Lax, I. and Schlessinger, J., 2005. Cellular signaling by fibroblast growth factor receptors. Cytokine Growth Factor Rev. 16, 139-149.

Eswarakumar, V.P., Ozcan, F., Lew, E.D., Bae, J.H., Tomé, F., Booth, C.J., Adams, D.J., Lax, I., Schlessinger, J., 2006. Attenuation of signalling pathways stimulated by pathologically activated FGF-receptor 2 mutants prevents craniosynostosis. Proc Natl Acad Sci U S A 49, 18603-8.

Fierek, O., Laskawi, R., Bönnemann, C., 2003. Das Levy-Hollister Syndrom: Ein Dysplasiesyndrom mit HNO-Manifestationen. HNO 51: 654-657

Flaumenhaft, R., Moscatelli, D. and Rifkin, D. B., 1990. Heparin and heparan sulfate increase the radius of diffusion and action of basic fibroblast growth factor. J Cell Biol. 111, 1651-1659.

Goldfarb, M., 2005. Fibroblast growth factor homologous factors: evolution, structure, and function. Cytokine Growth Factor Rev. 16, 215-220.

Hollister, D. W., Klein, S. H., De Jager, H. J., Lachman, R. S. and Rimoin, D. L., 1973. The lacrimo-auriculo-dento-digital syndrome. J Pediatr. 83, 438-444.

Hubbard, S. R. and Till, J. H., 2000. Protein tyrosine kinase structure and function. Annu Rev Biochem. 69, 373-398.

Ibrahimi, O. A., Yeh, B. K., Eliseenkova, A. V., Zhang, F., Olsen, S. K., Igarashi, M., Aaronson, S. A., Linhardt, R. J. and Mohammadi, M., 2005. Analysis of mutations in fibroblast growth factor (FGF) and a pathogenic mutation in FGF receptor (FGFR) provides direct evidence for the symmetric two-end model for FGFR dimerization. Mol Cell Biol. 25, 671-684.

Itoh, N. and Ornitz, D. M., 2004. Evolution of the Fgf and Fgfr gene families. Trends Genet. 20, 563-569.

Jabs, E. W., Li, X., Scott, A. F., Meyers, G., Chen, W., Eccles, M., Mao, J. I., Charnas, L. R., Jackson, C. E. and Jaye, M., 1994. Jackson-Weiss and Crouzon syndromes are allelic with mutations in fibroblast growth factor receptor 2. Nat Genet. 8, 275-279.

Levy, W. J., 1967. Mesoectodermal dysplasia. A new combination of anomalies. Am J Ophthalmol. 63, 978-982.

Miyakawa, K., Hatsuzawa, K., Kurokawa, T., Asada, M., Kuroiwa, T. and Imamura, T., 1999. A hydrophobic region locating at the center of fibroblast growth factor-9 is crucial for its secretion. J Biol Chem. 274, 29352-29357.

Miyake, A., Konishi, M., Martin, F. H., Hernday, N. A., Ozaki, K., Yamamoto, S., Mikami, T., Arakawa, T. and Itoh, N., 1998. Structure and expression of a novel member, FGF-16, on the fibroblast growth factor family. Biochem Biophys Res Commun. 243, 148-152.

Miyamoto, M., Naruo, K., Seko, C., Matsumoto, S., Kondo, T. and Kurokawa, T., 1993. Molecular cloning of a novel cytokine cDNA encoding the ninth member of the fibroblast growth factor family, which has a unique secretion property. Mol Cell Biol. 13, 4251-4259.

Mohammadi, M., Olsen, S. K. and Goetz, R., 2005. A protein canyon in the FGF-FGF receptor dimer selects from an a la carte menu of heparan sulfate motifs. Curr Opin Struct Biol. 15, 506-516.

Muenke, M., Schell, U., Hehr, A., Robin, N. H., Losken, H. W., Schinzel, A., Pulleyn, L. J., Rutland, P., Reardon, W., Malcolm, S. and et al., 1994. A common mutation in the fibroblast growth factor receptor 1 gene in Pfeiffer syndrome. Nat Genet. 8, 269-274.

Ohmachi, S., Watanabe, Y., Mikami, T., Kusu, N., Ibi, T., Akaike, A. and Itoh, N., 2000. FGF-20, a novel neurotrophic factor, preferentially expressed in the substantia nigra pars compacta of rat brain. Biochem Biophys Res Commun. 277, 355-360.

Orr-Urtreger, A., Bedford, M. T., Burakova, T., Arman, E., Zimmer, Y., Yayon, A., Givol, D. and Lonai, P., 1993. Developmental localization of the splicing alternatives of fibroblast growth factor receptor-2 (FGFR2). Dev Biol. 158, 475-486.

Ramirez, D. and Lammer, E. J., 2004. Lacrimoauriculodentodigital syndrome with cleft lip/palate and renal manifestations. Cleft Palate Craniofac J. 41, 501-506.

Reardon, W., Winter, R. M., Rutland, P., Pulleyn, L. J., Jones, B. M. and Malcolm, S., 1994. Mutations in the fibroblast growth factor receptor 2 gene cause Crouzon syndrome. Nat Genet. 8, 98-103.

Rutland, P., Pulleyn, L. J., Reardon, W., Baraitser, M., Hayward, R., Jones, B., Malcolm, S., Winter, R. M., Oldridge, M., Slaney, S. F. and et al., 1995. Identical mutations in the FGFR2 gene cause both Pfeiffer and Crouzon syndrome phenotypes. Nat Genet. 9, 173-176.

Sabatino, G., Di Rocco, F., Zampino, G., Tamburrini, G., Caldarelli, M. and Di Rocco, C., 2004. Muenke syndrome. Childs Nerv Syst. 20, 297-301.

Schlessinger, J., Plotnikov, A. N., Ibrahimi, O. A., Eliseenkova, A. V., Yeh, B. K., Yayon, A., Linhardt, R. J. and Mohammadi, M., 2000. Crystal structure of a ternary FGF-FGFR-heparin complex reveals a dual role for heparin in FGFR binding and dimerization. Mol Cell. 6, 743-750.

Schlessinger, J. and Ullrich, A., 1992. Growth factor signaling by receptor tyrosine kinases. Neuron. 9, 383-391.

Schoorlemmer, J. and Goldfarb, M., 2001. Fibroblast growth factor homologous factors are intracellular signaling proteins. Curr Biol. 11, 793-797.

Steinberger, D., Vriend, G., Mulliken, J. B. and Muller, U., 1998. The mutations in FGFR2-associated craniosynostoses are clustered in five structural elements of immunoglobulin-like domain III of the receptor. Hum Genet. 102, 145-150.

Toydemir, R. M., Brassington, A. E., Bayrak-Toydemir, P., Krakowiak, P. A., Jorde, L. B., Whitby, F. G., Longo, N., Viskochil, D. H., Carey, J. C. and Bamshad, M. J., 2006. A novel mutation in FGFR3 causes camptodactyly, tall stature, and hearing loss (CATSHL) syndrome. Am J Hum Genet. 79, 935-941.

Wilkie, A. O., Slaney, S. F., Oldridge, M., Poole, M. D., Ashworth, G. J., Hockley, A. D., Hayward, R. D., David, D. J., Pulleyn, L. J., Rutland, P. and et al., 1995. Apert syndrome results from localized mutations of FGFR2 and is allelic with Crouzon syndrome. Nat Genet. 9, 165-172.

Yamashita, T., 2005. [Regulatory effect of FGF23 on phosphate and vitamin D metabolism]. Nippon Rinsho. 63 Suppl 10, 519-522.

Yayon, A., Klagsbrun, M., Esko, J. D., Leder, P. and Ornitz, D. M., 1991. Cell surface, heparin-like molecules are required for binding of basic fibroblast growth factor to its high affinity receptor. Cell. 64, 841-848.

Yu, C., Wang, F., Kan, M., Jin, C., Jones, R. B., Weinstein, M., Deng, C. X. and McKeehan, W. L., 2000. Elevated cholesterol metabolism and bile acid synthesis in mice lacking membrane tyrosine kinase receptor FGFR4. J Biol Chem. 275, 15482-15489.

nature genetics

© 2006 Nature Publishing Group http://www.nature.com/naturegenetics

Mutations in different components of FGF signaling in LADD syndrome

Edyta Rohmann[1,2], Han G Brunner[3], Hülya Kayserili[4], Oya Uyguner[4], Gudrun Nürnberg[5,6], Erin D Lew[7], Angus Dobbie[8], Veraragavan P Eswarakumar[7], Abdullah Uzumcu[4], Melike Ulubil-Emeroglu[9], Jules G Leroy[10], Yun Li[1,2], Christian Becker[5,6], Kai Lehnerdt[11], Cor W R J Cremers[12], Memnune Yüksel-Apak[4], Peter Nürnberg[5,13], Chriiütian Kubisch[2,13], Joseph Schlessinger[7], Hans van Bokhoven[3] & Bernd Wollnik[1,2,4]

Lacrimo-auriculo-dento-digital (LADD) syndrome is characterized by lacrimal duct aplasia, malformed ears and deafness, small teeth and digital anomalies. We identified heterozygous mutations in the tyrosine kinase domains of the genes encoding fibroblast growth factor receptors 2 and 3 (*FGFR2*, *FGFR3*) in LADD families, and in one further LADD family, we detected a mutation in the gene encoding fibroblast growth factor 10 (*FGF10*), a known FGFR ligand. These findings increase the spectrum of anomalies associated with abnormal FGF signaling.

Autosomal dominant lacrimo-auriculo-dento-digital (LADD) syndrome (OMIM 149730), also known as Levy-Hollister syndrome, is a multiple congenital anomaly mainly affecting lacrimal glands and ducts, salivary glands and ducts, ears, teeth and distal limb segments[1,2]. In addition to these cardinal features, facial dysmorphism, malformations of the kidney and respiratory system and abnormal genitalia have been reported[3].

We have clinically examined five large LADD families and one sporadic case presenting a wide range of typical clinical symptoms with variable expression, even within a family (**Table 1** and **Fig. 1a–i**). Hypoplasia, atresia and aplasia of the nasolacrimal ducts and puncta led to frequent conjunctivitis in patients, and salivary gland abnormalities such as hypoplasia or aplasia of the parotid and submandibular glands caused xerostomia and early-onset caries. Frequently we observed hypo- and microdontia (**Fig. 1d**). External ear anomalies included cup-shaped, small and low-set ears (**Fig. 1a–c,e,f**), and in over 50% of the cases, we found sensorineural, conductive or mixed-type hearing loss. Limb defects most often involved the thumbs, ranging from total aplasia to hypoplastic, digitalized, triphalangeal and duplicated thumbs (**Fig. 1g–i**). Mild syndactylies of fingers or toes and lower-limb anomalies were less common. We did not find short stature or craniosynostosis in any of the affected individuals (**Fig. 1a–d**).

Initially, we genotyped available DNA samples from 12 affected and ten nonaffected members in three LADD families (LADD-Ist from Turkey, LADD-Nij from The Netherlands and LADD-Le from England) using the Affymetrix GeneChip Human Mapping 10K Array. We obtained a combined maximum parametric LOD score of 3.61 for a region located between SNPs rs36322 and rs718949 on chromosome 10q26 (**Supplementary Methods** and **Supplementary Fig. 1** online), defining a critical interval of about 8.7 Mb. By performing fine-mapping with microsatellite markers and including additional family members, we reduced the critical region to a 6.2-Mb interval between markers D10S1693 and D10S1723 with a maximum multipoint LOD score of 4.52 (**Supplementary Fig. 1** and **Supplementary Table 1** online). We considered the *FGFR2* gene a highly relevant positional candidate gene for the following reasons: (i) conditional knockout of *Fgfr2* or expression of a dominant interfering Fgfr2b mutant in mice results in limb and digit malformations[4,5]; (ii) Fgfr2b regulates submandibular gland morphogenesis[6] and (iii) haploinsufficiency of FGF10, a known ligand of FGFR2b, in mice and humans causes lacrimal and salivary gland abnormalities (OMIM 180920)[7]. We sequenced all 24 coding and noncoding exons of *FGFR2* (**Supplementary Table 2** online) in affected family members and identified a heterozygous mutation in each one of them (**Fig. 1j–m**). The mutations that cosegregated with the disease were present neither in unaffected family members nor in 200 ethnically matched control individuals. We found the 1942G→A transition in exon 16 in all five affected individuals of the Dutch LADD-Nij family (**Fig. 1j** and **Supplementary Fig. 2** online), predicting the substitution of the highly conserved Ala648 by threonine (**Supplementary Fig. 3** online). The same heterozygous A648T missense mutation was identified in all affected family members of the English LADD-Le family (**Fig. 1k** and **Supplementary Fig. 2**). We subsequently demonstrated by haplotype analysis that the A648T mutation most likely originated independently in both families, as it is not located on a common founder haplotype (**Supplementary Fig. 1**). All affected individuals in the LADD-Ist family carried a heterozygous 3-bp deletion, Δ1947-AGA-1949, in exon 16 of *FGFR2* (**Fig. 1m** and **Supplementary Fig. 2**), leading at position 649 to a substitution of the highly conserved arginine to

---

[1]Center for Molecular Medicine Cologne and [2]Institute of Human Genetics, University of Cologne, 50931 Cologne, Germany. [3]Department of Human Genetics, Radboud University Nijmegen Medical Center, 6500 HB Nijmegen, The Netherlands. [4]Medical Genetics Department, Istanbul Medical Faculty, Istanbul University, 34390 Istanbul, Turkey. [5]Cologne Center for Genomics, University of Cologne, 50674 Cologne, Germany. [6]RZPD Deutsches Ressourcenzentrum für Genomforschung GmbH, 14059 Berlin, Germany. [7]Department of Pharmacology, Yale University School of Medicine, New Haven, Connecticut 06520, USA. [8]Genetic Service, St. James's University Hospital, LS97TS Leeds, UK. [9]Ear, Nose and Throat Department, Istanbul Medical Faculty, Istanbul University, 34390 Istanbul, Turkey. [10]Department of Medical Genetics, Ghent University Hospital, 9000 Ghent, Belgium. [11]HNO-Abteilung, Klinikum Dortmund, 44137 Dortmund, Germany. [12]Otorhinolaryngology, Radboud University Nijmegen Medical Center, 6500 HB Nijmegen, The Netherlands. [13]Institute for Genetics, University of Cologne, 50674 Cologne, Germany. Correspondence should be addressed to B.W. (bwollnik@uni-koeln.de).

Received 19 December 2005; accepted 27 January 2006; published online 26 February 2006; doi:10.1038/ng1757

© 2006 Nature Publishing Group http://www.nature.com/naturegenetics

Table 1 Phenotypic characteristics of index cases in five LADD families and one sporadic LADD case

	LADD-Ist	LADD-Nij	LADD-Le	LADD-Be	LADD-Bo	LADD-Ala
	III-4	III-4	I-2	Sporadic	II-4	III-4
	FGFR2	*FGFR2*	*FGFR2*	*FGFR2*	*FGF10*	*FGFR3*
Lacrimal						
Alacrima	+	–	+	+	+	+
Aplastic or hypoplastic ducts, puncta	+	–	+	+	+	+
Aplastic or hypoplastic gland	+	–	–	U	–	–
Conjunctivitis	+	–	–	–	–	+
Aural						
Cup-shaped	+	+	+	+	+	+
Small sized	+	–	+	+	–	+
Hearing loss	+	+	+	+	U	+
Dental						
Peg-shaped	–	–	–	+	–	+
Microdontia	+	+	–	+	U	+
Hypodontia	–	–	+	+	U	+
Root anomalies	–	–	–	+	–	+
Dental caries	+	–	–	+	+	+
Digital						
Bifid thumb	–	–	+	–	+	–
Triphalangeal thumb	+	–	–	–	–	–
Digitalized thumb	–	–	–	–	–	–
Hypoplastic thumb	+	+	–	+	–	–
Missing thumb	–	–	–	–	–	–
Short radius and ulna	–	–	–	–	–	–
First toe abnormalities	–	–	–	–	–	+
Syndactyly in fingers/toes	–	–	+	–	–	–
Additional findings						
Salivary gland anomalies	–	–	+	+	U	–
Facial dysmorphism[a]	+	–	–	–	–	+

+, present. –, absent. U, unknown.

[a] Including, for example, high forehead, telecanthus, hypotelorism, downslanting palpebral fissures and prognathia.

serine and to the deletion of the neighboring aspartic acid (R649S ΔAsp650). We found further evidence for the involvement of *FGFR2* mutations in the pathogenesis of LADD syndrome by identifying a *de novo FGFR2* mutation, 1882G→A (A628T), in a sporadic LADD case from Belgium (**Fig. 1l** and **Supplementary Fig. 2**). Neither of the two healthy parents (paternity confirmed) carried this mutation. Dominant missense mutations in *FGFR2* have been implicated in various syndromic forms of craniosynostosis, including Pfeiffer (OMIM 101600), Crouzon (OMIM 123500), Apert (OMIM 101200), Jackson-Weiss (OMIM 123150), Antley-Bixler (OMIM 207410) and Beare-Stevenson (OMIM 123790) syndromes[8]. The vast majority of *FGFR2* mutations in these patients are located in the immunoglobulin-like IIIa and IIIc loops in the extracellular ligand-binding domain of FGFR2. Many of them recurred as *de novo* mutations exclusively on the paternal allele[8–10]. Individuals with Crouzon and Pfeiffer syndromes very rarely carried a mutation in the intracellular tyrosine kinase domains (TK1 or TK2)[11]. It is well established that *FGFR2* mutations found in craniosynostosis are gain-of-function mutations leading to an increased activation of FGFR2 (refs. 12,13). We describe for the first time *FGFR2* mutations associated with a different clinical entity that is associated neither with craniosynostosis nor with severe syndactyly. Notably, inspection of the three-dimensional structure of the tyrosine kinase domain shows that LADD mutations A648T and R649S ΔAsp650 are confined to the activation loop, and the A628T mutation is located in the catalytic loop of the kinase domain of FGFR2, respectively (**Fig. 1p** and **Supplementary Fig. 3**). This clustering suggests that these mutations might affect the tyrosine kinase activity of FGFR2 and generate developmental disturbances leading to LADD syndrome. The pathophysiological mechanism should differ significantly from that underlying the craniosynostosis syndromes caused by *FGFR2* mutations, which are believed to be most commonly mediated by constitutive tyrosine kinase activation leading to enhanced paracrine signaling in the embryonic mesoderm induced by either FGF10 or related FGFs[12].

We continued the molecular analysis in two newly ascertained LADD families, LADD-Bo from Germany (of Turkish origin) and LADD-Ala from Turkey, and excluded *FGFR2* in both families by haplotype analysis. Subsequently, we used a candidate gene approach for gene identification in these families and searched for mutations in other members of the *FGFR* gene family including *FGFR1*, *FGFR3*, *FGFR4* and two of the known ligands of *FGFR2*, *FGF10* and *FGF8* (**Supplementary Table 2**). We detected a 317G→T mutation in exon 1 of *FGF10* in the affected father and three affected children of the LADD-Bo family (**Fig. 1n** and **Supplementary Fig. 2**) that we did not observe in 200 matched control individuals. Recently, heterozygous loss-of-function mutations in *FGF10* caused by a nonsense mutation and gene deletion have been shown to cause lacrimal system and salivary gland aplasia in humans and in heterozygous $Fgf10^{+/-}$ knockout mice[7]. In contrast, the *FGF10* mutation we identified in LADD syndrome is a missense mutation affecting a conserved amino acid at position 106 (C106F). **Supplementary Figure 3** depicts the location of the mutation within the structure of FGF10. It is plausible that the effect of this missense mutation is different from the loss-of-function mutations described in isolated anomalies of the lacrimal system and salivary glands and that a dominant-negative effect of C106F might explain why this mutation affects additional organs in LADD syndrome.

Furthermore, we detected a mutation in *FGFR3* in the father and two children in the LADD-Ala family. The 1537G→A transition in exon 11 of *FGFR3* leads to the predicted amino acid substitution D513N in the conserved TK1 domain of FGFR3 (**Fig. 1o** and **Supplementary Fig. 2**). This mutation was not present in 200 control individuals. The finding that 1537G→A occurred *de novo* in the affected father and was subsequently transmitted to his affected offspring provides further evidence for the disease-causing nature of this mutation. Inspection of the structure of the tyrosine kinase domain has shown that the D513N mutation is located in a loop that connects the β3 sheet to the αC helix of the tyrosine kinase core (**Supplementary Fig. 3**). It is well established that activating *FGFR3* missense mutations cause short-limbed bone dysplasias and craniosynostosis syndromes, including achondroplasia (OMIM 100800), severe achondroplasia with developmental delay and acanthosis nigricans (SADDAN; OMIM 134934), hypochondroplasia (OMIM 146000), thanatophoric dysplasia I and II (OMIM 187600), Muenke

© 2006 Nature Publishing Group http://www.nature.com/naturegenetics

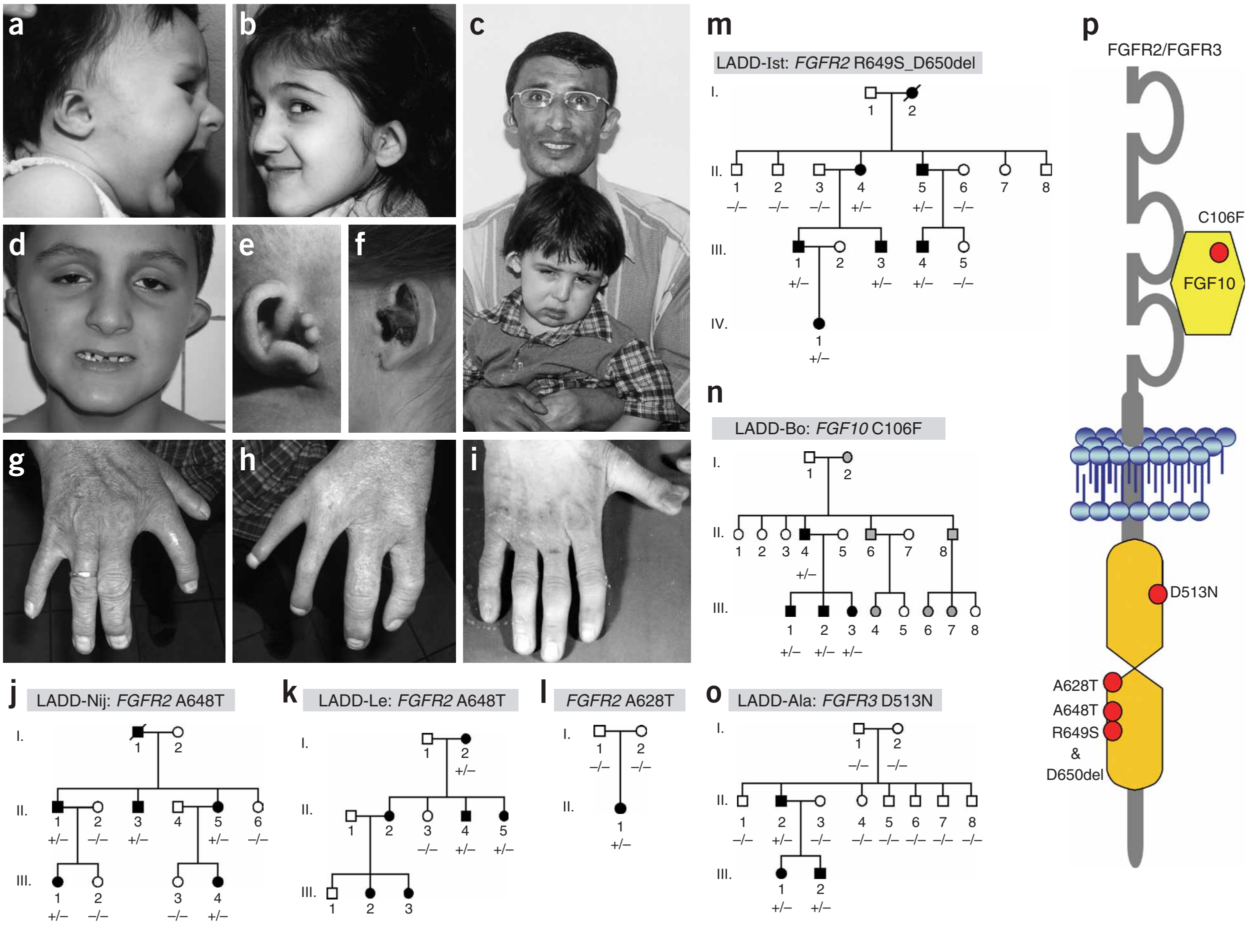

Figure 1 Clinical findings, pedigrees and mutations in FGFR2, FGFR3 and FGF10 in LADD syndrome. (**a**–**i**) Phenotypic characteristics of LADD patients from different families: (**a**,**d**) LADD-Ala, III-2; (**b**) LADD-Ala, III-1; (**c**) LADD-Ist, II-5 and III-4; (**e**) LADD-Be, II-1; (**f**) LADD-Nij, III-4; (**g**,**h**) LADD-Nij, II-3; (**i**) LADD-Bo, II-4. (**a**–**f**) Photographs show facial appearance and typical ear anomalies in LADD patients. Digital anomalies included hypoplastic (**g**), absent (**h**) and bifid (**i**) thumbs. (**j**–**o**) Pedigrees of LADD families. Family name, gene involved and identified mutation are given in the gray box on top of each pedigree. Symbols: +, mutation present; –, mutation absent. Filled black symbols indicate affected individuals; filled gray symbols in the LADD-Bo family represent individuals who were probably affected but for whom a detailed clinical description is lacking. (**p**) Schematic model of FGFR2 and FGFR3. The locations of different mutations are marked by red dots on the receptor or ligand (FGF10). The intracellular tyrosine kinase domains of FGFR2 and FGFR3 are shown in orange.

syndrome (OMIM 602849) and Crouzon syndrome with acanthosis nigricans (OMIM 134934)[13]. Similar to the spectrum of mutations in *FGFR2*, the *FGFR3* mutations are mainly confined to the extracellular immunoglobulin-like IIIa and IIIc domains, and few mutations have been identified in the tyrosine kinase domains[8,12,14]. In our LADD-Ala family, there is neither short-limbed bone dysplasia, nor is there craniosynostosis or severe syndactyly. As with the mutations in *FGFR2*, it is likely that the effect of this *FGFR3* mutation on the physiological role of FGF signaling during development substantially differs from the activating nature of mutations identified in short-limbed bone dysplasias and syndromic craniosynostosis. An *FGFR3* R621H mutation was identified previously (R. Toydemir *et al.*, *Am. J. Hum. Genet.* **73** (Suppl.), 171, 2003) in a family with an autosomal dominant inherited syndrome characterized by sensorineural hearing loss, camptodactyly, tall stature, microcephaly and developmental delay. Because of the phenotypic overlap with Fgfr3-deficient mice, a putative dominant-negative effect of R621H was hypothesized, although no experimental support was provided. We find a clear phenotypic difference between the family reported in that study and our LADD-Ala family, with only bilateral hearing loss as an overlapping feature, suggesting different functional effects of the two mutations.

We conclude that LADD syndrome is a genetically heterogeneous disorder caused by heterozygous missense mutations in *FGFR2*, *FGFR3* or *FGF10*. Notably, all FGFR mutations so far identified in LADD are located in the tyrosine kinase domains of FGFR2 or FGFR3, in loops that have a regulatory function in the control of tyrosine kinase activity. Although experimental support is needed, a reduced functional activity of FGFR2 and FGFR3 seems to be an attractive, plausible mechanism underlying the molecular basis for LADD.

Note: Supplementary information is available on the Nature Genetics website.

ACKNOWLEDGMENTS

We are thankful to all family members that participated in this study, M. Langen for excellent technical assistance and I. Feenstra and D. Koolen for sample collection and clinical analysis. This work was supported in part by the Turkish Academy of Sciences, in the framework of the Young Scientist Award Program (BW/TUBA-GEBIP/2002-1-20), European Commission FP6 Integrated

Project EUROHEAR, LSHG-CT-20054-512063, US National Institutes of Health grants RO1-AR051448 and RO1-AR051886 to J.S., and the German Federal Ministry of Science and Education through the National Genome Research Network (G.N., C.B. and P.N.).

COMPETING INTERESTS STATEMENT

The authors declare that they have no competing financial interests.

Published online at http://www.nature.com/naturegenetics
Reprints and permissions information is available online at http://npg.nature.com/reprintsandpermissions/

© 2006 Nature Publishing Group http://www.nature.com/naturegenetics

1. Levy, W.J. *Am. J. Ophthalmol.* **63**, 978–982 (1963).
2. Hollister, D.W., Klein, S.H., De Jager, H.J., Lachmann, R.S. & Rimoin, D.L. *J. Pediatr.* **83**, 438–444 (1973).
3. Bamforth, J.S. & Kaurath, P. *Am. J. Med. Genet.* **43**, 932–937 (1992).
4. Coumoul, X., Shukla, V., Li., C., Wang, R.H. & Deng, C.X. *Nucleic Acids Res.* **33**, e102 (2005).
5. Gorivodsky, M. & Lonai, P. *Development* **130**, 5471–5479 (2003).
6. Steinberg, Z. *et al. Development* **132**, 1223–1234 (2005).
7. Entesarian, M. *et al. Nat. Genet.* **37**, 125–127 (2005).
8. Wilkie, A.O. *Cytokine Growth Factor Rev.* **16**, 187–203 (2005).
9. Moloney, D.M. *et al. Nat. Genet.* **13**, 48–53 (1996).
10. Glaser, R.L. *et al. Am. J. Hum. Genet.* **66**, 768–777 (2000).
11. Kan, S.H. *et al. Am. J. Hum. Genet.* **70**, 472–486 (2002).
12. Wilkie, A.O., Patey, S.J., Kan, S.H., van den Ouweland, A.M. & Hamel, B.C. *Am. J. Med. Genet.* **112**, 266–278 (2002).
13. Eswarakumar, V.P., Lax, I. & Schlessinger, J. *Cytokine Growth Factor Rev.* **16**, 139–149 (2005).
14. Legeai-Mallet, L., Benoist-Lasselin, C., Munnich, A. & Bonaventure, J. *Bone* **34**, 26–36 (2004).

Molecular and Cellular Biology, Oct. 2007, p. 6903–6912 Vol. 27, No. 19
0270-7306/07/$08.00+0 doi:10.1128/MCB.00544-07
Copyright © 2007, American Society for Microbiology. All Rights Reserved.

Lacrimo-Auriculo-Dento-Digital Syndrome Is Caused by Reduced Activity of the Fibroblast Growth Factor 10 (FGF10)-FGF Receptor 2 Signaling Pathway[▽]

Imad Shams,[1] Edyta Rohmann,[2,3] Veraragavan P. Eswarakumar,[1] Erin D. Lew,[1] Satoru Yuzawa,[1]
Bernd Wollnik,[2,3] Joseph Schlessinger,[1] and Irit Lax[1]*

*Department of Pharmacology, Yale University School of Medicine, 333 Cedar Street, New Haven, Connecticut 06520,[1] and Center for Molecular Medicine Cologne[2] and Institute of Human Genetics,[3]
University of Cologne, Cologne, Germany*

Received 28 March 2007/Returned for modification 14 May 2007/Accepted 24 July 2007

Lacrimo-auriculo-dento-digital (LADD) syndrome is characterized by abnormalities in lacrimal and salivary glands, in teeth, and in the distal limbs. Genetic studies have implicated heterozygous mutations in fibroblast growth factor 10 (*FGF10*) and in FGF receptor 2 (*FGFR2*) in LADD syndrome. However, it is not clear whether LADD syndrome mutations (LADD mutations) are gain- or loss-of-function mutations. In order to reveal the molecular mechanism underlying LADD syndrome, we have compared the biological properties of FGF10 LADD and FGFR2 LADD mutants to the activities of their normal counterparts. These experiments show that the biological activities of three different FGF10 LADD mutants are severely impaired by different mechanisms. Moreover, haploinsufficiency caused by defective FGF10 mutants leads to LADD syndrome. We also demonstrate that the tyrosine kinase activities of FGFR2 LADD mutants expressed in transfected cells are strongly compromised. Since tyrosine kinase activity is stimulated by ligand-induced receptor dimerization, FGFR2 LADD mutants may also exert a dominant inhibitory effect on signaling via wild-type FGFR2 expressed in the same cell. These experiments underscore the importance of signal strength in mediating biological responses and that relatively small changes in receptor signaling may influence the outcome of developmental processes in cells or organs that do not possess redundant signaling pathway.

Fibroblast growth factors (FGFs) mediate their biological responses by binding to four receptor tyrosine kinases (RTKs) designated FGF receptor 1 (FGFR1) to FGF4 (25). The binding of FGF to FGFR in the presence of heparin sulfate glycosaminoglycan induces receptor dimerization and the activation of the protein tyrosine kinase domain (30). Tyrosine autophosphorylation and the recruitment of a complement of downstream signaling molecules result in the stimulation of various signaling cascades that play critical roles in mediating the pleiotropic responses of FGFs during development and in the adult organism (10).

Like all RTKs, FGFRs are composed of an extracellular ligand binding domain, a transmembrane region, and a cytoplasmic region containing a catalytic protein tyrosine kinase core and additional regulatory sequences. The extracellular domain is composed of three immunoglobulin-like domains (designated D1, D2, and D3), a stretch of negatively charged amino acids in the linker connecting D1 and D2 termed the acidic box, and a conserved positively charged region in D2 that serves as the binding site for heparin sulfate or heparin (13, 17, 30, 31). FGFR1, -2, and -3 transcripts are subject to alternative RNA splicing in which exon 7 of the FGFR gene codes for a common N-terminal half of D3 (referred to as IIIa) and exons 8 and 9 code for the C-terminal half of D3 to generate the IIIb and IIIc isoforms, respectively (21, 39). The IIIb isoforms are expressed exclusively in epithelial cells, while the IIIc isoforms are expressed only in mesenchymal cells (1, 9, 26, 38). Moreover, the IIIb and IIIc isoforms of FGFR1, -2, and -3 bind to different complements of FGFs that are expressed exclusively in mesenchymal or epithelial cells, respectively. For example, the FGFR2-IIIb isoform (also designated FGFR2b) binds FGF7, FGF10, and FGF22, while FGFR2-IIIc (also designated FGFR2c) binds FGF2, FGF8, FGF17, and FGF18 (14). FGF1, on the other hand, functions as a universal FGFR ligand, as it binds to all "b" and "c" FGFR isoforms. Strict lineage-specific expression of the two alternatively spliced isoforms of FGFR2 is essential for normal embryonic development.

Targeted disruption of the FGFR1 gene has shown that the FGFR1c isoform plays an essential role during early embryogenesis. The biological roles of FGFR2b, FGFR2c, and their specific ligands have also been explored by targeted disruption of isoform-specific genes fragments in the mouse by use of homologous recombination. Targeted disruption of the FGFR2b results in lethality at birth due to lung agenesis (7). Interestingly, the phenotype of the FGF10 null mice is similar to the phenotype of FGFR2b null mice (32). Characterizations of the phenotypes of mice deficient in FGF10 or FGFR2b have shown that FGF10 and FGFR2b play an essential role in the control of branching morphogenesis during the development of lung, pancreas, mammary gland, thyroid, lacrimal gland, and salivary gland. Moreover, aplasia of the lacrimal gland and hypoplasia of the salivary gland were observed for adult heterozygous FGF10 mice, indicating that the normal development of both glands depends on a precisely balanced dose of signaling stimulated by FGF10 (5, 17). Finally, human genetic

---

* Corresponding author. Mailing address: Department of Pharmacology, Yale University School of Medicine, 333 Cedar Street, SHM B-295, New Haven, CT 06520. Phone: (203) 785-7395. Fax: (203) 785-3879. E-mail: Irit.lax@yale.edu.

[▽] Published ahead of print on 6 August 2007.

Downloaded from mcb.asm.org at Deutsche Zentralbibliothek on September 25, 2007

studies and selective targeting of the FGFR3b and FGFR3c isoforms in mice have implicated the FGFR3c isoform in a variety of skeletal disorders (6, 8).

Recent studies have shown that patients with aplasia (or hypoplasia) of the lacrimal and salivary glands (ALSG) bear heterozygous mutations in the *FGF10* gene (4, 5). Mutations in *FGF10* were also detected for patients with lacrimo-auriculo-dento-digital (LADD) syndrome, which shows overlapping features with ALSG but in addition is characterized by facial dysmorphisms, outer and inner ear anomalies and hearing loss, teeth anomalies, distal limb malformations, and, more infrequently, impairment of kidney and lung development (2, 4, 12, 20, 22, 28). Genetic analysis has also revealed heterozygous mutations in *FGFR2* and *FGFR3* in LADD syndrome patients (28), implicating aberrant signaling by FGF10, FGFR2, or FGFR3 in this heterogeneous disorder.

In this report, we describe the biological properties of FGF10 and FGFR2b mutants implicated in LADD syndrome. We show that LADD syndrome mutations (LADD mutations) cause inactivation of FGF10 and that the tyrosine kinase activity of FGFR2b LADD mutants expressed in cultured cells is severely compromised. While the FGF10 mutation causes haploinsufficiency, the FGFR2b mutants may exert a dominant interfering effect on signaling via normal FGFR2b, causing LADD syndrome.

MATERIALS AND METHODS

Growth factors, antibodies, plasmids, and recombinant proteins. FGF1 and FGF2 were prepared and used as a stock solution at a concentration of 100 μg/ml with 5 mg/ml heparin for stimulation of cultured cells (33). Heparin agarose beads and Lipofectamine 2000 were purchased from Sigma and Invitrogen, respectively. Anti-FGFR2, anti-Grb2, anti-FRS2, and anti-Shc antibodies were previously described (6, 19). Antiphosphotyrosine (anti-p-Tyr) antibodies were purchased from Upstate Biotechnology. Anti-phospho-mitogen-activated protein kinase (anti-pMAPK) and anti-MAPK were purchased from Cell Signaling Technology. Horseradish peroxidase-conjugated protein A and horseradish peroxidase-conjugated goat anti-mouse antibodies were purchased from Kirkegaard & Perry Laboratories and Santa Cruz Biotechnology, respectively. Geneticin was purchased from GIBCO. Human FGF10 and FGF10 LADD mutants were expressed in *Escherichia coli* by use of the bacterial expression vector pET11c (Novagen) (3). Both Mirb and retroviral pBABE/*neo* expression vectors were used for human FGFR2 expression as previously described (11, 24). Point mutations in FGF10 and FGFR2 were generated using a QuikChange site-directed mutagenesis kit from Stratagene. pcDNA-3 expression vector (Invitrogen) was used for FGFR2b transient expression in 293 cells.

Purification of FGF10 and FGF10 LADD mutants. BL21(DE3) pLysS *E. coli* cells were transformed with expression vector for FGF10 or FGF10 LADD mutants and grown overnight in LB medium at 25°C. The bacterial cell pellet was resuspended in lysis buffer (20 mM HEPES, pH 7.4, 150 mM NaCl, 5% glycerol, 1 mM phenylmethylsulfonyl fluoride, and 2 mM EDTA), lysed by use of a French pressure cell (Thermo Electron Corp.), and centrifuged for 1 h at 32,000 × *g*. The cell supernatant was incubated with heparin-agarose beads for 1.5 h at 4°C, and FGF-bound beads were washed three times with lysis buffer. Washed beads were applied to a column and FGF10 or FGF10 LADD mutants were eluted using 20 mM HEPES buffer, pH 7.4, containing 1 M NaCl. Eluted proteins were further purified by fast-performance liquid chromatography (Amersham Biosciences) using a Mono S column (GE Healthcare). Protein purity was determined using sodium dodecyl sulfate-polyacrylamide gel electrophoresis (SDS-PAGE) analysis.

Cell lines. L6 cells devoid of endogenous FGFRs were cultured in Dulbecco's modified Eagle medium (DMEM) containing 10% fetal bovine serum (FBS), 2 mM L-glutamine with 100 μg/ml penicillin and 100 μg/ml streptomycin. L6 cells were transfected with expression vectors for wild-type (WT) FGFR2b and FGFR2b mutants that were cloned into the Mirb or pBABE/*neo* expression vectors. Cells were transfected with Lipofectamine 2000 and selected in growth medium containing 1 mg/ml geneticin. Individual clones as well as cell pools were screened for FGFR2 expression using anti-FGFR2 antibodies. Prior to growth factor stimulation, cells were starved overnight in medium containing 0.1% FBS. 293 cells were transfected with Lipofectamine 2000 and incubated in transfection medium for 6 h; this was followed by changing the medium to DMEM containing 10% FBS. Cells were harvested and lysed 18 h later.

Radiolabeling of FGF10 and ligand displacement assay. Human FGF10 (10 μg) was labeled with 0.5 mCi of ^{125}I by use of Iodo-Gen iodination tubes (Pierce) following the manufacturer's instructions. For the displacement binding assay, L6 cells expressing FGFR2b were grown in 24-well plates in DMEM containing 10% FBS. Confluent cells were washed with DMEM containing 0.5% bovine serum albumin (BSA) and then incubated for 1 h at room temperature with 2 ng of ^{125}I-labeled FGF10 in the presence of increasing concentrations of FGF1, FGF10, or the FGF10 LADD mutants. Cells were then washed three times with cold DMEM-BSA and lysed in 0.5 ml of 0.5 M NaOH for 30 min at room temperature, and 100 μl of the cell lysate was applied to 10 ml of Opti-Fluor scintillation cocktail (Perkin Elmer) in order to measure cell-associated radioactivity (using an LS6500 scintillation counter from Beckman Coulter).

Limited proteolysis. Limited proteolysis analysis of FGF10 or FGF10 LADD mutants was carried out using factor Xa (12×10^{-5} U/μl), endoproteinase Glu-C (V8 protease) (0.04 μg/μl), and endoproteinase Lys-C (12×10^{-4} U/μl). All enzymes were purchased from Roche and used in a series of 10-fold dilutions. FGF10 or FGF10 LADD mutants were incubated with the enzymes for 2 h at 25°C, and the proteolytic products were visualized by SDS-PAGE followed by Coomassie brilliant blue staining.

Intrinsic fluorescence spectrum measurements. FGF10 or the FGF10 LADD mutants (30 μg/ml in 20 mM HEPES, pH 7.4, 400 mM NaCl) were incubated at 37°C for various periods and then cooled to room temperature. To measure fluorescence emission, samples were excited at a wavelength of 285 nm, and emission was scanned at λ of between 300 and 380 nm by use of a fluorometer (Photon Technology International).

RESULTS

Several mutations in *FGF10* were identified in LADD patients, including a missense mutation in which cysteine 106 is substituted by a phenylalanine (p.C106F), a missense mutation in which isoleucine 156 is substituted by an arginine (p.I156R), and a nonsense mutation (p.K137X) causing a deletion of 71 carboxy-terminal residues of FGF10 (22, 28). To study the biological activities of the FGF10 LADD mutants, WT or mutant FGF10 proteins were expressed in *E. coli*. While the expression of WT FGF10 and the I156R mutant was detected in cells that were induced by isopropyl-β-D-thiogalactopyranoside (IPTG) at 37°C, expression of the C106F mutant was detected only in cells induced at 25°C, suggesting temperature sensitivity of the C106F LADD mutant (data not shown). Expression of the K137X mutant could not be detected for any experimental condition that was tried. We surmised that because of the large truncation, the K137X FGF10 mutant was probably misfolded, resulting in rapid degradation. For large-scale production of WT FGF10 and the two FGF10 LADD mutants, cells were induced at 25°C overnight. WT or mutant FGF10 was purified on a heparin affinity matrix followed by cation-exchange chromatography using a Mono S column. WT FGF10 and the LADD mutants were eluted from either heparin or the Mono S columns (Fig. 1) at similar salt concentrations, indicating that the surface charge of the FGF10 LADD mutants was not substantially altered.

Impaired activity of the I156R mutant is caused by deficiency in receptor binding. We first compared the capacities of WT FGF10 and the I156R LADD mutant to stimulate L6 cells expressing FGFR2b. Lysates of unstimulated or ligand-stimulated cells were subjected to immunoprecipitation with anti-FGFR2 antibodies followed by SDS-PAGE and immunoblotting with anti-p-Tyr antibodies. The experiment presented in

Downloaded from mcb.asm.org at Deutsche Zentralbibliothek on September 25, 2007

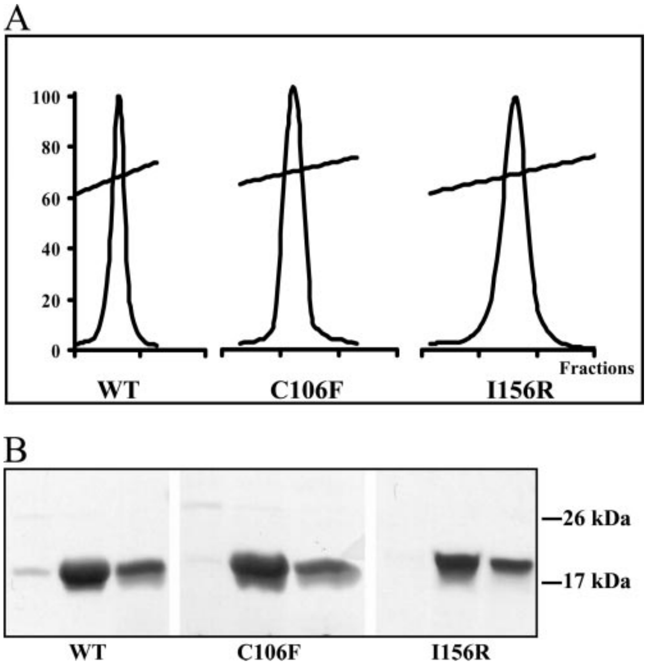

FIG. 1. Profiles of purification of WT FGF10 and LADD FGF10 mutants. (A) Mono S column elution profiles of FGF10 (WT) and the two FGF10 C106F and I156R LADD mutants. (B) Coomassie brilliant blue staining of FGF10 and the LADD mutants after SDS-PAGE analysis of two fractions of purified proteins.

Fig. 2A shows that unlike WT FGF10, which stimulated L6 cells, the I156R mutant was unable to stimulate the tyrosine autophosphorylation of FGFR2b or the tyrosine phosphorylation of the downstream signaling molecules FRS2 and Shc. Furthermore, MAPK stimulation was not detected in L6 cells stimulated with the I156R LADD mutant. To understand why the I156R FGF10 mutant was unable to induce receptor autophosphorylation, we next examined its binding affinity towards FGFR2b by using a displacement assay in which cell-bound ^{125}I-labeled WT FGF10 was displaced by increasing concentrations of native FGF10 (as a control) or the I156R FGF10 LADD mutant. The experiment presented in Fig. 2C shows that the 50% inhibitory concentration of ^{125}I-labeled FGF10 bound to FGFR2b of the I156R LADD mutant is approximately ninefold higher than the 50% inhibitory concentration of FGF10 towards FGFR2b expressed on the cell surfaces of L6 cells. This experiment demonstrates that the impaired biological activity of the I156R mutant is caused by compromised binding affinity towards FGFR2b.

Reduced stability of the C106F LADD mutant is responsible for its impaired biological activity. During the course of the expression and purification of FGF10 and the FGF10 LADD mutants, the production of the C106F LADD mutant after the *E. coli* cells were induced at 37°C was very low compared to the production of WT FGF10 and of the I156R LADD mutant under the same conditions. The displacement assay presented in Fig. 2C showed that the receptor binding profile of the purified C106F LADD mutant is similar to the binding characteristics of FGF10 towards FGFR2b expressed on the cell surfaces of L6 cells. Moreover, both WT FGF10 and the C106F LADD mutant showed similar levels of stimulation of tyrosine autophosphorylation of FGFR2b and similar MAPK responses upon cell stimulation when a broad range of FGF10 or C106F LADD mutant concentrations were applied (Fig. 2A and B). We next examined whether the C106F mutation affected FGF10 stability. Protein stability was first tested by comparing the susceptibilities of FGF10 and the C106F LADD mutant towards limited proteolysis by the enzymes V8 protease, factor Xa, and Lys-C. The experiment presented in Fig. 3A shows that unlike WT FGF10, the C106F LADD mutant undergoes rapid degradation, resulting in the formation of low-molecular-weight degradation products when treated with these enzymes.

The stabilities of WT FGF10 and the C106F and I156R LADD mutants at 37°C were further tested by comparing the intrinsic fluorescence spectra of FGF10 and the FGF10 LADD mutant as a function of time at 37°C. The experiments presented in Fig. 3B show that the fluorescence spectra of FGF10 and the I156R LADD mutant were stable over a period of 3 h of incubation at 37°C. By contrast, the fluorescence spectrum of the C106F LADD mutant changed within 2 min of incubation at 37°C. Moreover, a strong increase in the fluorescence intensity emitted from the C106F LADD mutant was observed after 20 min of incubation at 37°C. It is well established that fluorescence spectra of tryptophan and tyrosine residues of proteins can be used as a diagnostic tool to reveal local structural alterations that take place in host proteins (34). Since FGF10 and the FGF10 LADD mutants were excited at a wavelength of 285 nm, changes in fluorescence spectra will reflect local structural changes that take place in the vicinity of tryptophan residues of the proteins. The changes in the fluorescence spectrum of the C106F LADD mutant at 37°C may reflect the reduced stability of FGF10 mutant at a physiological temperature.

Since our results show that incubation of the C106F LADD mutant at 37°C affected the structural integrity of the mutant protein, we next examined the impact of these changes on cellular responses induced by the C106F LADD mutant at 37°C. Both FGF10 and the C106F LADD mutant were preincubated for various periods at 37°C in the absence or presence of heparin, and each sample was then used to stimulate, for an additional 5 minutes, L6 cells stably expressing FGFR2b. The experiment presented in Fig. 3C shows that the capacity of C106F LADD mutant to induce the tyrosine autophosphorylation of the FGFR2b and MAPK response was strongly compromised and that within 30 min of incubation at 37°C the activity of the C106F LADD mutant nearly vanished (Fig. 3C). Interestingly, in the presence of exogenous heparin the stability of C106F was protected. It is possible, however, that the majority of C106F LADD mutant molecules were not secreted from the cells after biosynthesis, as most of the unstable mutant molecules were degraded shortly after production.

Potential mechanism for impairment FGF10 LADD mutant activity. In order to gain insights into the mechanism underlying the diminished receptor binding activity of the I156R mutant, we examined the potential impact of the substitution of isoleucine 156 by an arginine residue on the receptor binding region of FGF10 in the X-ray crystal structure of FGF10 (40). Figure 4 shows that isoleucine 156 is located in the β8 strand of FGF10, in a region that forms contacts with the βF-βG loop of FGFR2b (23, 40). It is expected that the substitution of isoleucine 156 with the larger arginine residue will cause a

Downloaded from mcb.asm.org at Deutsche Zentralbibliothek on September 25, 2007

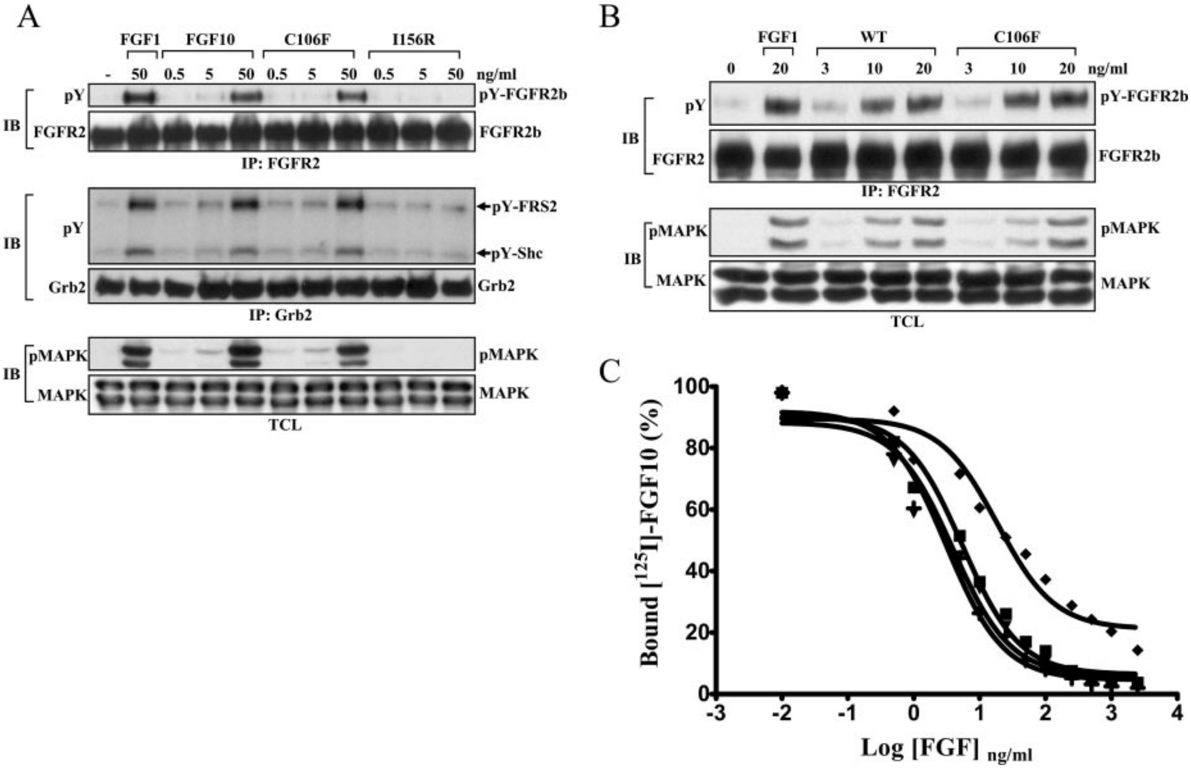

FIG. 2. Functional activities of LADD FGF10 mutants. (A) FGFR activation, substrate phosphorylation, and MAPK response following stimulation with FGF1, FGF10, or C106F and I156R LADD mutants. L6 cells stably expressing FGFR2b were stimulated with buffer alone or with FGF1, FGF10, or the C106F and I156R LADD mutants for 5 minutes at 37°C at different ligand concentrations as indicated. Lysates from unstimulated or ligand-stimulated cells were subjected to immunoprecipitation (IP) with anti-FGFR2 antibodies (top) or anti-Grb2 antibodies (middle). The bottom shows total cell lysates (TCL). The samples were subsequently subjected to immunoblotting (IB) with anti-FGFR2 or anti-p-Tyr antibodies (top), anti-Grb2 or anti-p-Tyr antibodies (middle), or anti-MAPK or anti-activated pMAPK antibodies (bottom). (B) Stimulation of FGFR2 activation and MAPK response by FGF1, FGF10, and the C106F mutant as a function of ligand concentration. L6 cells expressing FGFR2b were stimulated with buffer alone or with FGF1, FGF10, or the C106F LADD mutant at different ligand concentrations as indicated for 5 min at 37°C. Lysates from unstimulated or ligand-stimulated cells were subjected to immunoprecipitation with anti-FGFR2 antibodies (top) or presented as total cell lysates (bottom) followed by immunoblotting with anti-FGFR2 or anti-p-Tyr antibodies (top) and immunoblotting with anti-MAPK or anti-activated pMAPK antibodies (bottom). (C) Displacement assay of cell-bound ^{125}I-labeled FGF10 with FGF1, FGF10, or the FGF10 C106F and I156R LADD mutants. L6 cells expressing FGFR2b were incubated with ^{125}I-labeled FGF10 in the presence of increasing concentrations of FGF1, FGF10, or the two FGF10 C106F and I156R LADD mutants for 1 hour at room temperature. The cells were washed three times with DMEM containing 0.1% BSA, pH 7.5, and lysed in 0.1 M NaOH for 30 min at room temperature. Samples were collected and their radioactive contents were determined using a scintillation counter. Samples of displacement curves were done in duplicate for FGF1 (■), FGF10 (✚), C106F (▼), and I156R (◆).

steric clash with critical amino acids in the ligand binding pocket of FGFR2b (Fig. 4B). Moreover, the I156R LADD mutation may also destroy the highly conserved hydrogen bonds between Gly160 and Asn162 of FGF10 with Arg251 in the D2-D3 linker region of FGFR2, due to repulsion between Arg156 of the FGF10 LADD mutant and Arg251 of FGFR2b. The I156R mutation may also destroy the electrostatic interaction between Arg78 of FGFR10 with Arg251 and Asp283 of D3 of FGFR2b. Moreover, the Arg156 mutation in FGF10 may cause a steric clash and/or an electrostatic repulsion with Arg251 of FGFR2b that will disrupt three critical electrostatic interactions essential for FGF10 binding to FGFR2b.

We have also examined the potential impact of the substitution of cysteine 106 with a phenylalanine residue on the structure of FGF10 and its interactions with FGFR2b. Cysteine 106 is located in the β3-β4 loop of FGF10, a region that does not play a role in FGFR2b recognition (40). Indeed, the FGFR2b binding activity of the C106F LADD mutant remained unchanged. However, the replacement of cysteine 106 with a large hydrophobic residue such as phenylalanine may create a bulky region, which will become exposed, resulting in reduced stability and susceptibility to proteolytic digestion. Human mature FGF10 (amino acids 38 to 208) contains an additional cysteine residue at position 150. Inspection of the FGF10 structure (40) shows that Cys106 is located on the surface of FGF10, while Cys150 is buried in FGF10, and that the distance between Cys106 and Cys150 is 22 Å. The two cysteines are unlikely to form an intramolecular disulfide bond.

Reduced tyrosine kinase activity of FGFR2b LADD mutants. The mutations in FGFR2 that were identified for a variety of skeletal dysplasias have been mapped to the extracellular ligand binding domain in the vast majority of cases and less frequently in the tyrosine kinase domain, including the catalytic core and its regulatory activation loop. Biochemical characterization of mutant receptors has shown that FGFR2 mutations that are responsible for craniosynostosis and other

Downloaded from mcb.asm.org at Deutsche Zentralbibliothek on September 25, 2007

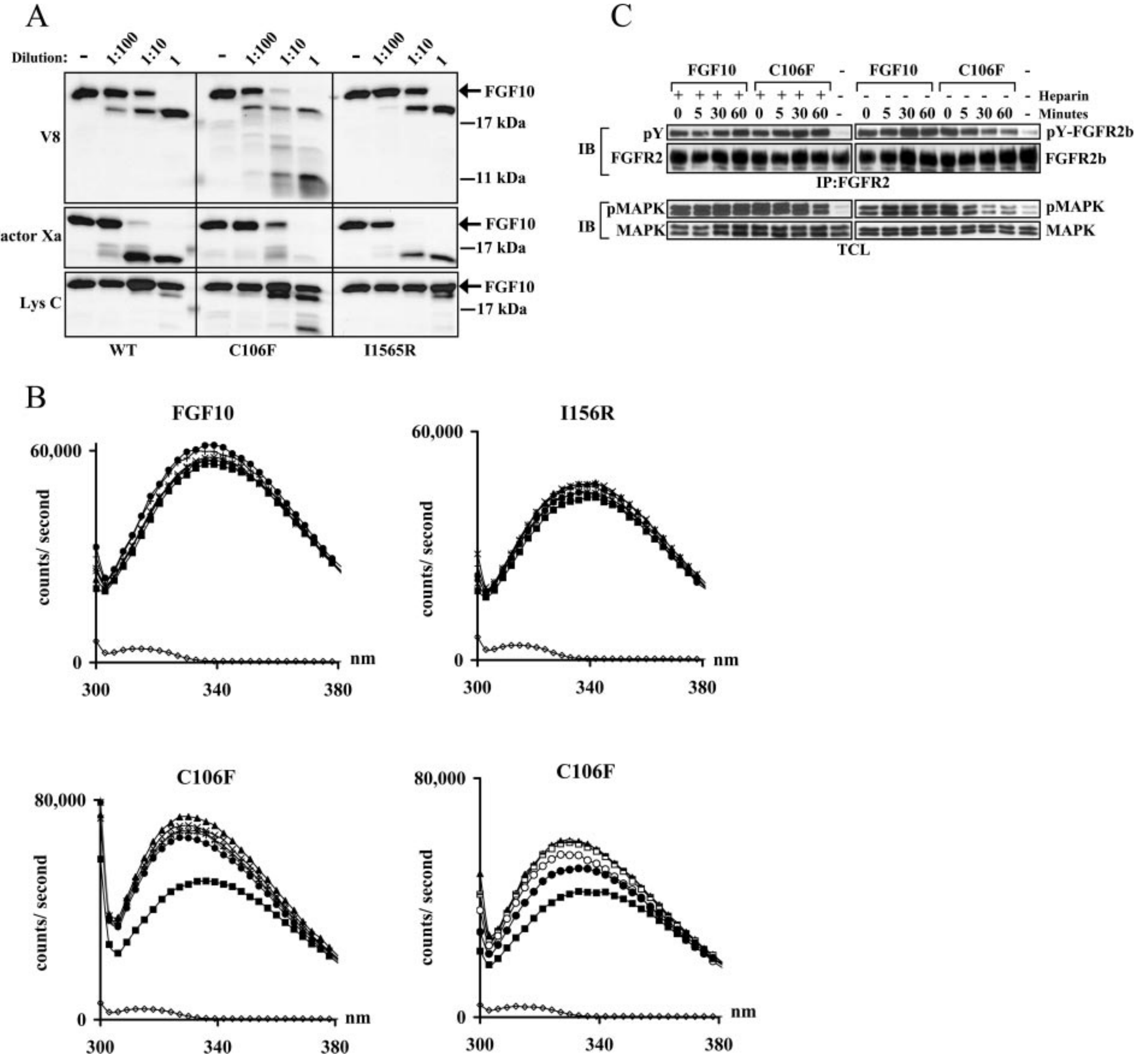

FIG. 3. Decreased stability of C106F FGF10 LADD mutants. (A) Enhanced susceptibility to proteolytic degradation of the C106F LADD mutant. Purified FGF10 or the two FGF10 LADD mutants, the C106F and I156R mutants (marked by arrows), were incubated with different amounts of V8 protease, factor Xa, or Lys-C for 2 hours at 25°C. The proteolytically digested samples were analyzed by SDS-PAGE and stained with Coomassie brilliant blue. (B) Fluorescence spectra of the C106F LADD mutant reveals structural changes after incubations at 37°C. Intrinsic fluorescence spectra of purified FGF10 or the two FGF10 LADD mutants incubated for increasing periods of time at 37°C. Shown are fluorescence spectra excited at a wavelength of 285 nm of buffer alone (◇) or of WT FGF10 and the I156R and C106F mutants after 0 (■)-, 20 (▲)-, 40 (×)-, 60 (★)-, 120 (●)-, or 180 (+)-min incubations at 37°C. The bottom right shows additional fluorescence spectra of the C106F mutant taken after 0 (■)-, 2 (●)-, 5 (○)-, 10 (×)-, 15 (□)-, and 20 (▲)-min incubations at 37°C. (C) Reduced activity of the C106F LADD mutant after incubations at physiological temperature. L6 cells expressing FGFR2b were stimulated for 5 min at 37°C with purified FGF10 or C106F mutant in the absence (left) or presence (right) of heparin that was preincubated for increasing periods at 37°C. Lysates from unstimulated and ligand-stimulated cells were subjected to immunoprecipitation (IP) with anti-FGFR2 antibodies (top). Shown at the bottom are total cell lysates (TCL). After SDS-PAGE, the samples were subjected to immunoblotting (IB) with anti-FGFR2 or anti-p-Tyr antibodies (top) or anti-MAPK or anti-activated pMAPK antibodies (bottom).

severe bone disorders are gain-of-function mutations that enhance the tyrosine kinase activity of the receptor molecules. The mutations in FGFR2 that have been implicated in LADD syndrome were mapped to the activation loop or the catalytic loop of FGFR2. However, it is not clear whether the LADD mutations in FGFR2 are gain- or loss-of-function mutations.

In order to reveal the molecular mechanism of the FGFR2 LADD mutations, expression vectors that direct the synthesis of FGFR2b carrying the LADD mutations were prepared and tested for their biological activity following transient expression in 293 cells or by stable expression in L6 cells. The tyrosine kinase activities of FGFR2b carrying LADD mutations in the activation loop (A648T and R649S) or in the catalytic loop (A628T) were compared to the tyrosine kinase activities of WT FGFR2b, of a kinase-defective (KD) FGFR2b mutant (K508A), and of a Pfeiffer syndrome gain-of-function FGFR2b

Downloaded from mcb.asm.org at Deutsche Zentralbibliothek on September 25, 2007

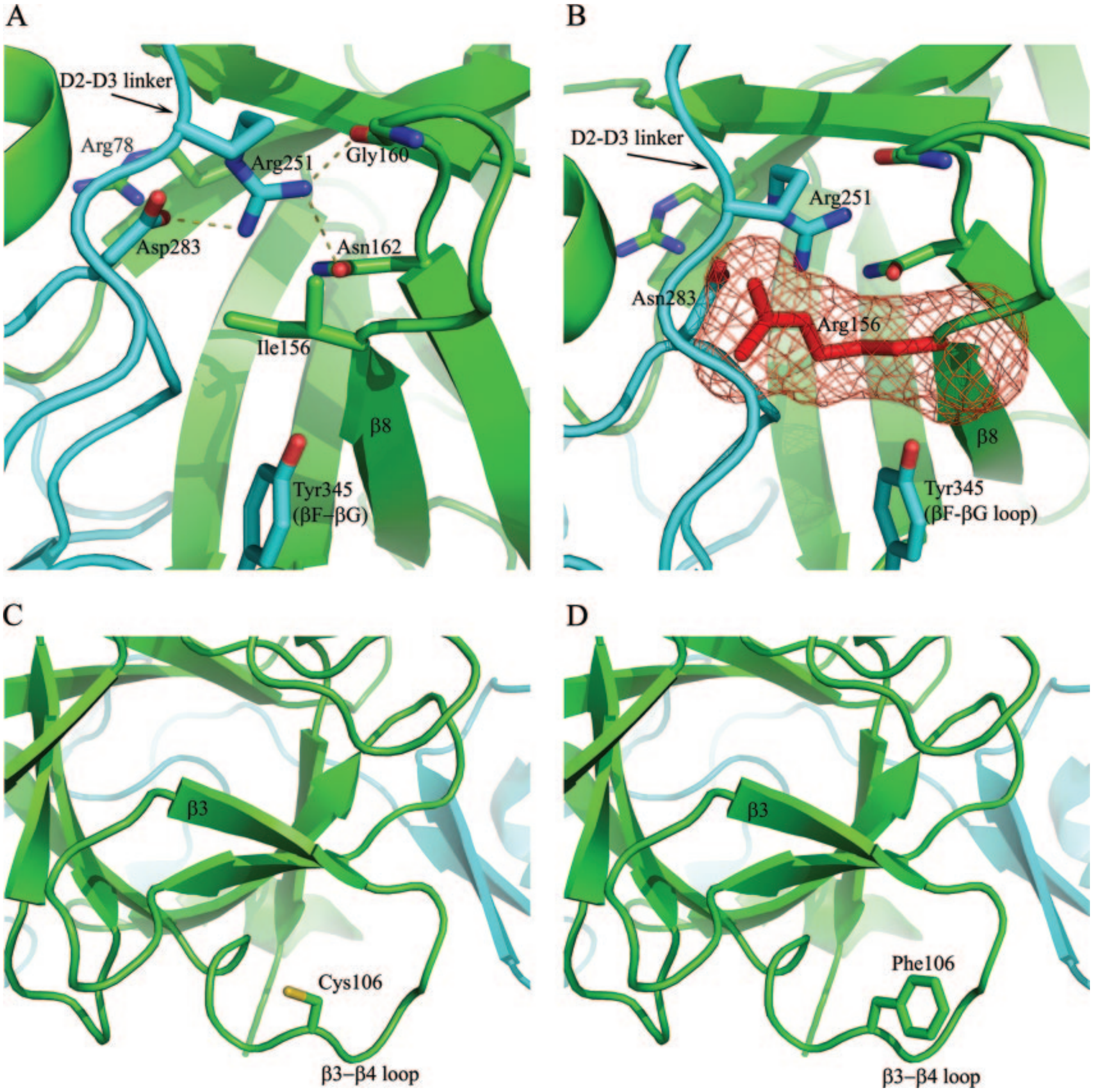

FIG. 4. Models of FGF10 LADD mutation based on the X-ray crystal structure of FGF10. (A) Ribbon diagram of part of the interface between FGF10 and the extracellular ligand binding domain of FGFR2b in the region that is mutated in the FGF10 I156R LADD mutant. Asn162 and Gly160 of FGF10 form hydrogen bonds with Arg251 of FGFR2b. Arg251 is also involved in mediating intramolecular interactions with Arg251 and Asp285 that contribute towards the formation of the D3 cleft of FGFR2b. FGF10 is colored in green and FGFR2b is colored in cyan. (B) The same view as in panel A; in this view, isoleucine 156 is replaced by an arginine residue in the FGF10 LADD mutant. It is expected that an arginine residue (shown in red mesh) in place of an isoleucine residue will interrupt FGF10 binding by steric clash and by introducing electrostatic repulsion between Arg251 of FGFR2b with Arg156 of the FGF10 LADD mutant. FGF10 is colored in green and FGFR2b is colored in cyan. (C) A ribbon diagram of FGF10 in the region that is mutated in the C106F LADD mutant. The LADD mutation is located in a region of FGF10 that does not participate in FGFR2b binding. FGF10 is colored in green and FGFR2b is colored in cyan. (D) The same view as in panel C; in this view, cysteine 106 in the β3-β4 loop is replaced by a phenylalanine residue in the FGF10 LADD mutant. Substitution of a cysteine residue by a hydrophobic bulky phenylalanine residue will perturb the structure of this region. This may result in decreased stability of the C106F LADD mutant. FGF10 is colored in green and FGFR2b is colored in cyan.

(K641R) mutant (18, 29) as controls. Cells expressing WT FGFR2b or the various mutants were stimulated with FGF10, and lysates from unstimulated or FGF10-stimulated cells were subjected to immunoprecipitation with anti-FGFR2 antibodies followed by SDS-PAGE and immunoblotting with anti-p-Tyr antibodies. The results presented in Fig. 5 show FGF10 stimulation of the tyrosine autophosphorylation of WT FGFR2b and the K641R Pfeiffer syndrome FGFR2b mutant. By contrast, FGF10 stimulation of the three FGFR2b LADD mutants led to very weak tyrosine autophosphorylation of mutant FGFR2b. Different degrees of tyrosine autophosphorylation were detected for the three LADD mutants, with the R649S mutant having the highest tyrosine kinase activity and the A628T mutant having the weakest tyrosine kinase activity. In addition, the three LADD mutants failed to stimulate tyrosine phosphorylation of two well-characterized FGFR substrates, FRS2 and Shc, as revealed by immunoprecipitation with anti-Grb2, anti-FRS2, or anti-Shc antibodies followed by SDS-PAGE and immunoblotting with anti-p-Tyr antibodies (Fig. 5B). We have also shown that MAPK stimulation in response

Downloaded from mcb.asm.org at Deutsche Zentralbibliothek on September 25, 2007

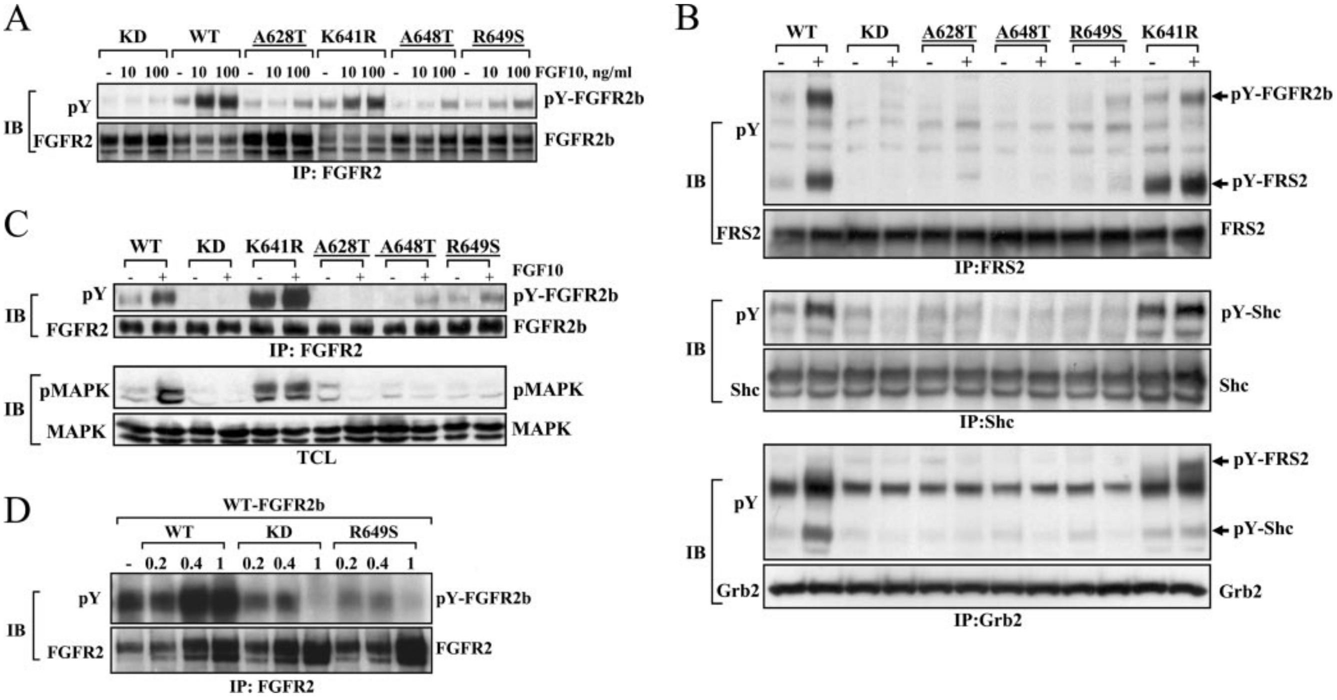

FIG. 5. Reduced tyrosine kinase activity, substrate phosphorylation, and MAPK response by FGFR2b LADD mutants. (A) Tyrosine kinase activity of FGFR2b LADD mutants. L6 cells expressing WT FGFR2b, a kinase-negative FGFR2b mutant (KD), a Pfeiffer syndrome FGFR2b mutant (K641R), or FGFR2b A628T, A648T, and R649S LADD mutants were stimulated with FGF10 for 5 minutes at 37°C as indicated. Lysates of unstimulated or FGF10-stimulated cells were subjected to immunoprecipitation (IP) with anti-FGFR2 antibodies followed by SDS-PAGE and immunoblotting (IB) with anti-FGFR2 or anti-p-Tyr antibodies. (B) Impaired substrate phosphorylation by FGFR2b LADD mutants. L6 cells expressing WT FGFR2b, a kinase-negative FGFR2b mutant (KD), a Pfeiffer syndrome FGFR2b mutant (K641R), or FGFR2b A628T, A648T, and R649S LADD mutants were stimulated with FGF10 for 5 minutes at 37°C. Lysates of unstimulated or FGF10-stimulated cells were subjected to immunoprecipitation with anti-FRS2 antibodies (top), anti-Shc antibodies (middle), or anti-Grb2 antibodies (bottom). After SDS-PAGE, the samples were subjected to immunoblotting with anti-FRS2 or anti-p-Tyr antibodies (top), anti-Shc or anti-p-Tyr antibodies (middle), or anti-Grb2 or anti-p-Tyr antibodies (bottom). (C) Impaired MAPK response in cells expressing FGFR2b LADD mutants. L6 cells expressing WT FGFR2b, a kinase-negative FGFR2b mutant (KD), a Pfeiffer syndrome FGFR2b mutant (K641R), or the FGFR2b A628T, A648T, and R649S LADD mutants were stimulated with FGF10 for 5 minutes at 37°C. Lysates of unstimulated or FGF10-stimulated cells were subjected to immunoprecipitation with anti-FGFR2 antibodies followed by SDS-PAGE and by immunoblotting with anti-FGFR2 or anti-p-Tyr antibodies (top). The bottom shows total cell lysates (TCL) subjected to SDS-PAGE and immunoblotting with anti-MAPK or anti-activated pMAPK antibodies. (D) Dominant interfering effect of the FGFR2b R649S LADD mutant on tyrosine kinase activity of WT FGFR2b. HEK 293 cells coexpressing WT FGFR2b (0.2 μg DNA/10-mm plate) together with increasing amounts (0.2, 0.4, and 1 μg DNA) of WT FGFR2b, a kinase-negative FGFR2b mutant (KD), and the FGFR2b R649S LADD mutant were analyzed. Cell lysates were subjected to immunoprecipitation with anti-FGFR2 antibodies followed by SDS-PAGE and immunoblotting with either anti-FGFR2 or anti-p-Tyr antibodies.

to FGF10 stimulation could barely be detected in L6 cells expressing the FGFR2b LADD mutants. By contrast, robust FGF10-dependent or FGF10-independent MAPK responses were detected in L6 cells expressing WT FGFR2b or the K641R Pfeiffer syndrome FGFR2b mutant, respectively (Fig. 5C). Furthermore, coexpression of WT FGFR2b with the R649S LADD mutant in transfected cells reveals a dominant interfering effect on the autophosphorylation of WT FGFR2 expressed in the same cells (Fig. 5D).

On the basis of these experiments, we conclude that the intrinsic tyrosine kinase activity of FGFR2 LADD mutants is strongly attenuated, resulting in impaired tyrosine phosphorylation of critical substrates and cell signaling. It is noteworthy, however, that weak tyrosine kinase activities could be detected for the LADD mutants that are above the background tyrosine kinase activity detected for the KD K508A mutant. Since all LADD mutations are clustered in the catalytic domain of FGFR2, a region common to both the b and c isoforms, these mutations will affect the tyrosine kinase activities of both the FGFR2b and FGFR2c isoforms.

DISCUSSION

Signaling pathways activated by FGFs and FGFRs have been identified in multicellular organisms from *Caenorhabditis elegans* to vertebrates. It is now well established that the FGFR family of RTKs and their numerous ligands play crucial roles in many developmental and physiological processes and that a variety of diseases are caused by aberrant signaling induced by FGFs or FGFRs (25, 30). The biological roles of individual FGFs and FGFRs have been analyzed by targeted disruption in mice of individual or combinations of FGF or FGFR genes or via analysis of disease-causing mutations in humans. In humans, both loss- and gain-of-function heterozygous mutations have been described. Several human skeletal dysplasias are caused by gain-of-function mutations in FGFR1, FGFR2,

Downloaded from mcb.asm.org at Deutsche Zentralbibliothek on September 25, 2007

and FGFR3. Activating mutations mapped in the extracellular ligand binding domain were found in FGFR1 and FGFR2 associated with Pfeiffer, Crouzon, Jackson-Weiss, and Apert syndromes and in the FGFR2 kinase domain associated with Pfeiffer and Crouzon syndromes. Likewise, activating mutations in FGFR3 were mapped to the transmembrane and the tyrosine kinase domains found for achondroplasia, thanatophoric dysplasia type I (TDI), and TDII (reviewed in references 6, 27, 35, and 36). Interestingly, the nature and severity of the disease might depend on the mutated amino acid; replacement of the same residue by different amino acids may strongly influence the severity of disease. For example, replacement of lysine 650 in the tyrosine kinase domain of FGFR3 by a methionine results in short limbs and developmental delay (dwarfism, severe achondroplasia with developmental delay and acanthosis nigricans), while replacement of the same lysine by a glutamic acid results in lethality (TDII) (15, 16, 35). These observations emphasize the complexity of molecular change that takes place as the consequence of mutations in FGFRs that may influence receptor activity, receptor stability, and receptor localization, among other changes. It is striking that all syndromes described above are caused by gain-of-function mutations in the c isoform of FGFRs, although in some cases mutations were also found in a region common to both b and c FGFR isoforms.

Genetic studies of families and patients with sporadic LADD syndrome revealed mutations in the tyrosine kinase domains of FGFR2 and FGFR3 (28). The three missense mutations identified in FGFR2 are located in catalytic (A628T) and activation (A648T, R649S) loops, and a single mutation was found in the tyrosine kinase domain of FGFR3 (D513N). Several mutations in LADD syndrome patients were identified in FGF10 (C106F, I156R), including a nonsense mutation leading to a premature stop of translation (K137X) (22, 28). A nonredundant role of the FGF10-FGFR2b signaling pathway in lacrimal and salivary gland development was proposed based on the phenotypes of mice deficient in these genes. Aplasia in the lacrimal gland and hypoplasia in the salivary gland were observed for FGF10$^{+/-}$ mice as well as for mice heterozygous for FGF10 and FGFR2b (FGF10$^{+/-}$ FGFR2b$^{+/-}$ mice) (5). Despite the observation that mutations in either FGF10 or FGFR2 cause LADD syndrome, the underlying mechanism is not clear. Moreover, in the absence of biochemical data, modeling of the mutations in the structures of FGF10 and FGFR2 kinase domain did not provide conclusive insights concerning molecular mechanisms.

To reveal the mechanism underlying the molecular basis of LADD syndrome, we have compared the biochemical and biological properties of FGF10 or FGFR2b LADD mutants to the properties of their normal counterparts. Our results show that each of the three LADD mutations affects FGF10 activity by a different mechanism. While the I156R mutant is deficient in binding to FGFR2b, the C106F mutant is unstable at physiological temperatures and is most likely degraded shortly after synthesis before being delivered to its target cell. The K137X mutant, lacking a large C-terminal part of the molecule, was not produced; if it is produced, this mutant will not have any biological activity because its FGF core will have been severely disrupted.

The biological characterization of the FGF10 LADD mutants shows that the activity of the three LADD mutants is strongly compromised. Haploinsufficiency caused by the severely impaired FGF10 mutant leads to LADD syndrome, as the signal induced by FGF10 coded by the normal allele of LADD syndrome patients is not sufficient for mediating the normal development of the salivary and lacrimal glands. This conclusion is supported by genetic studies with mice demonstrating that two copies of FGF10 are required for the normal development of the salivary and lacrimal glands (5). Moreover, the description of two additional FGF10 mutants (R80S and G138E) for patients with ALSG further emphasizes the critical and nonredundant role of FGF10 in salivary and lacrimal gland development (4). The reason why FGF10 haploinsufficiency causes ALSG and the more severe LADD syndrome remains to be elucidated.

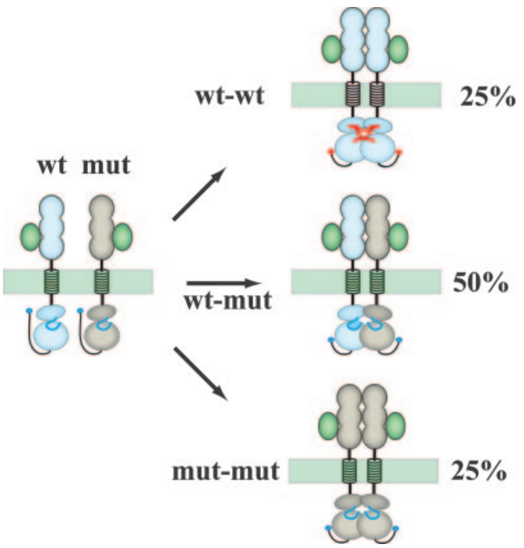

FIG. 6. A model for the dominant negative effect of the FGFR2 LADD mutant (mut) on activity and signaling by WT FGFR2. FGF10 stimulation of cells coexpressing WT FGFR2b together with the FGFR2b LADD mutant leads to the formation of three populations of receptor homodimers and heterodimers: 25% of the receptor molecules are homodimers of WT receptors with normal tyrosine kinase activity (wt-wt), 25% of the receptor molecules are homodimers of the FGFR2b LADD mutant with severely impaired tyrosine kinase activity (mut-mut), and 50% of the receptor molecules are heterodimers of WT and LADD mutant receptors (wt-mut). The tyrosine kinase activity of the heterodimers is strongly attenuated because of the dominant interfering effect exerted by the LADD mutant on the activity of WT FGFR2b.

Analysis of the biological properties of ectopically expressed FGFR2 LADD mutants in the activation loops (A648T and R649S) or in the catalytic loop (A628T) shows that the FGFR2b LADD mutants are deficient in tyrosine kinase activity. The A628T mutant has the weakest activity, the A648T mutant exhibits an intermediate activity, and the R649S mutant has the highest activity, albeit lower than the tyrosine kinase activity of WT FGFR2 following ligand stimulation. Unlike the LADD mutation in the ligand molecule that is caused by the haploinsufficiency of FGF10, the FGFR2 LADD mutation will have a dominant negative effect on signaling mediated via WT FGFR2 expressed in the same cell (Fig. 5D). Three types of FGFR2 dimers will be formed in cells expressing equal amounts of normal FGFR2 and the FGFR2 LADD

Downloaded from mcb.asm.org at Deutsche Zentralbibliothek on September 25, 2007

mutant in response to FGF10 stimulation (Fig. 6): one-fourth of the molecules are homodimers of WT FGFR2 with normal tyrosine kinase activity, one-fourth are homodimers of the FGFR2 LADD mutant with a very weak tyrosine kinase activity, and one-half of the molecules are heterodimers composed of WT and LADD FGFR2 with attenuated tyrosine kinase activities. Since the activation of FGFRs is mediated by ligand-induced receptor dimerization and transphosphorylation, mutant receptors are unable to efficiently phosphorylate WT receptors on autophosphorylation sites in the activation loop of the tyrosine kinase core, a step essential for enhanced and sustained tyrosine kinase activity. Consequently, the defective LADD mutant will exert a dominant inhibitory affect on normal FGFR2, resulting in a strongly attenuated signal.

It has been reported that FGFR2$^{+/-}$ mice are normal, indicating that a single FGFR2 allele (providing 50% of the signal that take place in normal mice) is sufficient to support normal mouse development, including development at the lacrimal and salivary glands. The attenuated signal transmitted in cells coexpressing an FGFR2 LADD mutant together with WT FGFR2 in response to ligand stimulation (assuming that the WT and the FGFR2 LADD mutant are equally expressed) is expected to be larger than 25% and lower than 50% ($25\% <$ signal $< 50\%$) of the signal transmitted by FGFR2 in normal mice. This conclusion underscores the importance of exact doses of receptor signaling in mediating biological responses; a small change in signal strength may have a strong impact on development and homeostasis in cells and tissues that do not possess a redundant signaling pathway.

On the basis of the previous genetic studies with and biochemical characterization of LADD mutations, it is possible to conclude that signaling pathways that are stimulated by FGF10 and mediated by FGFR2b play a critical role in the development and morphogenesis of branching organs such as salivary and lacrimal glands, kidneys, and lungs, which among other organs are affected by LADD syndrome. It has been shown that FGF10 expressed by mesenchymal cells will stimulate FGFR2b expressed in epithelial cells. Activation of FGFR2b in epithelial cells leads to the production of FGF8, which in turn stimulates the activity of FGFR2c and FGFR1c expressed in mesenchymal cells (37). Attenuation in signaling via FGF10 or FGFR2b will lead to the disruption of an important cell signaling circuit that takes place between epithelial and mesenchymal cells during development. Disruption of the epithelial-mesenchymal cell signaling circuit may lead to the dental and skeletal abnormalities seen for LADD syndrome patients.

We also conclude that normal development of lacrimal glands, salivary glands, ears, skeleton, and other organs relies on a correct dose of FGF10 signaling through FGFR2b and that both copies of the FGF10 gene are required for the normal development of these organs; these requirements are not met in the case of the ear, skeletal, and dental abnormalities associated with LADD syndrome. Unlike FGF10 mutations causing ligand haploinsufficiency without affecting the action of the product of the WT FGF10 allele, mutations in FGFR2 lead to more-severe diseases by exerting a dominant negative effect on WT FGFR2 and potentially also on other FGFRs that are expressed in the same cell.

No specific phenotypic differences were observed for patients with mutations in FGF10 and FGFR2 or by comparing phenotypes caused by different FGFR2 mutations. In general, a wide range of phenotypic variability of symptoms exists in LADD syndrome patients, even those within the same family and carrying the identical mutation. This fact makes genotype-phenotype correlations difficult. We propose that the phenotypic outcome of impaired FGF signaling caused by mutations in LADD genes is further modified by genetic, environmental, and stochastic factors which remain to be elucidated.

Finally, although both FGFR2b and FGFR2c carry the LADD mutations, LADD mutation is primarily mediated by the FGFR2b isoform, implying that the compromised signaling via the FGFR2c mutant seen for LADD syndrome is compensated for by other members of the FGFR family expressed in mesenchymal cells.

ACKNOWLEDGMENTS

This work was supported by NIH grants AR 05141448 (J.S.), AR 051886 (J.S.), and P50 AR 054086 (J.S.) and by the European Commission FP6 Integrated Project EUROHEAR, LSHG-CT-20054-512063 (B.W.). Satoru Yuzawa was supported by a fellowship from the Uehara Memorial Foundation.

We thank N. Itoh for the FGF10 plasmid.

REFERENCES

1. **Alarid, E. T., J. S. Rubin, P. Young, M. Chedid, D. Ron, S. A. Aaronson, and G. R. Cunha.** 1994. Keratinocyte growth factor functions in epithelial induction during seminal vesicle development. Proc. Natl. Acad. Sci. USA **91:**1074–1078.
2. **Bamforth, J. S., and P. Kaurah.** 1992. Lacrimo-auriculo-dento-digital syndrome: evidence for lower limb involvement and severe congenital renal anomalies. Am. J. Med. Genet. **43:**932–937.
3. **Emoto, H., S. Tagashira, M. G. Mattei, M. Yamasaki, G. Hashimoto, T. Katsumata, T. Negoro, M. Nakatsuka, D. Birnbaum, F. Coulier, and N. Itoh.** 1997. Structure and expression of human fibroblast growth factor-10. J. Biol. Chem. **272:**23191–23194.
4. **Entesarian, M., J. Dahlqvist, V. Shashi, C. S. Stanley, B. Falahat, W. Reardon, and N. Dahl.** 2007. FGF10 missense mutations in aplasia of lacrimal and salivary glands (ALSG). Eur. J. Hum. Genet. **15:**379–382.
5. **Entesarian, M., H. Matsson, J. Klar, B. Bergendal, L. Olson, R. Arakaki, Y. Hayashi, H. Ohuchi, B. Falahat, A. I. Bolstad, R. Jonsson, M. Wahren-Herlenius, and N. Dahl.** 2005. Mutations in the gene encoding fibroblast growth factor 10 are associated with aplasia of lacrimal and salivary glands. Nat. Genet. **37:**125–127.
6. **Eswarakumar, V. P., I. Lax, and J. Schlessinger.** 2005. Cellular signaling by fibroblast growth factor receptors. Cytokine Growth Factor Rev. **16:**139–149.
7. **Eswarakumar, V. P., E. Monsonego-Ornan, M. Pines, I. Antonopoulou, G. M. Morriss-Kay, and P. Lonai.** 2002. The IIIc alternative of Fgfr2 is a positive regulator of bone formation. Development **129:**3783–3793.
8. **Eswarakumar, V. P., and J. Schlessinger.** 2007. Skeletal overgrowth is mediated by deficiency in a specific isoform of fibroblast growth factor receptor 3. Proc. Natl. Acad. Sci. USA **104:**3937–3942.
9. **Gilbert, E., F. Del Gatto, P. Champion-Arnaud, M. C. Gesnel, and R. Breathnach.** 1993. Control of BEK and K-SAM splice sites in alternative splicing of the fibroblast growth factor receptor 2 pre-mRNA. Mol. Cell. Biol. **13:**5461–5468.
10. **Givol, D., V. Eswarakumar, and P. Lonai.** 2004. Molecular and cellular biology of FGF signaling, p. 367–379. *In* C. J. Epstein, R. P. Erickson, and A. J. Wynshaw-Boris (ed.), Inborn errors of development: the molecular basis of clinical disorders of morphogenesis. Oxford University Press, New York, NY.
11. **Hadari, Y. R., N. Gotoh, H. Kouhara, I. Lax, and J. Schlessinger.** 2001. Critical role for the docking-protein FRS2 alpha in FGF receptor-mediated signal transduction pathways. Proc. Natl. Acad. Sci. USA **98:**8578–8583.
12. **Hollister, D. W., S. H. Klein, H. J. De Jager, R. S. Lachman, and D. L. Rimoin.** 1973. The lacrimo-auriculo-dento-digital syndrome. J. Pediatr. **83:**438–444.
13. **Hunter, T.** 2000. Signaling—2000 and beyond. Cell **100:**113–127.
14. **Itoh, N., and D. M. Ornitz.** 2004. Evolution of the Fgf and Fgfr gene families. Trends Genet. **20:**563–569.
15. **Iwata, T., L. Chen, C. Li, D. A. Ovchinnikov, R. R. Behringer, C. A. Francomano, and C. X. Deng.** 2000. A neonatal lethal mutation in FGFR3 uncouples proliferation and differentiation of growth plate chondrocytes in embryos. Hum. Mol. Genet. **9:**1603–1613.
16. **Iwata, T., C. L. Li, C. X. Deng, and C. A. Francomano.** 2001. Highly activated

Downloaded from mcb.asm.org at Deutsche Zentralbibliothek on September 25, 2007

Fgfr3 with the K644M mutation causes prolonged survival in severe dwarf mice. Hum. Mol. Genet. **10:**1255–1264.

17. **Jaskoll, T., G. Abichaker, D. Witcher, F. G. Sala, S. Bellusci, M. K. Hajihosseini, and M. Melnick.** 2005. FGF10/FGFR2b signaling plays essential roles during in vivo embryonic submandibular salivary gland morphogenesis. BMC Dev. Biol. **5:**11.
18. **Kan, S. H., N. Elanko, D. Johnson, L. Cornejo-Roldan, J. Cook, E. W. Reich, S. Tomkins, A. Verloes, S. R. Twigg, S. Rannan-Eliya, D. M. McDonald-McGinn, E. H. Zackai, S. A. Wall, M. Muenke, and A. O. Wilkie.** 2002. Genomic screening of fibroblast growth-factor receptor 2 reveals a wide spectrum of mutations in patients with syndromic craniosynostosis. Am. J. Hum. Genet. **70:**472–486.
19. **Kouhara, H., Y. R. Hadari, T. Spivak-Kroizman, J. Schilling, D. Bar-Sagi, I. Lax, and J. Schlessinger.** 1997. A lipid-anchored Grb2-binding protein that links FGF-receptor activation to the Ras/MAPK signaling pathway. Cell **89:**693–702.
20. **Levy, W. J.** 1967. Mesoectodermal dysplasia. A new combination of anomalies. Am. J. Ophthalmol. **63:**978–982.
21. **Miki, T., D. P. Bottaro, T. P. Fleming, C. L. Smith, W. H. Burgess, A. M. Chan, and S. A. Aaronson.** 1992. Determination of ligand-binding specificity by alternative splicing: two distinct growth factor receptors encoded by a single gene. Proc. Natl. Acad. Sci. USA **89:**246–250.
22. **Milunsky, J. M., G. Zhao, T. A. Maher, R. Colby, and D. B. Everman.** 2006. LADD syndrome is caused by FGF10 mutations. Clin. Genet. **69:**349–354.
23. **Mohammadi, M., S. K. Olsen, and O. A. Ibrahimi.** 2005. Structural basis for fibroblast growth factor receptor activation. Cytokine Growth Factor Rev. **16:**107–137.
24. **Naski, M. C., Q. Wang, J. Xu, and D. M. Ornitz.** 1996. Graded activation of fibroblast growth factor receptor 3 by mutations causing achondroplasia and thanatophoric dysplasia. Nat. Genet. **13:**233–237.
25. **Ornitz, D. M., and N. Itoh.** 2001. Fibroblast growth factors. Genome Biol. **2:**REVIEWS3005.
26. **Orr-Urtreger, A., M. T. Bedford, T. Burakova, E. Arman, Y. Zimmer, A. Yayon, D. Givol, and P. Lonai.** 1993. Developmental localization of the splicing alternatives of fibroblast growth factor receptor-2 (FGFR2). Dev. Biol. **158:**475–486.
27. **Passos-Bueno, M. R., W. R. Wilcox, E. W. Jabs, A. L. Sertie, L. G. Alonso, and H. Kitoh.** 1999. Clinical spectrum of fibroblast growth factor receptor mutations. Hum. Mutat. **14:**115–125.
28. **Rohmann, E., H. G. Brunner, H. Kayserili, O. Uyguner, G. Nurnberg, E. D. Lew, A. Dobbie, V. P. Eswarakumar, A. Uzumcu, M. Ulubil-Emeroglu, J. G. Leroy, Y. Li, C. Becker, K. Lehnerdt, C. W. Cremers, M. Yuksel-Apak, P. Nurnberg, C. Kubisch, J. Schlessinger, H. van Bokhoven, and B. Wollnik.** 2006. Mutations in different components of FGF signaling in LADD syndrome. Nat. Genet. **38:**414–417.
29. **Schell, U., A. Hehr, G. J. Feldman, N. H. Robin, E. H. Zackai, C. de Die-Smulders, D. H. Viskochil, J. M. Stewart, G. Wolff, H. Ohashi, et al.** 1995. Mutations in FGFR1 and FGFR2 cause familial and sporadic Pfeiffer syndrome. Hum. Mol. Genet. **4:**323–328.
30. **Schlessinger, J.** 2000. Cell signaling by receptor tyrosine kinases. Cell **103:**211–225.
31. **Schlessinger, J., A. N. Plotnikov, O. A. Ibrahimi, A. V. Eliseenkova, B. K. Yeh, A. Yayon, R. J. Linhardt, and M. Mohammadi.** 2000. Crystal structure of a ternary FGF-FGFR-heparin complex reveals a dual role for heparin in FGFR binding and dimerization. Mol. Cell **6:**743–750.
32. **Sekine, K., H. Ohuchi, M. Fujiwara, M. Yamasaki, T. Yoshizawa, T. Sato, N. Yagishita, D. Matsui, Y. Koga, N. Itoh, and S. Kato.** 1999. Fgf10 is essential for limb and lung formation. Nat. Genet. **21:**138–141.
33. **Spivak-Kroizman, T., M. A. Lemmon, I. Dikic, J. E. Ladbury, D. Pinchasi, J. Huang, M. Jaye, G. Crumley, J. Schlessinger, and I. Lax.** 1994. Heparin-induced oligomerization of FGF molecules is responsible for FGF receptor dimerization, activation, and cell proliferation. Cell **79:**1015–1024.
34. **Steinberg, I. Z.** 1971. Long-range nonradiative transfer of electronic excitation energy in proteins and polypeptides. Annu. Rev. Biochem. **40:**83–114.
35. **Webster, M. K., and D. J. Donoghue.** 1997. FGFR activation in skeletal disorders: too much of a good thing. Trends Genet. **13:**178–182.
36. **Wilkie, A. O.** 1997. Craniosynostosis: genes and mechanisms. Hum. Mol. Genet. **6:**1647–1656.
37. **Xu, X., M. Weinstein, C. Li, M. Naski, R. I. Cohen, D. M. Ornitz, P. Leder, and C. Deng.** 1998. Fibroblast growth factor receptor 2 (FGFR2)-mediated reciprocal regulation loop between FGF8 and FGF10 is essential for limb induction. Development **125:**753–765.
38. **Yan, G., Y. Fukabori, G. McBride, S. Nikolaropolous, and W. L. McKeehan.** 1993. Exon switching and activation of stromal and embryonic fibroblast growth factor (FGF)-FGF receptor genes in prostate epithelial cells accompany stromal independence and malignancy. Mol. Cell. Biol. **13:**4513–4522.
39. **Yayon, A., Y. Zimmer, G. H. Shen, A. Avivi, Y. Yarden, and D. Givol.** 1992. A confined variable region confers ligand specificity on fibroblast growth factor receptors: implications for the origin of the immunoglobulin fold. EMBO J. **11:**1885–1890.
40. **Yeh, B. K., M. Igarashi, A. V. Eliseenkova, A. N. Plotnikov, I. Sher, D. Ron, S. A. Aaronson, and M. Mohammadi.** 2003. Structural basis by which alternative splicing confers specificity in fibroblast growth factor receptors. Proc. Natl. Acad. Sci. USA **100:**2266–2271.

Downloaded from mcb.asm.org at Deutsche Zentralbibliothek on September 25, 2007

Structural basis for reduced FGFR2 activity in LADD syndrome: Implications for FGFR autoinhibition and activation

Erin D. Lew*, Jae Hyun Bae*, Edyta Rohmann†‡, Bernd Wollnik†‡, and Joseph Schlessinger*§

*Department of Pharmacology, Yale University School of Medicine, 333 Cedar Street, New Haven, CT 06510; and †Center for Molecular Medicine Cologne (CMMC) and ‡Institute of Human Genetics, University of Cologne, 50923 Cologne, Germany

Contributed by Joseph Schlessinger, October 23, 2007 (sent for review September 25, 2007)

Mutations in fibroblast growth factor receptor 2 (FGFR2) and its ligand, FGF10, are known to cause lacrimo-auriculo-dento-digital (LADD) syndrome. Multiple gain-of-function mutations in FGF receptors have been implicated in a variety of severe skeletal disorders and in many cancers. We aimed to elucidate the mechanism by which a missense mutation in the tyrosine kinase domain of FGFR2, described in the sporadic case of LADD syndrome, leads to reduced tyrosine kinase activity. In this report, we describe the crystal structure of a FGFR2 A628T LADD mutant in complex with a nucleotide analog. We demonstrate that the A628T LADD mutation alters the configuration of key residues in the catalytic pocket that are essential for substrate coordination, resulting in reduced tyrosine kinase activity. Further comparison of the structures of WT FGFR2 and WT FGFR1 kinases revealed that FGFR2 uses a less stringent mode of autoinhibition than FGFR1, which was also manifested in faster *in vitro* autophosphorylation kinetics. Moreover, the nearly identical conformation of WT FGFR2 kinase and the A628T LADD mutant to either the phosphorylated FGFR2 or FGFR2 harboring pathological activating mutations in the kinase hinge region suggests that FGFR autoinhibition and activation are better explained by changes in the conformational dynamics of the kinase rather than by static crystallographic snapshots of minor structural variations.

cell signaling | genetic disease | growth factor receptors | protein kinases | structural biology

Lacrimo-auriculo-dento-digital (LADD) syndrome is characterized by multiple congenital anomalies including aplasia of the lacrimal and salivary glands, cup-shaped, small, and low-set ears, hypo- and microdentia, hearing loss, and malformation of the digits, most commonly the thumb (1). Patients with LADD syndrome exhibit overlapping phenotypic features with aplasia (or hypoplasia) of lacrimal and salivary gland (ALSG) syndrome. Recent genetic studies have implicated mutations in fibroblast growth factor 10 (FGF10) and the "IIIb" isoform of FGFR2 (also designated FGFR2b) in LADD syndrome (2–4).

FGFR2 is a member of the FGFR family of receptor tyrosine kinases (RTK) that includes three additional receptors. FGF-receptors play an important role in the control of diverse cellular processes including cell proliferation, differentiation, migration, and maintenance of cellular homeostasis (5). The four members of the FGFR family (FGFR 1–4) each consist of an extracellular ligand-binding region composed of three Ig-like domains designated D1, D2, and D3, a single transmembrane-spanning domain, and an intracellular tyrosine kinase domain with additional regulatory sequences. FGFRs 1–4 exhibit different temporal and spatial expression patterns, and FGFRs 1–3 are additionally subject to alternative splicing in the C-terminal half of D3 to generate either the "IIIb" or the "IIIc" spliced isoforms. It was shown that the IIIb isoforms are expressed in epithelial cells, and the IIIc isoforms are expressed in the mesenchymal cells. Moreover, FGFs that activate the IIIb FGFR isoforms are expressed in mesenchyme, whereas FGFs that activate the IIIc FGFR isoforms are produced in epithelial cells (6).

After ligand binding, FGFRs undergo receptor-mediated dimerization and subsequent transautophosphorylation on numerous tyrosine residues in the tyrosine kinase core and in other parts of the cytoplasmic region (7). The tyrosine kinase domain catalyzes the transfer of the γ-phosphate of ATP to the hydroxyl group of tyrosine residues, which serves to both increase the intrinsic catalytic activity of the kinase and recruit a number of downstream signaling molecules via their conserved Src homology-2 (SH2) or phosphotyrosine-binding (PTB) domains (8). The x-ray crystal structure of the tyrosine kinase domain of FGFR1 revealed that in the inactive state, FGFR1 exists in an autoinhibited conformation in which the nucleotide-binding loop is open, but the catalytic loop is occluded by residues from the C terminus of the activation loop (9). Crystal structures of tyrosine kinase domains of other RTKs have shown a variety of autoinhibitory conformations (10), highlighting the requirement for precise regulation of the tyrosine kinase activity, a principle exemplified by the discovery of numerous gain-of-function and loss-of-function mutations in the kinase domain of FGFRs responsible for a variety of clinical entities including Crouzon syndrome, Pfeiffer syndrome, Kallmann syndrome, various cancers, and LADD syndrome, among others (11).

More recent biochemical evidence suggests that FGFR2 mutations responsible for LADD syndrome exhibit decreased tyrosine phosphorylation as well as decreased ligand-induced recruitment of downstream signaling molecules (12). However, the precise mechanism governing how these point mutations in highly conserved regions of the FGFR kinase domain lead to partial inactivation or a loss-of-function phenotype is poorly understood.

In this article, we describe the crystal structure at 1.8 Å resolution of the tyrosine kinase domain of FGFR2 harboring a single missense mutation, A628T, described in a sporadic case of LADD syndrome, in complex with a nucleotide analog. The structure precisely revealed that the A628T LADD mutation altered the catalytic pocket, which would compromise the ability of the tyrosine kinase to coordinate its substrate and thus, lead to the partial FGFR2 inactivation found in LADD syndrome. Moreover, the structure provides more detailed insight into RTK-mediated phosphotransfer and provides a molecular mechanism at atomic resolution for how this single point mutation directly affects FGFR2

Author contributions: E.D.L. and J.S. designed research; E.D.L., J.H.B., and E.R. performed research; E.D.L., J.H.B., E.R., B.W., and J.S. analyzed data; and E.D.L. and J.S. wrote the paper.

The authors declare no conflict of interest.

Data deposition: The atomic coordinates have been deposited in the Protein Data Bank, www.pdb.org (PDB accession code: 3B2T).

§To whom correspondence should be addressed. E-mail: joseph.schlessinger@yale.edu.

This article contains supporting information online at www.pnas.org/cgi/content/full/0709905104/DC1.

© 2007 by The National Academy of Sciences of the USA

19802–19807 | PNAS | December 11, 2007 | vol. 104 | no. 50 www.pnas.org/cgi/doi/10.1073/pnas.0709905104

enzymatic activity. We also show that FGFR2 adopts a less autoinhibited conformation relative to FGFR1, suggesting that FGFR2 uses a somewhat different mode of autoregulation to maintain its tyrosine kinase domain in an inactive state. Finally, the nearly identical conformation of WT FGFR2 kinase to those of A628T LADD mutant and various forms of activated FGFR2 kinase underscores the significance of conformational dynamics in the control of FGFR autoinhibition and activation.

Results and Discussion

In a sporadic LADD case, a *de novo* missense mutation was found in the catalytic loop in the tyrosine kinase domain of FGFR2 resulting in the substitution of a highly conserved alanine to a threonine (A628T) residue (13). Although recent biochemical evidence has shown that this mutation leads to decreased tyrosine phosphorylation of FGFR2 and recruitment of downstream signaling molecules (12), we sought to precisely determine how this mutation affects the intrinsic properties of the FGFR2 kinase domain. We first purified the intact kinase domains of both wild-type FGFR2 (WT) and FGFR2 harboring a single A628T point mutation (A628T) [supporting information (SI) Fig. 5]. Both WT FGFR2 and A628T-FGFR2 migrated as a monomer of ≈36 kDa on an SDS/PAGE gel and had very similar elution profiles from an anion exchange column, suggesting that the A628T mutant remained intact and that the surface charge was comparable to the WT FGFR2 tyrosine kinase.

Reduced Kinase Activity of LADD Mutant Is Not Caused by Impairment of ATP Binding. We next asked whether the A628T mutation had a direct effect on the intrinsic catalytic activity of FGFR2 kinase. The mutation resides in center of the catalytic loop, which is a highly conserved region within the FGFR family and among other RTKs (14). An *in vitro* kinase assay was performed by incubating 69.4 μM WT FGFR2 or A628T-FGFR2 with ATP and $MgCl_2$ to a final concentration of 10 mM and 25 mM at 4°C, respectively (Fig. 1*A*). The reaction was stopped at various time points upon addition of EDTA to a final concentration of 100 mM, and the formation of phosphorylated species was followed by native gel electrophoresis. For WT kinase, formation of a monophosphorylated species (1P) was detected as early as 3 min, and formation of a fully phosphorylated species (5P) was visible by 45 min. In contrast, the A628T mutant failed to undergo autophosphorylation even after a 5-h incubation with ATP/$MgCl_2$, suggesting that the A628T mutation greatly impaired FGFR2 catalytic activity. The kinase assay was also performed at room temperature (5 mM ATP and 10 mM $MgCl_2$, final concentration) to determine whether the mutation renders the kinase inactive (Fig. 1*B*). Although tyrosine phosphorylation of the A628T-FGFR2 mutant was observed, the kinetics of autophosphorylation were significantly slower than those observed for WT FGFR2 and were similar to the phosphorylation kinetics of WT FGFR2 observed at 4°C. These results show that the A628T mutation directly compromises the intrinsic catalytic activity of FGFR2 kinase, which would account for the decreased tyrosine phosphorylation of ectopically expressed A628T-FGFR2 mutant in transfected L6 cells (12).

To examine the structural basis for the decreased catalytic activity of the A628T mutant, we crystallized the kinase domain of the A628T LADD mutant in complex with a nucleotide analog, AMP-PCP, in the inactive state. The 1.8 Å resolution structure revealed that the kinase domain adopts the classical RTK bilobate architecture, and clear density was observed for the activation loop, the catalytic loop including the A628T mutation, and the ATP analog (Fig. 2*A* and SI Fig. 6 *A* and *C*). AMP-PCP resides in the nucleotide-binding pocket between the N- and C-terminal lobes, and the adenine ring is hydrogen-bonded to the backbone of Glu-565 and Ala-567, analogous to the interactions observed between inactive FGFR1 and AMP-PCP and in other RTKs (Fig. 2*B*) (9, 15). The nucleotide analog does not appear to be in a productive binding mode because the γ-phosphates in both molecules in the asymmetric unit were disordered, and Mg^{2+} ions were not observed in coordination with AMP-PCP. The α-, and β-phosphate groups extend in a configuration parallel to the nucleotide-binding loop, in contrast to what was seen in the structure of inactive FGFR1 (9), but they do not make direct contacts with the protein backbone.

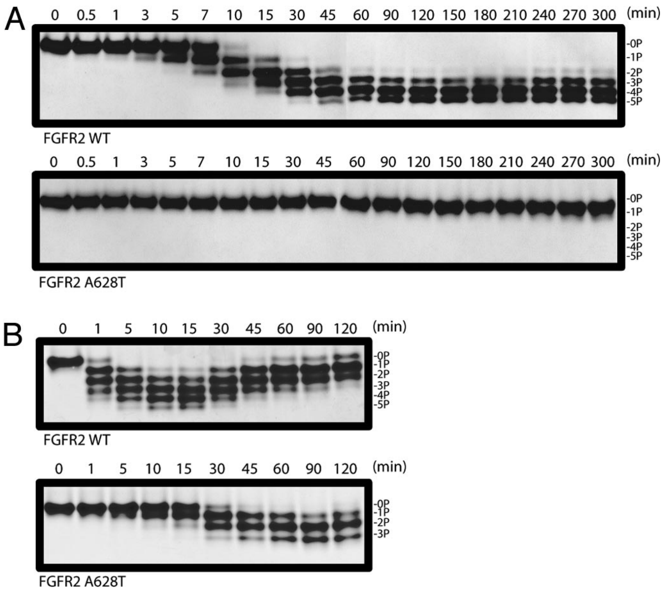
A
0 0.5 1 3 5 7 10 15 30 45 60 90 120 150 180 210 240 270 300 (min)
-0P -1P -2P -3P -4P -5P
FGFR2 WT
0 0.5 1 3 5 7 10 15 30 45 60 90 120 150 180 210 240 270 300 (min)
-0P -1P -2P -3P -4P -5P
FGFR2 A628T
B
0 1 5 10 15 30 45 60 90 120 (min)
-0P -1P -2P -3P -4P -5P
FGFR2 WT
0 1 5 10 15 30 45 60 90 120 (min)
-0P -1P -2P -3P
FGFR2 A628T

Fig. 1. Reduced tyrosine kinase activity of the A628T LADD FGFR2 mutant. (*A*) FGFR2 WT or FGFR2-A628T (69.4 μM final concentration) were incubated with ATP and $MgCl_2$ at 4°C to a final concentration of 10 mM and 25 mM, respectively. Reactions were quenched at each time point upon addition of EDTA (100 mM final concentration), and the phosphorylation states were visualized by native gel electrophoresis. (*B*) Autophosphorylation reaction was similarly performed at room temperature upon addition of ATP and $MgCl_2$ to a final concentration of 5 mM and 10 mM, respectively. Reactions were quenched with EDTA (100 mM final concentration), and results were visualized by native gel electrophoresis. The positions of unphosphorylated (0P) and FGFR2 phosphorylated on 1 to 5 tyrosine residues are marked (1P–5P).

The rate of catalysis can also be affected by a change in the affinity of the tyrosine kinase for ATP. To determine whether the A628T LADD mutation affected ATP binding, we performed fluorescence titration experiments where WT FGFR2 or A628T-FGFR2 were incubated with increasing concentrations of AMP-PNP in the presence of excess $MgCl_2$. The kinase was excited at 285 nm, and the change in intrinsic protein fluorescence due to binding of the ATP analog was monitored between 300 and 420 nm (Fig. 2*C*). Decrease in fluorescence intensity was observed with increasing concentrations of AMP-PNP, and the data were fit to a quadratic equation. The dissociation constants obtained for WT and A628T were $K_D = 4.56 \pm 1.27$ μM and $K_D = 6.21 \pm 2.10$ μM, respectively, indicating that the LADD mutation did not affect ATP binding and that the diminished FGFR2 catalytic activity in the A628T mutant was not caused by decreased ATP binding.

FGFR2 Kinase Is Less Autoinhibited Than FGFR1 Kinase. Recent crystal structures have shown that, in the inactive state, RTKs adopt a number of autoinhibitory configurations often involving inhibition of the substrate-binding pocket or blockage of the nucleotide-binding pocket (10). The structure of the A628T-FGFR2 mutant revealed that in the inactive state, both the nucleotide binding site and the substrate-binding pocket appeared accessi-

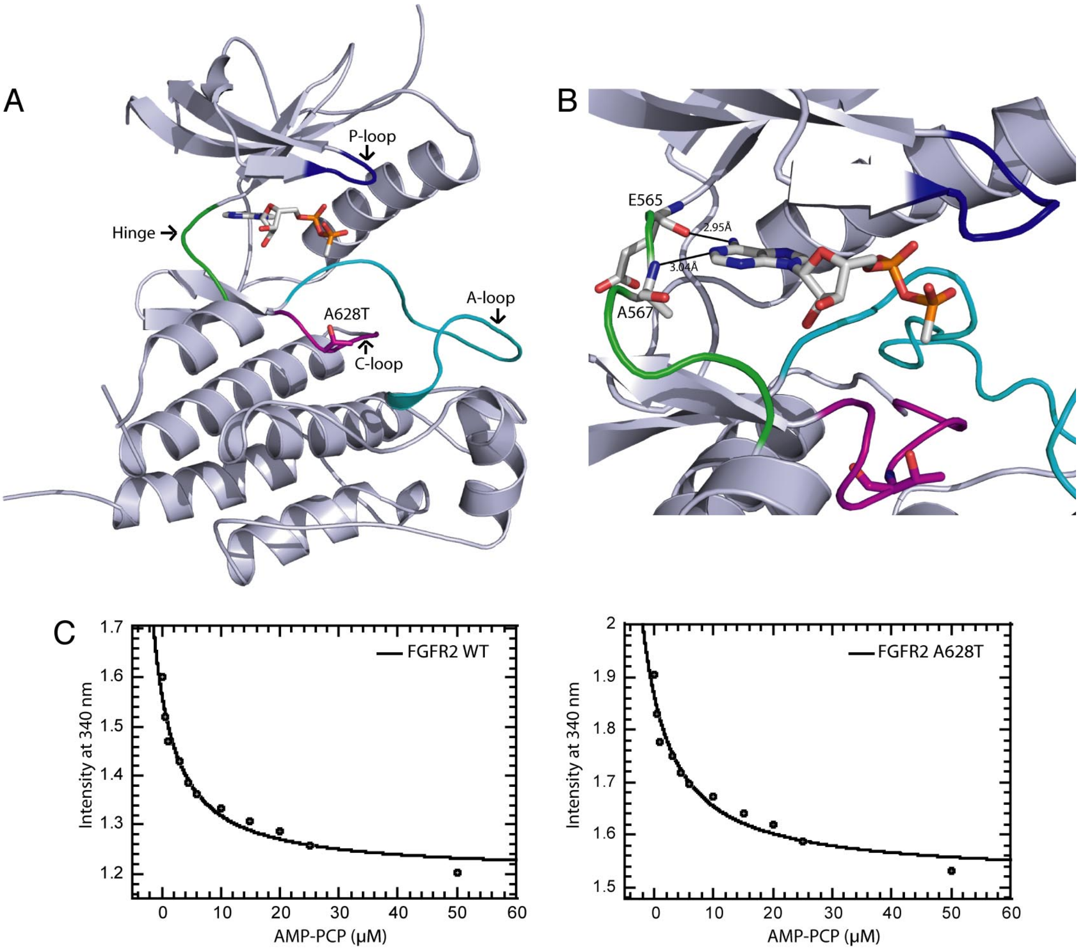

Fig. 2. Overview of the structure of FGFR2 A628T LADD mutant and effect of LADD mutations on ATP binding. (*A*) Ribbon diagram of A628T FGFR2 structure in complex with nucleotide analog, AMP-PCP. The mutation in the catalytic loop is indicated. The nucleotide-binding loop is shown in blue, the hinge region in green, the catalytic loop in purple, and the activation loop in cyan. AMP-PCP is shown in stick representation with nitrogen atoms blue, carbon atoms white, oxygen atoms red, and phosphate atoms orange. (*B*) Close view of nucleotide-binding pocket. Hydrogen bonds are indicated by solid black lines. Coloring is as in *A* (*C*) Fluorescence titration experiments measuring FGFR WT or FGFR2 A628T intrinsic protein fluorescence at 340 nm in the presence of increasing concentrations of AMP-PNP from 0 to 50 μM. Data were fit to a quadratic equation by nonlinear regression (Kaleidograph). AMP-PNP-binding values for FGFR2 WT and FGFR2 A628T were $K_D = 4.56 \pm 1.27$ μM and $K_D = 6.21 \pm 2.10$ μM, respectively.

ble, and the kinase adopted a configuration much different from that observed in the structure of inactive FGFR1 (Figs. 2*A* and 3*A*) (9). To determine whether this altered configuration was due to the A628T point mutation or whether it is an intrinsic property of FGFR2 kinase, the tyrosine kinase domain of WT FGFR2 (PDB ID code, 1GJO) and the A628T-FGFR2 mutant were compared (Fig. 3*C*). The two FGFR2 structures were nearly identical, with an overall r.m.s.d. value of 0.7 Å. The tyrosine kinase domains of FGFR1 and FGFR2 share >90% sequence identity; however, the divergence of their three-dimensional structures warranted a detailed comparison of the two structures (Fig. 3*A*). Overall, the conformation of the C-terminal lobe was nearly identical, whereas the N-terminal lobe of FGFR2 relative to FGFR1 (PDB ID code, 1FGK) appeared rotated toward the C-lobe with movement of αC 20° downward in a configuration reminiscent of an active state. In addition, the activation loop of FGFR2 is flipped outward and adopts a conformation more favorable to αC downward movement as well as more conducive to substrate binding. This conformation was observed for both WT FGFR2 and the A628T-FGFR2, which were crystallized in two different space groups and had different crystal-packing arrangements, suggesting that the conformation is intrinsic to FGFR2 kinase. Comparison of FGFR2 to activated insulin receptor kinase (IRK-3P) (PDB ID code, 1IR3) (Fig. 3*B*) (15) showed that the positions of αC and the activation loop, especially near the $P + 1$ loop, were very similar, further suggesting that FGFR2 kinase is less autoinhibited than FGFR1 kinase. Furthermore, in FGFR1 kinase, substrate binding is occluded by Pro-663 and Arg-661, which appear to directly interfere with the binding of a substrate Tyr (P-site). In contrast, in FGFR2, the corresponding residues, Pro-666 and Arg-664, are away from the catalytic pocket (Fig. 4 *A* and *I*). Pro-666 is in a conformation very similar to that found for the equivalent residue in IRK-3P and appears poised to form favorable van der Waals interactions with a substrate Tyr(P) residue. Arg-664 forms an ion pair with Asp-530 in αC, preventing it from adopting the autoinhibitory conformation found in the structure of FGFR1 and furthermore, stabilizing the active configuration of the αC helix (Fig. 4*I*). To determine whether the less autoinhibited conformation may affect the intrinsic catalytic activity of FGFR2 relative to FGFR1, we next incubated either 69.4 μM purified FGFR2 WT kinase or FGFR1 WT kinase with ATP and $MgCl_2$ to a final concentration of 10 mM and 25 mM, respectively, at 4°C and quenched the reaction mixture with 100 mM EDTA at different time points. The experiment presented in Fig. 3*D* shows that formation of mono-phosphorylated and

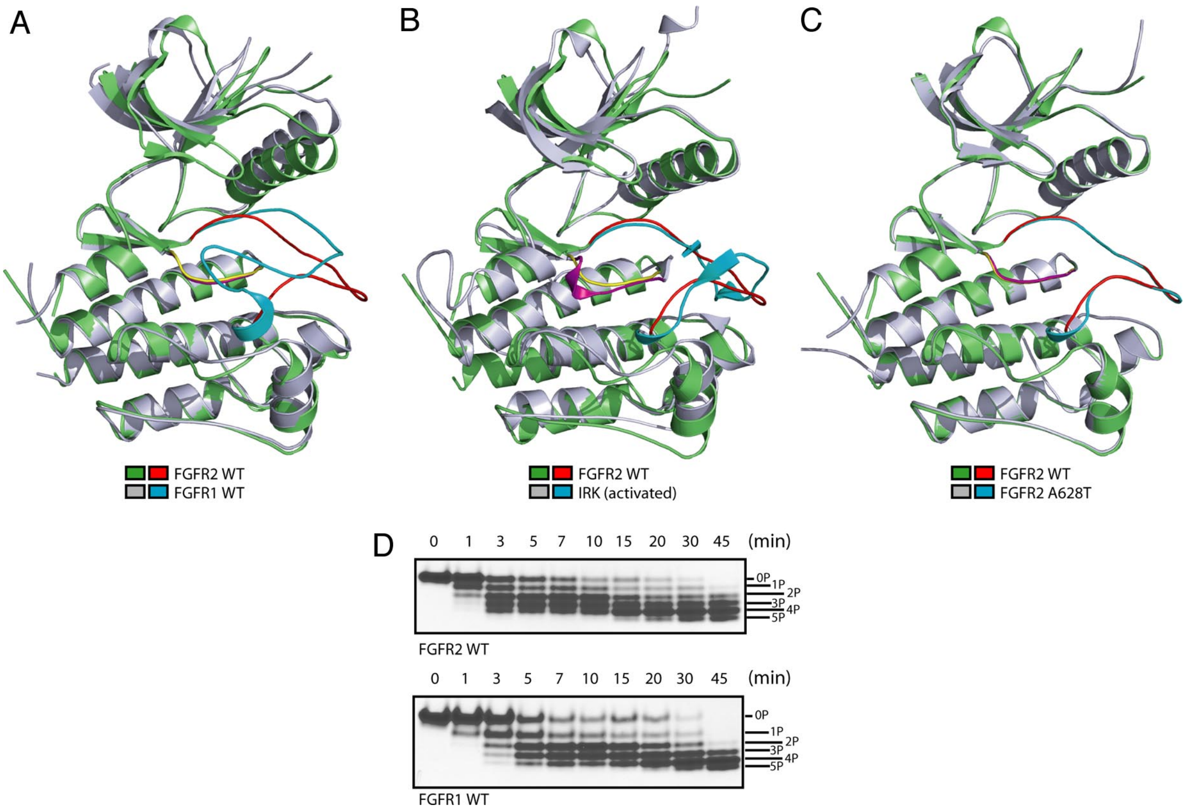

Fig. 3. Comparison of the structure of the tyrosine kinase domains of FGFR1, FGFR2, and insulin receptor. (*A*) Overlay of inactive FGFR2 kinase (PDB ID code, 1GJO) and inactive FGFR1 kinase (PDB ID code, 1FGK). FGFR2 WT is shown in green, its activation loop in red, and its catalytic loop in yellow. FGFR1 WT is illustrated in gray, its activation loop in cyan, and its catalytic loop in purple. (*B*) Overlay of inactive FGFR2 WT kinase (PDB ID code, 1GJO) and activated IRK (PDB ID code, 1IR3). Colors for FGFR2 WT are as in *A*. Activated IRK is shown in gray, its activation loop in cyan, and its catalytic loop in purple. (*C*) Overlay of inactive FGFR2 WT (PDB ID code, 1GJO) and FGFR2 A628T LADD mutant. Colors for FGFR2 WT are as in *A*. FGFR2 A628T is illustrated in gray, its activation loop in cyan, and its catalytic loop in purple. (*D*) FGFR2 WT or FGFR1 WT (69.4 μM final concentration) were incubated with ATP and $MgCl_2$ at 4°C to a final concentration of 10 mM and 25 mM, respectively. Reactions were quenched at each time point upon addition of EDTA (100 mM final concentration), and the phosphorylation states were visualized by native gel electrophoresis.

bis-phosphorylated FGFR2 was observed by 1 min, with formation of the fully phosphorylated species visible by 15 min. In contrast, by 1 min, only monophosphorylated FGFR1 was visible, with formation of the fully phosphorylated species visible by 30 min, suggesting that FGFR2 is modestly more catalytically active than FGFR1, most prominently in the initial stages of phosphorylation. Despite its less autoinhibited conformation, unphosphorylated FGFR2 kinase does not fully adopt an active conformation. The N-lobe of FGFR2 was not fully closed for proper coordination of the Mg^{2+} ions or full interaction with the nucleotide analog, AMP-PCP, as evidenced from the lack of clear electron density for both the Mg^{2+} ions and the γ-phosphate of AMP-PCP and also from lack of engagement of the α- and β-phosphate groups of AMP-PCP with the protein backbone (Figs. 2*B* and 3*B*). In addition, αC is oriented such that the highly conserved Lys-517 and Glu-534 (Lys-514 and Glu-531 in FGFR1), found $\approx$4 Å apart after activation of IRK, are hydrogen-bonded, which prevents proper orientation of the five-stranded β-sheets of the N-lobe relative to αC and may also be inhibitory for Mg^{2+} binding. In addition, structures of activated kinases in complex with peptide analogs have shown that, in addition to accommodating the substrate Tyr(P) moiety, residues C-terminal to Tyr(P) comprise a β-strand that forms an antiparallel sheet with β11 at the C terminus of the activation loop (Fig. 4*B*) (15, 16). In FGFR2, residues in the C terminus of the activation loop fail to adopt this configuration but, rather, are internally stabilized by a hydrogen-bonding network consisting of Arg-649, Thr-660, Asn-662, and Arg-625 (Fig. 4*I*). Transition from the inactive to the active state most likely involves rearrangement of these hydrogen-bond interactions upon autophosphorylation, including the hydrogen bond between Arg-664 with Asp-530 on αC, and rearrangement of the activation loop to form interactions more similar to those seen in the crystal structure of IRK-3P and other phosphorylated RTKs.

A628T LADD Mutation Alters the Conformation of Key Residues Essential for Substrate Coordination. Despite the structural differences observed within the FGFR family and the conformational changes associated with the transition from the inactive to active state, the catalytic loop is a highly conserved region in the kinase, and superimposition of the catalytic loops revealed a high degree of structural similarity among both active and inactive RTKs (Figs. 3*B* and 4*H*) (17). In the structures of the activated IRK (15) and IGFR1 (18) in complex with peptide substrate, both the catalytic base (D1132 in IRK) and the conserved arginine residue within the catalytic loop (R1136 in IRK) are hydrogen-bonded to the hydroxyl group of the substrate Tyr(P), presumably in position for proton abstraction and charge neutralization, respectively (Fig. 4*B*). The A628T LADD mutation resides in the center of the catalytic loop and results in substitution of a small hydrophobic residue with a more bulky, polar residue (Fig. 4*E*). The A628T-FGFR2 structure revealed that the threonine substitution resulted in movement of the conserved Arg-630 $\approx$160° away from the catalytic base, Asp-626, in a position stabilized by interaction with Asp-521 from the neighboring molecule in the asymmetric unit. Structures of both inactive and active RTKs in the presence and absence of substrate

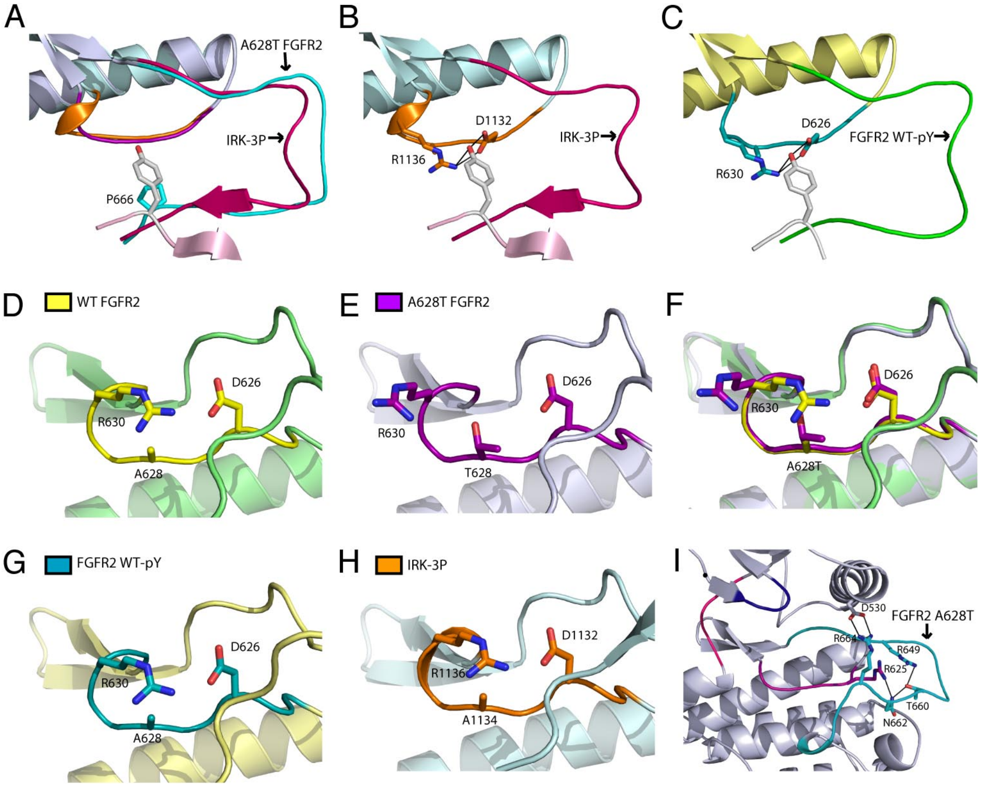

Fig. 4. A628T LADD FGFR2 mutation compromises substrate binding. (*A*) Comparison of A-loop orientations of IRK-3P in complex with peptide substrate and A628T FGFR2 mutant. A-loop of IRK-3P is shown in magenta and the catalytic loop in orange. The peptide substrate is shown in pink, and the tyrosine phosphorylation site is indicated by a stick representation. The A-loop of A628T FGFR2 is colored in cyan, and the catalytic loop is shown in purple. The corresponding proline residue in FGFR2 that plays an autoregulatory role in the inactive structure of FGFR1 is indicated. (*B*) Catalytic pocket of IRK-3P with peptide substrate. Colors are as in *A*, and key hydrogen-bonding interactions are indicated by solid black lines. (*C*) Catalytic pocket of phosphorylated FGFR2 WT with peptide substrate (PDB ID code, 2PVF). The peptide substrate is shown in white, and the tyrosine phosphorylation site is indicated by stick representation. The A-loop of activated FGFR2 WT is shown in green, and the catalytic loop is shown in teal. Hydrogen-bonding interactions are indicated by solid black lines. (*D*–*F*) Catalytic loop of FGFR2 WT (*D*, yellow), A628T FGFR2 LADD mutant (*E*, purple), and overlay (*F*). Key residues involved in catalysis are indicated. (*G* and *H*) Catalytic pocket of phosphorylated WT FGFR2 (*G*, PDB ID code, 2PVF) and IRK-3P (*H*) in complex with peptide substrate. Residues involved in catalysis are indicated. (*I*) Interactions within the A-loop of A628T-FGFR2 LADD mutant. The activation loop is shown in cyan, the catalytic loop is shown in purple, and key hydrogen bonds are indicated by solid black lines.

have shown that the hydrogen bond between Arg-630 and Asp-626 in the catalytic pocket is highly conserved (Fig. 4*H*), and in the A628T-FGFR2 mutant, movement of Arg-630 is most likely due to steric hindrance between Arg-630 and Thr-628, because superimposition of the catalytic loops of WT FGFR2 and the A628T-FGFR2 mutant showed that the Arg-630 cannot be accommodated in the catalytic pocket upon substitution of Ala-628 with threonine (Fig. 4 *D*–*F*). The position of Asp-626 remains roughly unchanged (Fig. 4*F*) and seemingly, would still be in position to interact with the substrate Tyr(P). The position of Arg-630, however, is too far from the catalytic pocket to contact the substrate Tyr(P), and this conformation would hinder phosphotransfer by failing to stabilize the substrate interaction and, thus, result in severely compromised catalytic activity as seen in LADD syndrome. The crystal structure of the A628T-FGFR2 mutant presented in this study is also in agreement with the crystal structure of WT FGFR2 kinase that was recently described, most notably in the $P + 1$ loop (SI Fig. 7) (19). Furthermore, despite similar crystal-packing arrangements, the two structures differ in the orientation of the Arg-630 side chain in the catalytic loop (Fig. 4*C*, *E*, and *G*), further supporting the notion that the A628T LADD mutation is responsible for disruption of the catalytic pocket.

Inactive LADD Mutant Adopts a Virtually Identical Conformation to both Phosphorylated FGFR2 and Activated Pathological FGFR2 Mutants. Comparison of the structure of the kinase domain of the inactive A628T-FGFR2 LADD mutant to the crystal structures of either phosphorylated or activated FGFR2 mutants (19) that have been implicated in severe bone disorders or other pathological conditions revealed nearly identical structures (SI Fig. 7). The virtually identical conformations of the kinase domain of the inactive A628T LADD mutant, unphosphorylated WT FGFR2, phosphorylated FGFR2, and several pathological activating FGFR2 mutants (SI Fig. 7) support the argument that autoinhibition is likely not caused by a static and crystallographically defined "molecular brake" in the hinge region of FGFRs and other RTKs (19), but, instead, it seems likely that the activating mutations in the hinge region exert their effects by altering the conformational dynamics. Interestingly, despite the compromised catalytic activity observed with the A628T LADD mutant, the triad of residues that comprise the molecular brake in the LADD mutant are partially disengaged in this structure and participate in a different network of hydrogen bonding interactions, suggesting that minor variations in the hinge and other flexible regions may be influenced by crystallization conditions and crystal lattices. The surprising similarity of activated and inactive forms of FGFR2 when viewed as static crystal structures suggest that both autoinhibition and activation of FGFRs and other RTKs may be dictated, to a large extent, by conformational dynamics rather than by well defined minor changes observed in FGFR2 kinase (19).

Materials and Methods

Expression, Purification, and Crystallization of A628T FGFR2 Tyrosine Kinase Domain. A bacterial expression vector was engineered to encode residues 461–768 of the human fibroblast growth factor receptor 2 (FGFR2). For crystallization studies, a tobacco etch virus (TEV) enzymatic cleavage site was introduced after the N-terminal His_6-tag by PCR, and a single point mutation, A628T, was introduced by site-directed mutagenesis (Stratagene). Bacteria were grown at 37°C to an OD_{600} of 1.3 and induced with 1 mM IPTG overnight at 20°C. The cells were lysed by French press (Thermo Scientific), and the protein was purified by using a Ni-NTA-His resin (Novagen). After elution from the column, the protein was incubated with a 1:100 molar ratio of TEV protease to A628TFGFR2 and simultaneously dialyzed in buffer containing 20 mM Tris, pH 8, and 5 mM DTT overnight at 4°C. The reaction mixture was subsequently passed over a Superdex200 HR10/30 (GE Healthcare) and further purified by using an anion exchange column on a Mono Q HR16/10 (GE Healthcare). Purified A628T FGFR2 was concentrated to 20 mg/ml in 20 mM Tris, pH 8, 200 mM NaCl, and 5 mM DTT.

Crystals were grown at 4°C by vapor diffusion in hanging drops containing 1 μl of protein solution (20 mg/ml A628T-FGFR2, 5 mM AMP-PCP, 10 mM $MgCl_2$) and 1 μl of reservoir solution (0.6 M NaH_2PO_4, 0.6 M KH_2PO_4, 0.1 M Hepes, pH 8). The crystals belonged to the orthorhombic space group $P2_12_12$ and had unit cell dimensions $a = 67.7$ Å, $b = 80.3$ Å, $c = 118.6$ Å, $\alpha = \beta = \gamma = 90°$. There were two molecules per asymmetric unit, and the solvent content was ≈45% (*SI Materials and Methods* and SI Tables 1 and 2).

Data Collection, Structure Determination, and Analysis. One cryo-cooled crystal was used for data collection. The crystal was transferred stepwise into a cryosolution containing 0.6 M NaH_2PO_4, 0.6 M KH_2PO_4, 0.1 M Hepes, pH 8, with increasing concentrations of glycerol (5%, 15%, 20%, 25%, and 30%). After ≈1 min in the final cryosolution, the crystal was flash-cooled in liquid nitrogen and transferred to the goniostat, which was bathed in a dry nitrogen stream at −180°C. Data were collected at beamline X29 at Brookhaven National Laboratory. All data were processed by using DENZO and SCALEPACK (20). A molecular replacement solution was found by using the program PHASER (21) with the FGFR2 tyrosine kinase domain (PDB ID code, 1GJO) as the search molecule. The A628T structure was subject to rigid body refinement from 50 to 3 Å by using REFMAC (22), resulting in a R_{cryst} value of 33.9%. Model building and refinement were carried out from 50 to 1.8 Å by using COOT (23) and CNS (24), respectively, to an R_{cryst} and R_{free} value of 20.1% and 23.1%, respectively. For calculation of R_{free}, 7% of the data were omitted. Figures were generated by using PyMOL (25). The stereochemistry of the model was analyzed with PROCHECK (26).

We thank Dr. Satoru Yuzawa for helpful crystallization and structure determination suggestions, Dr. Titus Boggon for critical reading of the manuscript, Dr. Mark Lemmon and Dr. Kate Ferguson for helpful discussions, and the staff at the National Synchrotron Light Source Beamline X29 for assistance. This work was supported by National Institutes of Health Grants AR 051448, AR 051886, and P50 AR 054086 (to J.S.).

1. Bamforth J, Kaurah P (1992) *Am J Med Genet* 43:932–937.
2. Entesarian M, Dahlqvist J, Shashi V, Stanley CS, Falahat B, Reardon W, Dahl N (2007) *Eur J Hum Genet* 15:379–382.
3. Hollister D, Klein SH , De Jager HJ, Lachman RS, Rimoin DL (1973) *J. Pediatr* 83:438–444.
4. Milunsky J, Zhao G, Maher T, Colby R, Everman D (2006) *Clin Genet* 69:349–354.
5. Eswarakumar VP, Lax I, Schlessinger J (2005) *Cytokine Growth Factor Rev* 16:139–149.
6. Johnson DE, Lu J, Chen H, Werner S, Williams LT (1991) *Mol Cell Biol* 11:4627–4634.
7. Schlessinger J (2000) *Cell* 103:211–225.
8. Schlessinger J, Lemmon MA (2003) *Sci STKE* 2003.
9. Mohammadi M, Schlessinger J, Hubbard SR (1996) *Cell* 86:577–587.
10. Hubbard SR (2002) *Front Biosci* 7:330–340.
11. Wilkie AO (2005) *Cytokine Growth Factor Rev* 16:187–203.
12. Shams I, Rohmann E, Eswarakumar VP, Lew ED, Yuzawa S, Wollnik B, Schlessinger J, Lax I (2007) *Mol Cell Biol* 27:6903–6912.
13. Rohmann E, Brunner HG, Kayserili H, Uyguner O, Nurnberg G, Lew ED, Dobbie A, Eswarakumar VP, Uzumcu A, Ulubil-Emeroglu M, *et al.* (2006) *Nat Genet* 38:414–417.
14. Nolen B, Taylor S, Ghosh G (2004) *Mol Cell* 15:661–675.
15. Hubbard SR (1997) *EMBO J* 16:5572–5581.
16. Zheng J, Trafny EA, Knighton DR, Xuong N, Taylor SS, Ten Eyck LF, Sowadski JM (1993) *Acta Crystallogr D* 49:362–365.
17. Madhusudan E, Trafny A , Xuong NH, Adams JA, Eyck LFT, Taylor SS, Sowadski JM (1994) *Protein Sci* 3:176–187.
18. Favelyukis S, Till JH, Hubbard SR, Miller WT (2001) *Nat Struct Biol* 8:1058–1063.
19. Chen H, Ma J, Li W, Eliseenkova AV, Xu C, Neubert TA, Miller WT, Mohammadi M (2007) *Mol Cell* 27:717–730.
20. Otwinowski Z, Minor W (1997) *Methods Enzymol* 276:307–326.
21. Read RJ (2001) *Acta Crystallogr D* 57:1378–1382.
22. Murshudov GN, Vagin AA, Dodson EJ (1997) *Acta Crystallogr D* 53:240–255.
23. Emsley P, Cowtan K (2004) *Acta Crystallogr D* 60:2126–2132.
24. Brunger AT, Adams PD, Clore GM, DeLano WL, Gros P, Grosse-Kunstleve RW, Jiang JS, Kuszewski J, Nilges M, Pannu NS, *et al.* (1998) *Acta Crystallogr D* 54:905–921.
25. DeLano WL (2002) *PyMOL* (DeLano Scientific, Palo Alto, CA).
26. Laskowski RA, MacArthur MW, Moss DS, Thornton JM (1993) *J Appl Crystallogr* 26:283–291.

Downloaded from bjo.bmj.com on 17 April 2008

Skewed X inactivation in an X linked nystagmus family resulted from a novel, p.R229G, missense mutation in the FRMD7 gene

Y Kaplan, I Vargel, T Kansu, B Akin, E Rohmann, S Kamaci, E Uz, T Ozcelik, B Wollnik and N A Akarsu

Br. J. Ophthalmol. 2008;92;135-141; originally published online 25 Oct 2007;
doi:10.1136/bjo.2007.128157

Updated information and services can be found at:
http://bjo.bmj.com/cgi/content/full/92/1/135

These include:

Data supplement *"web only table"*
http://bjo.bmj.com/cgi/content/full/bjo.2007.128157/DC1

References This article cites 14 articles, 3 of which can be accessed free at:
http://bjo.bmj.com/cgi/content/full/92/1/135#BIBL

Rapid responses You can respond to this article at:
http://bjo.bmj.com/cgi/eletter-submit/92/1/135

Email alerting service Receive free email alerts when new articles cite this article - sign up in the box at the top right corner of the article

Notes

To order reprints of this article go to:
http://journals.bmj.com/cgi/reprintform

To subscribe to *British Journal of Ophthalmology* go to:
http://journals.bmj.com/subscriptions/

Downloaded from bjo.bmj.com on 17 April 2008

Skewed X inactivation in an X linked nystagmus family resulted from a novel, p.R229G, missense mutation in the *FRMD7* gene

Y Kaplan,[1] I Vargel,[2] T Kansu,[3] B Akin,[4] E Rohmann,[5,6] S Kamaci,[7] E Uz,[8] T Ozcelik,[8] B Wollnik,[5,6] N A Akarsu[4,9]

► The supplementary table is published online only at http://bjo.bmj.com/content/vol92/issue1

[1] Department of Neurology, Gaziosmanpaşa University, Medical Faculty, Tokat, Turkey; [2] Department of Plastic and Reconstructive Surgery, Hacettepe University Medical Faculty, Ankara, Turkey; [3] Department of Neurology, Hacettepe University Medical Faculty, Ankara, Turkey; [4] Gene Mapping Laboratory, Pediatric Hematology Unit, Hacettepe University Medical Faculty, Ankara, Turkey; [5] Center for Molecular Medicine Cologne (CMMC), University of Cologne, Cologne, Germany; [6] Institute of Human Genetics, University of Cologne, Cologne, Germany; [7] Department of Orthodontics, Hacettepe University, Faculty of Dentistry, Ankara, Turkey; [8] Department of Molecular Biology and Genetics, Bilkent University, Faculty of Science, Ankara, Turkey; [9] Department of Medical Genetics, Hacettepe University Medical Faculty, Ankara, Turkey

Correspondence to:
N A Akarsu, Hacettepe University Medical Faculty, Department of Pediatrics, Pediatric Hematology Unit, Gene Mapping Laboratory, Room No. 24, Sihhiye, 06100, Ankara, Turkey; nakarsu@hacettepe.edu.tr

Accepted 6 October 2007
Published Online First
25 October 2007

ABSTRACT

Aims: This study aimed to identify the underlying genetic defect of a large Turkish X linked nystagmus (NYS) family.

Methods: Both Xp11 and Xq26 loci were tested by linkage analysis. The 12 exons and intron–exon junctions of the *FRMD7* gene were screened by direct sequencing. X chromosome inactivation analysis was performed by enzymatic predigestion of DNA with a methylation-sensitive enzyme, followed by PCR of the polymorphic CAG repeat of the androgen receptor gene.

Results: The family contained 162 individuals, among whom 28 had NYS. Linkage analysis confirmed the Xq26 locus. A novel missense c.686C>G mutation, which causes the substitution of a conserved arginine at amino acid position 229 by glycine (p.R229G) in exon 8 of the *FRMD7* gene, was observed. This change was not documented in 120 control individuals. The clinical findings in a female who was homozygous for the mutation were not different from those of affected heterozygous females. Skewed X inactivation was remarkable in the affected females of the family.

Conclusions: A novel p.R229G mutation in the *FRMD7* gene causes the NYS phenotype, and skewed X inactivation influences the manifestation of the disease in X linked NYS females.

Congenital nystagmus (NYS) is an ocular oscillatory movement disorder caused by a motor instability that can manifest with or without afferent visual system dysfunction. This entity is defined both clinically and by electronystagmography. Certain clinical features usually differentiate congenital NYS from other oscillations. NYS may be irregular, but is always conjugate and horizontal, though very rarely vertical. There may be a torsional component. Some patients with this abnormality also show head oscillations, which tend to increase when the patient attends to an object, an effort that also increases the NYS. Therefore, it seems probable that both the head tremor and the ocular oscillations are the consequence of a common disordered neural mechanism.[1]

The underlying defect in congenital NYS remains elusive. The Eye Movement Abnormalities and Strabismus Working Group proposed the term, infantile nystagmus syndrome, for the NYS that is known as congenital NYS. Although there is some controversy concerning classification of NYS in infancy, it has been suggested that NYS with an onset before 6 months of age can be divided into three categories:[2] (1) congenital idiopathic NYS in which no visual or associated neurological impairment can be found; (2) sensory deficit NYS in which there is a visual abnormality, such as ocular albinism, optic nerve hypoplasia, congenital stationary night blindness and blue cone monochromatism; (3) neurological NYS, which is associated with a neurological disorder. Category 1 is also called congenital motor NYS, which is presumed to have a primary defect in the part of the brain responsible for ocular motor control.[3]

Congenital motor NYS is a genetically heterogeneous disorder. Autosomal dominant (MIM 164100), recessive (MIM 257400) and X linked (MIM 310700) patterns of inheritance are described for this disorder. X linked inheritance is the most common form of NYS (NYS1). An irregular dominant pattern of X linked inheritance has been frequently reported, although some pedigrees support X linked recessive inheritance.[4] The penetrance is full in males and approximately 50% to 29% in females.[5 6] Large intrafamilial variance in waveforms can be observed. Two distinct loci, one on the Xq26–q27[3] and the other on the Xp11.4[7] regions have been reported as the likely loci for X linked dominant NYS. The locus on the long arm (Xq26) has been confirmed by subsequent reports of various ethnic populations.[8–10] To the best of our knowledge, there are only two reports supporting the Xp11.4 locus.[7 11] The pattern of inheritance and clinical profile of Xp11-linked families are not different from Xq26-linked pedigrees. X linked recessive NYS has also been mapped to the Xq26 region, which harbours the X linked dominant NYS locus.[10] Recently, mutations in the *FRMD7* (FERM domain-containing 7) gene have been reported as a molecular cause in Xq26-linked families.[6] Little is known about the function of the *FRMD7* gene; however, the restricted expression pattern of this gene in the human embryonic brain and developing neural retina suggests a role in eye movement and gaze stability.[6]

Herein, we report an extensive NYS pedigree, including 162 individuals across six generations from southeastern Turkey. The mode of inheritance is clearly X linked, demonstrating a reduced penetrance in female obligate gene carriers. Genetic linkage analysis confirmed the Xq26–q27 locus, and further mutation analysis identified a novel p.R229G missense mutation in the *FRMD7* gene that causes this disorder. We also detected a predisposition to skewed X inactivation in affected

Downloaded from bjo.bmj.com on 17 April 2008

females, suggesting that the X inactivation mechanism might have a role in manifestation of the disease in females.

METHODS

Clinical evaluation

The family was identified during fieldwork to study a large craniosynostosis pedigree in Antakya, Turkey. The complete pedigree structure contains over 427 individuals, including a separate branch of congenital idiopathic NYS. Only the NYS branch is included in this study, and the pedigree structure is shown in fig 1. Pedigree formation was completed in the field by NA, IV and SK. Neurological evaluation of 23 individuals was conducted by YK, a neurologist and member of the family. The recruitment criteria were NYS noted at birth or during the first 3 months of life, and no abnormalities of the ocular or neural visual pathway. Visual acuity of all the patients was measured by Snellen card. Eye movements were recorded by a video camera in 16 patients. Video recordings were further reviewed by a neuro-ophthalmologist (TK). Peripheral blood samples were collected from 48 individuals with informed consent for further molecular studies. The Hacettepe University Ethics Committee approved the study (FON 02/6-13)

Genetic linkage analysis

The family was tested for linkage to two reported loci on chromosome regions Xp11[7] and Xq26.[3] Map order and physical positions (Mb) of the polymorphic markers were obtained from the University of California Santa Cruz (USCS), Genome Bioinformatics Center (http://genome.ucsc.edu). Oligonucleotide samples were purchased from MWG-Biotechnology (Ebersberg, Germany). Site-specific PCR, 7% polyacrylamide gel electrophoresis and silver staining technique were used in genotyping the individuals. Gels were manually pictured. The Cyrillic program was used to generate haplotype and input files for linkage analysis. Two-point linkage was performed with the MLINK component of the LINKAGE package, assuming X linked dominant inheritance with 0.36 penetrance in females. Mutant allele frequencies were kept as 0.0001. Equal marker allele frequency of DNA markers was assumed.

Mutation analysis

We designed primers to amplify all 12 protein-coding exons and adjacent intronic sequences of the *FMRD7* gene by PCR using standard conditions (supplementary table). Due to its size, exon 12 was amplified in three overlapping fragments. Subsequent to amplification, PCR fragments were purified, with QIAquick spin columns (Qiagen), and directly sequenced using the corresponding forward primers with the ABI PRISM® BigDye™ Terminator v2.0 cycle sequencing ready reaction kit and an ABI PRISM® 3100 genetic analyser (Applied Biosystems). We re-sequenced all identified mutations in independent experiments, tested for co-segregation within the families, and screened 120 Turkish control individuals for the c.686C>G mutation by PCR and subsequent restriction digestion using *Bcc*I (MBI Fermentas, Germany).

Evaluation of X chromosome inactivation (XCI)

Genotyping of a highly polymorphic CAG repeat in the androgen-receptor (*AR*) gene was performed to assess the XCI patterns.[12] DNA was divided into two identical aliquots, one of

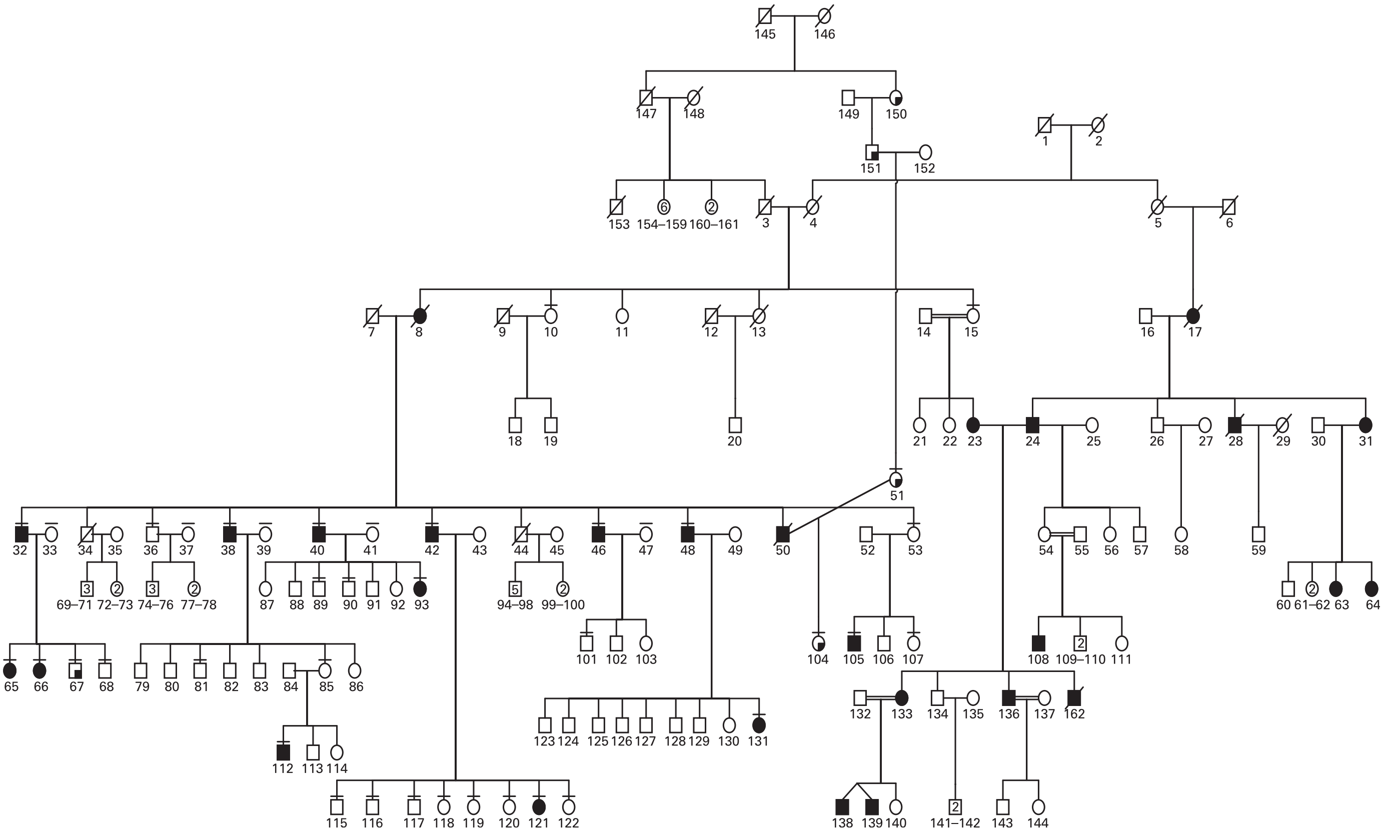
145 146
147 148 149 150
1 2
151 152
6 2
153 154–159 160–161 3 4 5 6
7 8 9 10 11 12 13 14 15 16 17
18 19 20 21 22 23 24 25 26 27 28 29 30 31
51
32 33 34 35 36 37 38 39 40 41 42 43 44 45 46 47 48 49 50 52 53 54 55 56 57 58 59
3 2 3 2 5 2 2
69–71 72–73 74–76 77–78 87 88 89 90 91 92 93 94–98 99–100 60 61–62 63 64
101 102 103 104 105 106 107 108 109–110 111
65 66 67 68 79 80 81 82 83 84 85 86
132 133 134 135 136 137 162
123 124 125 126 127 128 129 130 131
112 113 114
2
115 116 117 118 119 120 121 122 138 139 140 141–142 143 144

Figure 1 Complete pedigree structure of X linked idiopathic congenital NYS. Full shaded symbols indicate the NYS phenotype. Quarter shaded symbols demonstrate individuals with craniosynostosis. The craniosynostosis branch (relatives of individuals 150, 151 and 51) was not included in this study.

Downloaded from bjo.bmj.com on 17 April 2008

Table 1 Examination findings of the family members

PID	Gender	DOB	Nystagmus	Head oscillations	DM type II	Obesity	Other findings
23	F	1939	Pendular	+	–	–	–
24	M	1929	Pendular	+	+	+	Asthma, corneal opacity on the left, hypertension
32	M	1961	Pendular + jerk	+	+	+	Diabetic neuropathy, cataract, hypertension
38	M	1950	Pendular	–	+	+	Diabetic neuropathy, amyloid lichenosis
40	M	1945	Pendular	+	+	+	–
42	M	1943	Pendular	+	+	+	Diabetic neuropathy, psoriasis, hypertension
46	M	1939	Pendular	+	+	+	Diabetic neuropathy, ptosis on the left
48	M	1930	Pendular	+	+	+	Diabetic neuropathy, hypertension, ptosis on the right
65	F	1981	Pendular + jerk	+	–	–	–
66	F	1982	Pendular + jerk	–	–	–	Strabismus
93	F	1980	Pendular	–	–	–	–
105	M	1986	Pendular + jerk	+	–	+	Febrile convulsion
108	M	1985	Pendular	+	–	–	–
112	M	1998	Pendular	–	–	–	–
121	F	1971	Pendular	+	–	+	–
131	F	1965	Pendular	+	–	–	–
133	F	1969	Pendular	–	–	–	–
136	M	1968	Pendular	+	–	+	–
138	M	1993	Pendular	–	–	–	–
139	M	1993	Pendular	–	–	–	–
36	M	1957	–	–	+	+	–
39	F	1951	–	–	–	+	–
43	F	1951	–	–	–	+	–
53	F	1959	–	–	+	+	Psoriasis, hypertension
54	F	1960	–	–	–	+	–
69	M	1978	–	–	–	+	–
79	M	1971	–	–	–	+	–
80	M	1974	–	–	–	+	–
81	M	1976	–	–	–	+	–
82	M	1989	–	–	–	+	–
87	F	1970	–	–	–	+	–
91	M	1969	–	–	–	+	–
94	M	1989	–	–	–	+	Allergic conjuctivitis
95	M	1976	–	–	–	+	–
107	F	1983	–	–	–	+	–
115	M	1975	–	–	–	+	–
116	M	1979	–	–	–	+	–
117	M	1980	–	–	–	+	Asthma bronchiale
118	F	1970	–	–	–	+	–
119	F	1978	–	–	–	+	Asthma bronchiale
120	F	1984	–	–	–	+	–
122	F	1986	–	–	–	+	–
123	M	1967	–	–	–	+	–
124	M	1968	–	–	–	+	–
125	M	1969	–	–	–	+	–
126	M	1960	–	–	–	+	–
134	M	1968	–	–	–	+	–

DM, diabetes mellitus; DOB, date of birth; PID, Personal Identification Number presented in fig 1.

which was incubated overnight at 37°C with the methylation-sensitive restriction enzyme *Hpa*II (MBI Fermentas, Vilnius, Lithuania), for the digestion of unmethylated (or active) alleles. A second restriction enzyme, *Rsa*I (MBI Fermentas, Vilnius, Lithuania), which recognises a four-base-pair sequence not present in the amplified region of the *AR* locus, was also included in the reaction to facilitate the *Hpa*II digestion process. Male DNA with a cytogenetically verified 46,XY karyotype was used as the control for complete digestion. The other half of the DNA was treated similarly, but without *Hpa*II. After restriction-enzyme digestion, residual DNA was amplified using the primers 5′-GTC CAA GAC CTA CCG AGG AG-3′ and 5′-CCA GGA CCA GGT AGC CTG TG-3′. PCR products were separated on 10% denaturing 29:1 acrylamide-bisacrylamide gel for 5 h at 20 W. Gels were stained with ethidium bromide and visualised under UV light. Densitometric analysis of the alleles was performed at least twice for each sample using the appropriate software (MultiAnalyst v1.1; Bio-Rad, Hercules, CA). A corrected ratio (CrR) was calculated by dividing the ratio of the predigested sample (upper/lower allele) by the ratio of the non-predigested sample for normalisation of the ratios that were obtained from the densitometric analyses. The use of a CrR compensates for preferential amplification of the shorter allele when the number of PCR cycles increases.[13] A skewed population is defined as a cell population with >80% expression of one of the AR alleles. This corresponds to CrR values of <0.25 or >4.0.

Downloaded from bjo.bmj.com on 17 April 2008

Table 2 Two point LOD scores with the DNA markers selected from Xp11 and Xq26 regions

	Recombination fraction (θ) cM					
Marker	**0.00**	**0.01**	**0.05**	**0.10**	**0.20**	**Exclusion (cM)**
Xp11						
DXS6810	−∞	−5.35	−2.64	−1.54	−0.58	7
GATA144D03	−∞	−5.19	−2.50	−1.43	−0.52	6
DXS7132	−∞	−5.32	−2.62	−1.53	−0.57	7
Xq26						
GATA172D05	−∞	−1.78	−0.53	−0.11	0.12	–
GATA165B12	−∞	0.54	1.07	1.16	1.00	–
DXS1047	−∞	1.08	1.58	1.62	1.37	–
DXS8068	−∞	0.38	0.93	1.03	0.91	–
DXS8072	3.74	3.68	3.44	3.12	2.45	–
DXS8071	0.82	0.80	0.72	0.62	0.43	–
DXS1187	3.37	3.32	3.10	2.81	2.21	–
DXS8033	3.68	3.62	3.38	3.07	2.41	–
DXS8094	4.04	3.98	3.72	3.38	2.65	–
DXS1062	2.55	2.51	2.33	2.09	1.59	–
DXS1192	0.48	0.47	0.43	0.38	0.29	–
DXS984	3.74	3.68	3.44	3.12	2.45	–
GATA31E08	3.37	3.32	3.10	2.81	2.21	–

Exclusion area = recombination fraction (cM) at which the LOD score was ⩽ −2. Significant LOD scores were obtained with the DNA markers from the Xq26 region.

RESULTS

Clinical presentation and formal genetics of the family

The most striking findings of this pedigree were, 1, NYS and, 2, obesity and type 2 diabetes in some family members (table 1). Other findings included craniosynostosis and allergic complaints, such as bronchial asthma. In all, 20 patients had rhythmic pendular type NYS, with varying frequencies and amplitudes. Video recordings of 16 individuals supported the clinical observations. On lateral gaze, four individuals had horizontal jerk NYS, whereas six patients had spontaneous head oscillations, and 13 had oscillations during fixation (table 1). Visual acuity among the patients varied from 20/20 to 20/100. Direct ophthalmoscopic findings were unremarkable. In all, seven NYS patients had diabetes, and 10 were obese. Among the non-NYS family members, 27 were obese (two of them with diabetes) (table 1) suggesting independent segregation of the two disorders (NYS and obesity and/or type 2 diabetes) in the same family. Regarding the NYS phenotype, male-to-male transmission was not observed. This finding supported X linked inheritance. There were 33 obligate gene carrier females in this family, and only 12 of them developed NYS (fig 1); therefore, the penetrance of the NYS phenotype in females was estimated to be approximately 36% for this family.

Linkage studies

The family was tested for a linkage to both Xp11.4-p11.3[7] and Xq26–q27[3] loci. The NYS phenotype was previously mapped between the DNA markers DXS8015 and DXS1003 on the Xp11.4 locus. The DNA markers DXS6810, GATA144D04 and DXS7132 were used in this study, and the physical positions of these markers are: DXS8015 (39.44 Mb)-DXS6810, (42.57 Mb)-GATA144D04 and (44.67 Mb)-DXS1003 (46.19 Mb)-DXS7132 (64.33 Mb). Four NYS patients were recombinant for the entire region (data not shown). Negative LOD scores were also obtained. The excluded region was 6–7 cM for each DNA marker (table 2).

Significant LOD scores were obtained for the entire region, with a maximum of 4.04 at $\theta = 0$ cM for the DNA marker DXS8094 (table 2) in the Xq26–q27 region (fig 2). A single cross-over event in an NYS patient (person 40) positioned the disease gene telomeric to the DNA marker DXS8068. We also observed the first homozygote female case of the NYS phenotype (fig 1, person 133). No phenotypic differences were observed among the females, in terms of homozygote and heterozygote states (table 1).

Mutation results

We sequenced all 12 coding exons of the recently described X linked NYS gene *FRMD7*, which was located in the critical region in two affected male individuals of the family, and identified the c.686C>G mutation in exon 8 of the gene (fig 3A). The mutation co-segregated with the disease in the family (fig 3B) and was not observed in 120 healthy individuals of the same ethnic background. The novel c.686C>G mutation predicted a substitution of a conserved arginine at amino acid position 229 in the functionally important FERM-C domain of the protein by glycine (p.R229G). Interestingly, three other missense mutations in the FERM-C domain of FRMD7 have been described in the original gene identification paper[6] (fig 3C), suggesting an important role for this domain in the pathogenesis of congenital NYS.

X chromosome inactivation results

Since at least seven females in the pedigree had NYS, we analysed the XCI patterns to verify if skewed XCI could be responsible for the clinical manifestation of the disease. Skewed patterns with ratios of 81:19 per cent in individual 65, 85:15 per cent in 121, and 80:20 per cent in 131 and 133 was apparent, while individual 23 was not informative, and only individuals 93 and 66 displayed random XCI with ratios of 57:43 per cent and 62:38 percent, respectively. Among the non-NYS females, XCI status was analysed in 18 individuals. With the exception of individual 35, who had a skewed XCI (93:7) pattern, and four more non-informative females (individuals 41, 43, 54 and 86), all women displayed random XCI profiles (table 3). Skewed X inactivation was significantly increased in the NYS females when compared with the non-NYS females in the family (odds ratio was 26:1; 95% CI = 1.83 to 367.7).

Downloaded from bjo.bmj.com on 17 April 2008

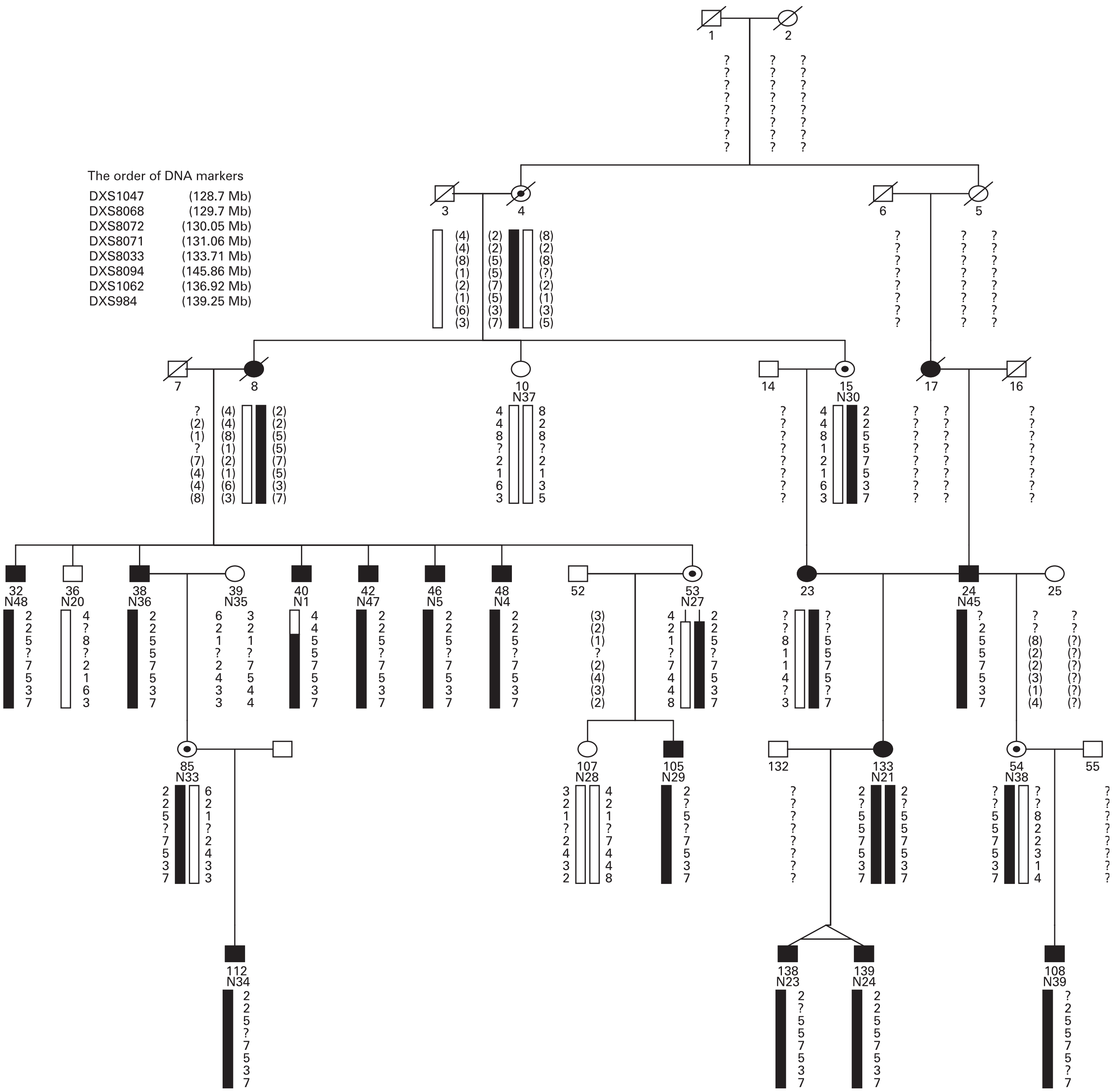

Figure 2 Haplotype structure between the NYS phenotype and the DNA markers selected from Xq26. The order and the physical locations (Mb) of the DNA markers are shown to the upper left. A single recombination event in affected individual 40 positioned the disease gene telomeric to DXS8068 containing the *FRMD7* gene (130.93 Mb).

DISCUSSION

In this study, we described a large family with X linked congenital NYS. The disorder was completely penetrant in males; however, reduced penetrance was observed in females. Various penetrance rates, ranging from 54% to 29%, are suggested to be due to family size.[3 5 6] Our study also supported 36% penetrance in females. This extremely low penetrance rate in females might challenge the mode of inheritance estimations. For genetic counselling purposes, it might be difficult to distinguish X linked recessive and dominant patterns in small family trees. Genetic linkage analysis provided strong evidence of linkage to the previously established locus on Xq26–27, which is the major locus for X linked NYS (NYS1). A recombination event in a single affected male positioned the disease gene telomeric to the DNA marker DXS8068 (fig 2). Combining these data with previous studies, the 8 Mb region residing between DNA markers DXS8068 and DXS1211 containing the recently reported *FRMD7* gene[6] was critical for this family.

We identified the novel p.R229G missense mutation in the *FRMD7* gene in the study family. The following points support the disease-causing nature of this mutation: (i) p.R229G co-segregated with the disease in this family; (ii) our control studies excluded p.R229G as a non-synonymous polymorphism

Downloaded from bjo.bmj.com on 17 April 2008

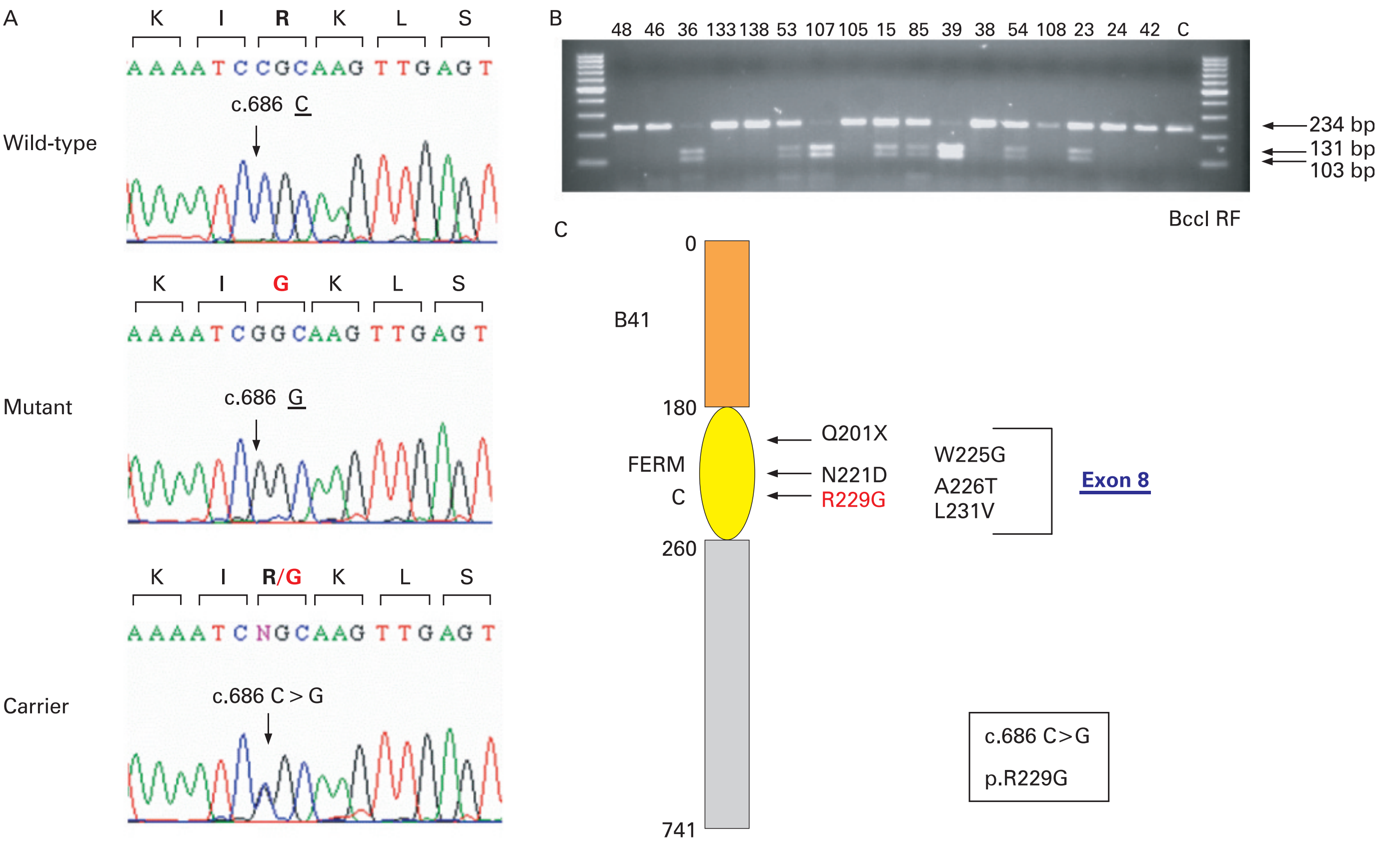
A
K I R K L S
AAAATCCGCAAGTTGAGT
c.686 C
Wild-type
K I G K L S
AAAATCGGCAAGTTGAGT
c.686 G
Mutant
K I R/G K L S
AAAATCNGCAAGTTGAGT
c.686 C > G
Carrier
B
48 46 36 133 138 53 107 105 15 85 39 38 54 108 23 24 42 C
234 bp
131 bp
103 bp
BccI RF
C
0
B41
180
FERM C
260
741
Q201X
N221D
R229G
W225G
A226T
L231V
Exon 8
c.686 C>G
p.R229G

Figure 3 Identification of a novel missense mutation in the *FRMD7* gene. (A) Representative sequence chromatograms of the identified c.686C>G (p.R229G) mutation in an affected male (mutant), a carrier female (carrier) and an unaffected male (wild-type). (B) Co-segregation of the mutation in the family. Results of *Bcc*I restriction fragment analysis presenting an undigested 234 bp PCR-fragment in affected male individuals, a fully digested PCR fragment in unaffected males (two fragments 131 bp and 101 bp in size), and one undigested and one digested allele in carrier females (three fragments 234 bp, 131 bp and 101 bp in size). A non-digested sample, labelled as C, was included as a control (C) schematic view of conserved *FRMD7* domains and locations of described mutations located in the FERM-C domain.

Table 3 Distribution of skewed x-inactivation between nystagmus and normal members of the family

	PID	DNA no.	Status	Skewing degree
Skewed				
1	35	N42	Normal	93:7
2	121	N46	Affected	85:15
3	65	N31	Affected	81:19
4	131	N40	Affected	80:20
5	133	N21	Affected	80:20
Random				
1	33	N18	Normal	72:28
2	45	N11	Normal	71:29
3	107	N28	Normal	71:29
4	72	N41	Normal	69:31
5	15	N30	Normal	67:33
6	11	N37	Normal	67:33
7	53	N27	Normal	63:37
8	66	N16	Affected	62:38
9	93	N26	Affected	57:43
10	118	N13	Normal	56:44
12	99	N10	Normal	54:46
13	122	N14	Normal	54:46
14	119	N43	Normal	53:47
15	120	N12	Normal	51:49
16	Spouse of 129	N7	normal	50:50

PID reflects personal identification numbers on fig 1. A total of five individuals (fig 1, individuals 23, 41, 43, 54 and 86) were not informative. The disease status of non-informative individuals was normal except person 23.

Downloaded from bjo.bmj.com on 17 April 2008

in the Turkish population; (iii) the mutation is located in the FERM-C domain in the surrounding of previously described missense mutations in families with congenital NYS.[6 14]

The functional role of *FRMD7* remains to be elucidated. The *FRMD7* transcript is abundantly expressed in most tissues, and a localised and restricted expression was found to be involved in embryonic development in regions affecting motor control of eye development.[6] Homologies of the B41 and FERM-C domains of *FRMD7* to other proteins, such as *FARP1* and *FARP2*, which are involved in neurite branching of cortical neurons, led to the hypothesis that *FRMD7* could also be involved in the development of similar neuronal pathways.

Skewed X inactivation has consistently been suggested as a mechanism that may influence the penetrance of X linked NYS in females;[3 7 8 9] however, except for only one study,[7] an X inactivation pattern was not previously studied in NYS families. No correlation between X inactivation patterns and the NYS phenotype was observed in this sole study.[7] Nevertheless, NYS in the family used in that study was linked to the Xp11 region rather than the major NYS locus on Xq26–q27. Our Xq26-linked NYS family implies that skewed XCI could be a factor that influences the clinical manifestation of NYS in females. It is well established that skewed XCI is a rare event in a diverse group of control females.[15 16] In agreement with this prior observation, we only observed skewed X inactivation in a single healthy spouse (individual 35). None of the obligate gene carrier females and none of the remaining healthy spouses demonstrated skewed X inactivation (table 3); however, increased susceptibility to skewed X inactivation was apparent in the clinically affected females. On the other hand, we observed random X inactivation in two affected females, individuals 66 and 93, with XCI scores of 62:38 and 57:43, respectively. This finding may be a reflection of tissue mosaicism, which has been clearly shown in women.[16] To the best of our knowledge, inactivation status of the *FRMD7* gene has not been studied. Further investigations of the X inactivation status of *FRMD7* might help contribute to an understanding of the irregular pattern of inheritance of NYS1.

Acknowledgements: We are grateful to the family members for their participation in the study. We thank the Hacettepe University Craniofacial Surgery Study Group members: Yucel Erk, Emin Mavili, and Gokhan Tuncbilek (Plastic and Reconstructive Surgery), Kemal Benli (Neurosurgery), Aysenur Cila (Radiology), and Sevim Balci (Genetics) for their evaluation of the family members with craniosynostosis. This work was presented in the 8th European Neuro-Ophthalmology Society (EUNOS) Meeting, 26–29 May 2007, Istanbul, Turkey.

Funding: This study was supported by The Hacettepe University Research Foundation (number 00-01-101-010), The Scientific and Technological Research Council of Turkey (number TUBITAK-SBAG 3334) and The International Centre for Genetic Engineering and Biotechnology (ICGEB-CRP/TUR04-01).

Competing interests: None.

REFERENCES

1. **Leigh RJ,** Averbuch-Heller L. Nystagmus and related ocular motility disorders. In: *Walsh & Hoyt's clinical neuro-ophthalmology, Vol. 1*. 5th edn. In: N R Miller, NJ Newman, eds. Williams & Wilkins, Baltimore, 1998:1483.
2. **Hoyt C.** *Clinical congenital nystagmus. Evaluation and treatment. North American Neuro-Ophthalmology Society 31st Annual Meeting Syllabus,* 2005:319.
3. **Kerrison JB,** Vagefi MR, Barmada MM, *et al*. Congenital motor nystagmus linked to Xq26–q27. *Am J Hum Genet* 1999;**64**:600–7.
4. **Forrsman B,** Ringer B. Prevalence and inheritance of congenital nystagmus in a Swedish population. *Ann Hum Genet* 1971;**35**:139–47.
5. **Kerrison JB,** Giorda R, Lenart TD, *et al*. Clinical and genetic analysis of a family with X linked congenital nystagmus (NYS1). *Ophthalmic Genet* 2001;**22**:241–8.
6. **Tarpey P,** Thomas S, Sarvananthan UM, *et al*. Mutations in FRMD7, a newly identified member of the FERM family, cause X linked idiopathic congenital nystagmus. *Nat Genet* 2006;**38**:1242–4.
7. **Cabot A,** Rozet JM, Gerber S, *et al*. A gene for x-linked idiopathic congenital nystagmus (NYS1) maps to chromosome Xp11.4–p11.3. *Am J Hum Genet* 1999;**64**:1141–6.
8. **Mellot M,** Brown J, Fingert JH, *et al*. Clinical characterization and linkage analysis of a family with congenital X linked nystagmus and deuteranomaly. *Arch Ophthalmol* 1999;**117**:1630–3.
9. **Zhang B,** Xia K, Ding M, *et al*. Confirmation and refinement of a genetic locus of congenital motor nystagmus in Xq26.3–q27.1 in a Chinese family. *Hum Genet* 2005;**116**:128–31.
10. **Guo X,** Li S, Jia X, *et al*. Linkage analysis of two families with x-linked recessive congenital motor nystagmus. *J Hum Genet* 2006;**51**:76–80.
11. **Oetting WS,** Armstrong CM, Holleschau AM, *et al*. Evidence for genetic heterogeneity in families with congenital motor nystagmus (CN). *Ophthalmic Genet* 2000;**21**:227–33.
12. **Allen RC,** Zoghbi HY, Moseley AB, *et al*. Methylation of *Hpa*II and *Hha*I sites near the polymorphic CAG repeat in the human androgen-receptor gene correlates with X chromosome inactivation. *Am J Hum Genet* 1992;**51**:1229–39.
13. **Delforge M,** Demuynck H, Vandenberghe P, *et al*. Polyclonal primitive hematopoietic progenitors can be detected in mobilized peripheral blood from patients with high-risk myelodysplastic syndromes. *Blood* 1995;**86**:3660–7.
14. **Schorderet DF,** Tiab L, Gaillard MC, *et al*. Novel mutations in FRMD7 in X linked congenital nystagmus. *Hum Mutat* 2007;**28**:525.
15. **Busque L,** Mio R, Mattioli J, *et al*. Nonrandom X-inactivation patterns in normal females: lyonization ratios vary with age. *Blood* 1996;**88**:59–65.
16. **Sharp A,** Robinson D, Jacobs P. Age- and tissue-specific variation of X chromosome inactivation ratios in normal women. *Hum Genet* 2000;**107**:343–9.

Clin Res Cardiol
DOI 10.1007/s00392-007-0574-0

ORIGINAL PAPER

S. Pabst
B. Wollnik
E. Rohmann
Y. Hintz
K. Glänzer
H. Vetter
G. Nickenig
C. Grohé

A novel stop mutation truncating critical regions of the cardiac transcription factor NKX2-5 in a large family with autosomal-dominant inherited congenital heart disease

Received: 15 May 2007
Accepted: 18 July 2007
Published online: 25 September 2007

Prof. Dr. med. Christian Grohé (✉)
S. Pabst · G. Nickenig
Medizinische Klinik II
S.-Freud-Str. 25
Universitätsklinikum Bonn
53105 Bonn, Germany
E-Mail: c.grohe@poliklinik-bonn.de

B. Wollnik · E. Rohmann
Zentrum für Molekulare Medizin Köln
(ZMMK) und Institut für Humangenetik
Universität zu Köln
Köln, Germany

Y. Hintz · K. Glänzer · H. Vetter
Medizinische Univ. Poliklinik
Bonn, Germany

Abstract We report on a familial screen of five female members in three generations affected by an autosomal-dominant inherited atrioventricular (AV) conduction block associated with atrial septal defects (ASD) and other congenital cardiovascular diseases (CCVD), such as pulmonary artery stenosis (PAS), patent foramen ovale (PFO) and ventricular septal defect (VSD). We tested the cardiac transcription factor *NKX2-5* which is known to cause CCVD with variable phenotype and penetrance by direct sequencing of the two *NKX2-5* coding exons in the index patient and identified a novel heterozygous c.325G > T mutation in exon 1 of the gene. This mutation co-segregated with the disease in the family and was present in all five affected family members, but not in 100 control chromosomes. The c.325G > T mutation is predicted to introduce a stop codon at amino-acid position 109 (p.E109X). The truncated protein lacks all of the functionally important domains of the cardiac transcription factor. Therefore, it is very likely that this novel mutation causes a complete loss of *NKX2-5* function and haploinsufficiency is the pathophysiological mechanism underlying the disease in the family.

Key words
congenital heart disease – mutation – NKX2-5 – AV conduction block

Introduction

Congenital cardiovascular diseases (CCVDs) are the most common developmental anomalies, and are diagnosed in 1% of newborns. Failure of atrial or ventricular septation accounts for nearly 50% of CCVDs. The secundum atrial septal defect (ASD) accounts for ~10% of congenital cardiac malformations, affecting 1 in 1000 live births [1].

ASD, as the most often inherited CCVD, can occur in monogenic familial conditions, sometimes in association with other cardiac malformations, or as one feature of syndromes. Large ASDs can lead to heart failure in childhood, pulmonary hypertension and right heart dilatation due to smaller untreated defects can develop in later life. In adults, percutaneous closure techniques via catheterization are mostly used to occlude the ASD.

An association of ASD with AV conduction block and other CCVDs was previously described in sporadic patients and families with heterozygous mutations in the cardiac transcription factor *NKX2-5* gene [2–6].

The human *NKX2-5* gene is located on chromosome 5q31.1 and the two protein-coding exons encode a 324 amino-acid protein with several important functional domains for transcriptional activation and gene regulation. Mutations in *NKX2-5* were described in patients with variable clinical presentation of CCVD including missense, nonsense, and frame-shifting mutations such as small deletions and insertions [2]. Patients with *NKX2-5* mutations are known to have a higher incidence of ASD, with or without concomitant AV conduction defects. However, many other cardiac malformations, such as tetralogy of Fallot (TOF), VSD, hypoplastic left heart syndrome and L-transposition of the great arteries, have been reported in association with mutations of *NKX2-5*. No genotype-phenotype correlation between the functional consequence of *NKX2-5* mutation and clinical phenotype could be established.

Deletion of both *NKX2-5* alleles in mice result in lethality due to impaired cardiac looping [7]. Interestingly, heterozygosity resulted in hypoplasia of the atrioventricular conduction system in mice [8].

We report a family with five female members in three generations affected by an autosomal-dominant inherited atrioventricular (AV) conduction block associated with atrial septal defects (ASD) and other congenital cardiovascular diseases (CCVD), such as pulmonary artery stenosis (PAS), patent foramen ovale (PFO) and ventricular septal defect (VSD).

The aim of the study was to identify the molecular basis of this autosomal-dominant disorder causing CCVD in the family. The primary candidate gene to examine was *NKX2-5* for the reasons described above.

Patients and methods

The female index patient (Fig. 1a, II.5) was 63 years old. She presented with bradyarrhythmia absoluta (pacemaker since 1984) and an ASD. She had two daughters (III.2 and III.3). Both daughters also had a first-degree AV-block (Fig. 1d) and an ASD. While the elder daughter had a VSD, the younger one presented with an additional pulmonary artery stenosis (PAS). PQ interval was progredient over the last 20 years. The elder sib had two daughters (IV.1 and IV.2), both of them affected by a first-degree AV-block and an ASD. Moreover, they both presented with a patent foramen ovale (PFO). Both children had a second-degree AV-block at night. Being without clinical symptoms, they have not yet received a pacemaker. Both parents of the index patient had died and there was no information about CCVD. PQ interval, QTc time and clinical presentation of affected family members are shown in Table 1. We also examined all three sibs (one sister, two brothers) of the index patient (II.5), as well as the husbands of patients II.5 and III.2 Blood samples were taken from the five affected family members and the three sibs of the index patient.

Table 1 Clinical characterization of the affected family members. *AF* atrial fibrillation, *ASD* atrial septal defect, *AV-B* atrioventricular block, *CCVD* congenital cardiovascular diseases, *OP* operation, *PAS* pulmonary artery stenosis, *PFO* patent foramen ovale, *PM* pacemaker, *s* seconds, *VSD* ventricular septal defect

Patient	Year of birth	CCVD (therapy)	PQ interval (ms)		QTC time (ms)	
II.5	1942	ASD, AV-B I°, AF (PM 1984)	1984: 293	2007: AF	1984: 320	2007: 351
III.2	1967	ASD, VSD, AV-B I°	1984: 282	2007: 320	1984: 324	2007: 346
III.3	1971	ASD, PAS, AV-B I° (ASD-OP 1976)	1984: 278	2007: 344	1984: 328	2007: 364
IV.1	1983	ASD, PFO, AV-B I°, II°a	1996: 151	2005: 392	1996: 314	No data
IV.2	1997	ASD, PFO, AV-B I°, II°b	1997: 120	2005: 212	1997: 305	No data

DNA was isolated from blood samples taken by venous puncture. Informed consent of all individuals or parents of minors was obtained before examination. The study was approved by the Ethics Committee of the University Hospital Bonn.

Mutation analysis

The two protein-coding exons and adjacent intronic sequences of the *NKX2-5* gene were amplified by PCR using standard conditions (exon 1, forward primer 5′-ggcaccatgcagggaagctg-3′ and reverse primer 5′-caccaggcatcttacattctgaac-3′; exon 2: forward primer 5′-ccacgaggatcccttaccatta-3′ and reverse primer 5′-ggtctccgcaggagtgaatg-3′). Subsequently, PCR fragments were purified using QiaQuick spin columns (Qiagen) and completely sequenced with an ABI 3100 sequencer (Applied Biosystems).

Identified mutations were resequenced in independent experiments, tested for co-segregation within the family, and we screened 50 matched healthy control individuals with the same ethnical background (non-familial, equal amount of males and females without any history for cardiac anomalies, not matched for age) for the mutation by direct sequencing.

Molecular results

After detailed clinical characterization of the autosomal-dominant inherited phenotype in the family, we considered the *NKX2-5* cardiac transcription gene as a highly relevant functional candidate gene, because *NKX2-5* mutation had previously been described in ASD patients associated with AV conduction block.

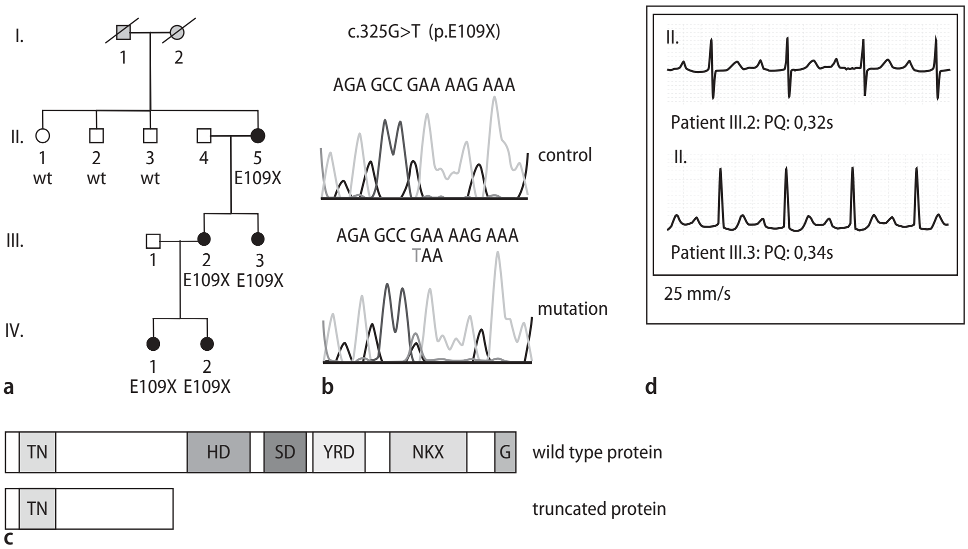

Fig. 1 Pedigree and mutation analysis. **a** Pedigree of the family studied. Affected individuals are shown by filled symbols. Results of the molecular analysis are given for each family member tested (E109X in all affected family members, wild type (wt) in three healthy individuals in the second generation). **b** Sequence chromatograms showing the identified c.325G>T mutation in comparison to a control sequence. **c** Functional effect of the p.E109X nonsense mutation on the protein. Comparison of wild-type and truncated protein. **d** Electrocardiogram showing a first-degree AV conduction block in individual III.2 and III.3; ECG 25 mm/s

Therefore, we initially sequenced the two *NKX2-5* coding exons in the index patient and identified the novel heterozygous c.325G > T mutation in exon 1 of the gene that was present in all five affected family members, but neither in the three healthy sibs of the index patient (II.5), nor in 100 control chromosomes (Figs. 1 a, b). The penetrance of the mutation in the family was 100%. The c.325G > T mutation predicts the introduction of a stop codon at amino-acid position 109 (p.E109X). The truncated protein lacks all of the functionally important domains of the cardiac transcription factor (Fig. 1 c). Therefore, it is very likely that this novel mutation causes a complete loss of *NKX2-5* function and haploinsufficiency is the pathophysiological mechanism underlying the disease in the family.

Discussion

Our study identified a novel nonsense mutation in the cardiac transcription factor *NKX2-5* in the presented family. Evidence for the disease-causing nature of this mutation includes: (i) co-segregation with the disease in the family; (ii) absence of the disease in 100 healthy control individuals; and (iii) the predicted loss of function of the mutant allele. The mutation is predicted to truncate the protein after 109 amino-acids and, thereby, the mutant protein lacks all known domains that are important for its functionality including the homeodomain (Fig. 1 c). This clearly shows that haploinsufficiency by loss of function is the pathophysiological mechanism in this family. It is interesting to note that haploinsufficiency in *NKX2-5* ± mice caused alterations of the AV-node, which is in accordance with the clinical phenotype in the family we are reporting on.

In the presented family we could observe a complex pattern of CCVD. Though ASD and AV block are the most frequent CCVD in different *NKX2-5* mutations, they are not found in all cases and, furthermore, the combination with other congenital heart disorders is common, but very unpredictable [9]. The phenotype of CCVD is also distinct in each affected family member presented here, only ASD and AV block are found in each patient. We emphasize the fact that the AV block is progredient in each individual as described before, but it also seems to be progressive in the descendants compared to the respective mother (Fig. 1 d). Although there are numerous reports of tetralogy of Fallot or isolated pulmonary valve stenosis, there has been no description of patent foramen ovale and pulmonary artery stenosis in a family before. Atrial fibrillation though, as seen in our index patient, seems to be common in patients with *NKX2-5* mutations. Taken together, the phenotype of patients with defects in *NKX2-5* mutations is highly variable, even within families. Thus, it is difficult to outline any significant genotype-phenotype correlation.

Genetic factors play an important role in the development of congenital heart disease, especially ASD/VSD, and previous studies showed that heterozygous mutations in *NKX2-5* cause a subset of familial ASD [9–11]. ASD is the most common CCVD in over 1 in

© Steinkopff Verlag 2007

1000 live births and its association with other AV block types of cardiac arrhythmias increases the symptomatic risk for patients. Therefore, a molecular genetic analysis, as presented in this study, can identify the underlying cause as well as identify family members at risk for the disease. Genetic and clinical screening will appear to be most helpful in identifying individuals who await operative reconstruction during the progressive course of the underlying congenital heart disease [12, 13].

Conclusion

As AV block seems to be progredient in most *NKX2-5* mutations and often requires the implantation of a pacemaker in the course of disease, identification of patients carrying *NKX2-5* mutations is important for accurate and early therapy.

References

1. Burn J, Goodship J (1996) Congenital heart disease. In: Rimoin DL, Connor JM, Pyeritz RE (eds) Emery and Rimoin's Principals and Practice of Medical Genetics. Churchill-Livingstone, New York, NY, pp 767–828
2. Hirayama-Yamada K, Kamisoago M, Akimoto K et al (2005) Phenotypes with GATA4 or NKX2-5 mutations in family atrial septal defect. Am J Med Genet A 135:47–52
3. Ikeda Y, Hiroi Y, Hosoda T et al (2002) Novel point mutation in the cardiac transcription factor CSX/NKX2-5 associated with congenital heart disease. Circ J 66:561–563
4. Elliot DA, Kirk EP, Yeoh T et al (2003) Cardiac homeobox gene NKX2-5 mutations and congenital heart disease. JACC 11:2072–2076
5. Benson DW, Silberbach GM, Kavanaugh-McHugh A et al (1999) Mutations in the cardiac transcription factor NKX2-5 affect diverse cardiac developmental pathways. J Clin Invest 104:1567–1573
6. König K, Will JC, Berger F, Müller D, Benson DW (2006) Familial congenital heart disease, progressive atrioventricular block and the cardiac homeobox transcription factor gene NKX2-5. Clin Res Cardiol 9:499–503
7. Lyons I, Parsons LM, Hartley L et al (1995) Myogenic and morphogenetic defects in the heart tubes of murine embryos lacking the homeo box gene NKX2-5. Genes Dev 9:1654–1666
8. Jay PY, Harris BS, Maguire CT et al (2004) NKX2-5 mutation causes anatomic hypolasia of the cardia conduction system. J Clin Invest 113:1130–1137
9. Schott JJ, Benson DW, Basson CT et al (1998) Congenital heart disease caused by mutations in the transcription factor NKX2-5. Science 281:108–101
10. Engberding R, Yelbuz TM, Breithardt G (2007) Isolated noncompaction of the left ventricular myocardium. Clin Res Cardiol 7:481–488
11. Mayer B, Erdmann J, Schunkert H (2007) Genetics and heritability of coronary artery disease and myocardial infarction. Clin Res Cardiol 1:1–7
12. Tagarakis GI, Tsolaki-Tagaraki F, Tsolaki M, Diegele A, Kazis D, Rouska E (2007) The role of SOAT-1 polymorphisms in cognitive decline and delirium after bypass heart surgery. Clin Res Cardiol, in press
13. Norozi K, Wessel A, Buchhorn R, Alpers V, Arnhold JO, Zoege M, Geyer S (2007) Comparison of two classification scales in adolescents and adults with operated congenital heart defects. Clin Res Cardiol, in press

HUMAN MUTATION 27(7), 633–639, 2006

RAPID COMMUNICATION

Mutations in the *lipoma HMGIC fusion partner-like 5* (*LHFPL5*) Gene Cause Autosomal Recessive Nonsyndromic Hearing Loss

Ersan Kalay,[1–3] Yun Li,[4,5] Abdullah Uzumcu,[6] Oya Uyguner,[6] Rob W. Collin,[2] Refik Caylan,[7] Melike Ulubil-Emiroglu,[8] Ferry F.J. Kersten,[2] Gunter Hafiz,[8] Erwin van Wijk,[2] Hulya Kayserili,[6] Edyta Rohmann,[4,5] Janine Wagenstaller,[9] Lies H. Hoefsloot,[1] Tim M. Strom,[9,10] Gudrun Nürnberg,[11,12] Nermin Baserer,[8] Anneke I. den Hollander,[1,13] Frans P.M. Cremers,[1,13] Cor W.R.J. Cremers,[2] Christian Becker,[11,12] Han G. Brunner,[1,13] Peter Nürnberg,[11,14] Ahmet Karaguzel,[3] Seher Basaran,[6] Christian Kubisch,[4,5,14] Hannie Kremer,[2] and Bernd Wollnik[4–6]*

[1]Department of Human Genetics, Radboud University Nijmegen Medical Centre, Nijmegen, The Netherlands; [2]Department of Otorhinolaryngology, Radboud University Nijmegen Medical Centre, Nijmegen, The Netherlands; [3]Department of Medical Biology, Faculty of Medicine, Karadeniz Technical University, Trabzon, Turkey; [4]Center for Molecular Medicine Cologne (CMMC), University of Cologne, Cologne, Germany; [5]Institute of Human Genetics, University of Cologne, Cologne, Germany; [6]Medical Genetics Department, Istanbul Medical Faculty, Istanbul University, Istanbul, Turkey; [7]Department of Otorhinolaryngology, Faculty of Medicine, Karadeniz Technical University, Trabzon, Turkey; [8]Department of Otorhinolaryngology, Istanbul Medical Faculty, Istanbul University, Istanbul, Turkey; [9]Institute of Human Genetics, GSF National Research Center for Environment and Health, München, Germany; [10]Institute of Human Genetics, Klinikum Rechts der Isar, Technical University, München, Germany; [11]Cologne Center for Genomics, University of Cologne, Cologne, Germany; [12]RZPD Deutsches Ressourcenzentrum für Genomforschung GmbH, Berlin, Germany; [13]Nijmegen Centre for Molecular Life Science, Nijmegen, The Netherlands; [14]Institute for Genetics, University of Cologne, Cologne, Germany

Communicated by Henrik Dahl

In two large Turkish consanguineous families, a locus for autosomal recessive nonsyndromic hearing loss (ARNSHL) was mapped to chromosome 6p21.3 by genome-wide linkage analysis in an interval overlapping with the loci *DFNB53* (*COL11A2*), *DFNB66*, and *DFNB67*. Fine mapping excluded *DFNB53* and subsequently homozygous mutations were identified in the *lipoma HMGIC fusion partner-like 5* (*LHFPL5*) gene, also named *tetraspan membrane protein of hair cell stereocilia* (*TMHS*) gene, which was recently shown to be mutated in the "hurry scurry" mouse and in two *DFNB67*-linked families from Pakistan. In one family, we found a homozygous one-base pair deletion, c.649delG (p.Glu216ArgfsX26) and in the other family we identified a homozygous transition c.494C>T (p.Thr165Met). Further screening of index patients from 96 Turkish ARNSHL families and 90 Dutch ARNSHL patients identified one additional Turkish family carrying the c.649delG mutation. Haplotype analysis revealed that the c.649delG mutation was located on a common haplotype in both families. Mutation screening of the *LHFPL5* homologs *LHFPL3* and *LHFPL4* did not reveal any disease causing mutation. Our findings indicate that LHFPL5 is essential for normal function of the human cochlea. Hum Mutat 27(7), 633–639, 2006. © 2006 Wiley-Liss, Inc.

KEY WORDS: deafness; hearing loss; autosomal-recessive; gene identification; *LHFPL5*

INTRODUCTION

Hearing impairment is the most common inherited disorder of a person's senses; therefore, understanding the various pathophysiological processes causing hearing loss has an important impact on advanced therapeutic strategies. The approximate prevalence of hearing loss caused by genetic factors has been estimated to

Received 28 February 2006; accepted revised manuscript 27 April 2006.

*Correspondence to: Bernd Wollnik, MD, Center for Molecular Medicine Cologne (CMMC) and Institute of Human Genetics, University of Cologne, Kerpener Str. 34, 50931 Cologne, Germany. E-mail: bwollnik@uni-koeln.de

Grant sponsor: National Genome Research Network, German Federal Ministry of Science and Education; Grant sponsor: Young Scientist Award Program, Turkish Academy of Sciences; Grant number: BW/TUBA-GEBIP/2002-1-20; Grant sponsor: European Commission FP6 Integrated Project EUROHEAR; Grant number: LSHG-CT-20054-512063; Grant sponsor: Research Fund of Istanbul University Grant number: T-1255/01112001; Grant sponsor: Karadeniz Technical University Research Fund; Grant number: 2002.114.001.3.

Ersan Kalay and Yun Li contributed equally to this work.

Senior authors Hannie Kremer and Bernd Wollnik contributed equally to this work.

DOI 10.1002/humu.20368

Published online in Wiley InterScience (www.interscience.wiley.com).

© 2006 WILEY-LISS, INC.

be at least 1 per 2,000 [Mehl and Thomson, 1998, 2002]. The spectrum of hereditary hearing loss is broad and ranges from nonsyndromic hearing loss without any other phenotypic abnormality to various forms of syndromic hearing loss. Overall, the most common hereditary form is autosomal recessive nonsyndromic hearing loss (ARNSHL), accounting for >70% of the cases [Morton, 1991]. In recent years, improved molecular genetic techniques have led to the identification of more than 67 loci for ARNSHL (*DFNB*) and to date 23 of the corresponding genes have been identified (Hereditary Hearing loss Homepage; http://webhost.ua.ac.be/hhh/). Analysis of the physiological and pathophysiological functions of the disease-associated proteins have provided intriguing insights into the complex structure of the inner ear and mechanisms of hearing. Although the progress in the field is remarkable, further identification of novel deafness genes and analyses of the function of the encoded proteins will enlarge our knowledge of the highly complex regulation of inner ear development and function.

Our strategy to identify novel deafness genes is based on a collection of large consanguineous families with ARNSHL; a genomewide, homozygosity mapping approach was used to identify novel *DFNB* loci and subsequently novel disease-causing genes. In the course of this study, we mapped two Turkish families to the *DFNB67* locus on chromosome 6p21.3–p21.1 and identified homozygous mutations in the gene named *lipoma HMGIC fusion partner-like 5* (*LHFPL5*) gene (MIM# 609427), alias *tetraspan membrane protein of hair cell stereocilia* (*TMHS*), which was recently shown to be mutated in the "hurry scurry" mouse [Longo-Guess et al., 2005] and in two *DFNB67*-linked families from Pakistan [Shabbir et al., 2006].

MATERIALS AND METHODS

Subjects

Participating family members underwent otoscopy and pure-tone audiometry. Hearing loss was quantified by pure-tone audiometry with aerial and bone conduction at 250, 500, 1,000, 2.000, 4,000, 6,000, and 8,000 Hz in a sound-treated room. The air conduction pure-tone average (ACPTA) threshold in the conversational frequencies (0.5, 1, and 2 kHz) was calculated for each ear, and hearing loss was classified as mild (20<ACPTA<40 dB), moderate (40<ACPTA<70 dB), severe (70<ACPTA<90 dB), or profound (ACPTA>90 dB). Vestibular areflexia was evaluated by the Romberg test and a questionnaire including questions of childhood motor development, insecure feeling during walking in darkness and on an uneven surface, problems with gymnastics and sports, motion sickness, and visual fixation (reading during walking) (Gendeaf homepage; www.gendeaf.org). Written informed consent was obtained from adults and the parents of children. The local ethics committee approved this study. DNA was extracted from peripheral blood lymphocytes by standard extraction procedures. We used control DNAs from 170 unrelated individuals of Turkish origin and over 90 Caucasian individuals from The Netherlands.

Linkage Analysis

The *GJB2* (MIM# 121011) gene was excluded as the causative gene in all families by sequencing of the 5′-untranslated region and the protein coding exon of the gene. In addition, all other 22 known ARNSHL genes were excluded in Family TR77 by analysis of flanking microsatellite markers. We performed genomewide linkage analysis in Family DF44 and homozygosity mapping in Family TR77 using the Affymetrix GeneChip Human Mapping 10K Array, version 2.0 (Affymetrix, Santa Clara, CA). This version of the Mapping 10K array comprises a total of 10,204 SNPs with a mean intermarker distance of 258 kb, equivalent to 0.36 cM. Genotypes were called by the GeneChip DNA Analysis Software (GDAS v2.0; Affymetrix). We verified the gender of the samples by counting heterozygous SNPs on the X chromosome. Relationship errors were evaluated with the help of the program Graphical Relationship Representation [Abecasis et al., 2001]. The program PedCheck was applied to detect Mendelian errors [O'Connell and Weeks, 1998] and data for SNPs with such errors were removed from the data set. Non-Mendelian errors were identified by using the program MERLIN [Abecasis et al., 2002] and unlikely genotypes for related samples were deleted. Nonparametric linkage analysis using all genotypes of a chromosome simultaneously was carried out with MERLIN. Parametric linkage analysis was performed by a modified version of the program GENEHUNTER 2.1 [Kruglyak et al., 1996; Strauch et al., 2000] through stepwise use of a sliding window with sets of 110 or 200 SNPs. In addition, the ExcludeAR Excel sheet was used for autozygosity mapping [Woods et al., 2004]. We analyzed additional microsatellite markers for fine-mapping of the critical regions and calculated multipoint logarithm of the odds (LOD) scores using SimWalk2 [Sobel and Lange, 1996] and the following markers: Family DF44: D6S273, D6S2443, D6S2444, D6S1583, D6S1629, D6S291, D6S943, D6S389, D6S426, D6S1575, D6S1549, D6S400, D6S1582; Family TR77: D6S1615, D6S1666, D6S2414, D6S1701, D6S1583, D6S1568, D6S1618, D6S1611, D6S291, D6S1602, D6S943, D6S1019, D6S1610, D6S1575, D6S282. Markers were taken from the ENSEMBL (www.ensembl.org) and UCSC (www.genome.ucsc.edu) human genome databases.

Mutation Analysis

We identified candidate genes in the critical region using the ENSEMBL and UCSC human genome databases. The three protein-coding exons and adjacent intronic sequences of the *LHFPL5* gene were amplified by PCR (MJ Research DNA, Bio-Rad, Munich, Germany; www.mjr.com) using standard conditions (exon 1, forward primer 5′-GTCATCTCGGTTCAGGAAGG-3 and reverse primer 5′-TCTGGGCTCAGAACCTCATC-3′ exon 2: forward primer 5′-GTGAGGAGAATGGCTGAAGG-3′ and reverse primer 5′-TGATTTCAGGGAGGACAAGG-3′; exon 3: forward primer 5′-CCATCTGCCCAACCAATAAC-3′ and reverse primer 5′-AAAATTAGCCAGGCATGGTG-3′). Subsequently, PCR fragments were purified with QiaQuick spin columns (Qiagen, Hilden, Germany; www.qiagen.com) and directly sequenced using the corresponding forward primers with the ABI PRISM Big Dye Terminator cycle sequencing V2.0 ready reaction kit and an ABI PRISM 3730 DNA analyzer (Applied Biosystems, Darmstadt, Germany; www.appliedbiosystems.com). Primer sequences for amplification of coding exons of *LHFPL3* and *LHFPL4* genes are available on request. DNA mutation numbering of identified mutations was given based on cDNA sequence of *LHFPL5* GenBank entry NM_182548.2 with +1 corresponding to the A of the ATG translation initiation codon.

We resequenced all identified mutations in independent experiments, tested for cosegregation within the families, and screened more than 170 Turkish control individuals for the mutations c.649delG and c.494C>T by PCR and subsequent restriction digestion (using *BshTI* or *BccI*, respectively; Fermentas, St. Leon-Rot, Germany; www.fermentas.com) or direct sequencing. The c.527G>T mutation was not found in 90 Dutch control individuals. The presence of this mutation was analyzed by an Amplification-Refractory Mutation System (ARMS) assay with for the wild-type allele the forward primer 5′-aagtacacgctgggccactg caccatcag-3′ and for the mutant allele the forward primer 5′-aagtacacgctgggccactgcaccatcat-3′. As reverse primer was used 5′-ccaagccttagaggactggctaagatgaac-3′. The PCR was performed with 1.5 mM $MgCl_2$ and an annealing temperature of 58°C.

Accession Numbers

LHFPL5 mRNA: GenBank NM_182548.2; *LHFPL4* mRNA: GenBank AY278320.1; *LHFPL3* mRNA: GenBank NM_199000.1.

RESULTS

Patients and Clinical Evaluation

Participating members of Families DF44, TR44, and TR77 underwent general otological examinations, pure-tone audiometry, and affected individuals were diagnosed with nonsyndromic, bilateral, severe to profound, sensorineural hearing loss. In each affected individual hearing impairment was noticed by the parents in the first six months of life. Vestibular evaluation did not display any symptoms of vestibular dysfunction. Childhood milestones were normal and the Romberg test was negative in all patients. Most of the affected individuals were born to consanguineous parents and an autosomal recessive inheritance pattern was suggested in all families analyzed.

Homozygosity Mapping

After exclusion of *GJB2* as the causative gene by direct sequencing in Families DF44 and TR77, and exclusion of 22 known ARNSHL genes by linkage analysis in Family TR77, we initially genotyped DNA samples from six affected and nine nonaffected members in Family DF44, and five affected individuals in Family TR77 using the Affymetrix GeneChip Human Mapping 10K Array. The combined maximum parametric LOD score of 3.56 was obtained in Family DF44 for a region located between SNPs rs718254 and rs571770 on chromosome 6p21.3–p21.1 (Fig. 1A and D) defining a critical interval of about 14 Mb. By fine-mapping with microsatellite markers and inclusion of additional family members, we reduced the critical region to an 8.4-Mb interval between markers *D6S1629* and *D6S400* with a maximum multipoint LOD score of 4.44 for markers between *D6S291* and *D6S389*, calculated by using SimWalk2 [Sobel and Lange, 1996] (Fig. 1B and D; Fig. 2A). Analyses of genotype data of the TR77 family revealed two significant homozygous regions for the four affected individuals in loop II (Fig. 2B). These regions were interrupted by several heterozygous SNPs in individual V:1 in loop I (Fig. 2B). One significant homozygous region was detected on chromosome 6p22.3-p21.2 between the SNPs rs1022558 and rs976482 and another region was found on chromosome 20q13.12 between the SNPs rs3908612 and rs869136. Analysis of microsatellite markers of these regions in additional family members excluded the putative locus on chromosome 20 (data not shown).

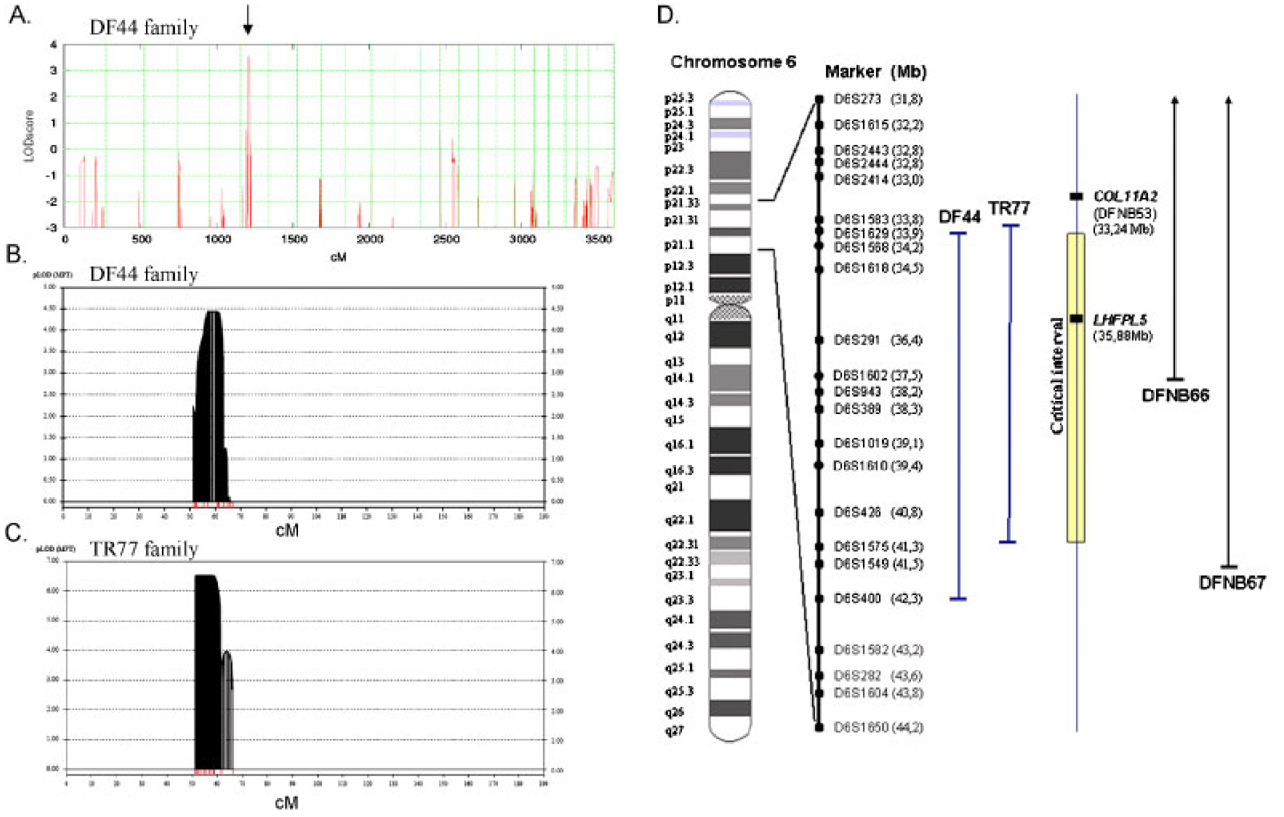

FIGURE 1. **Mapping of the 6p21.3–p21.1 locus. A: Graphical view of additive LOD score calculations of genomewide SNP mapping in family DF44 indicating a single locus on 6p21.3–p21.1 (marked by the arrow). B and C. Multipoint analysis of microsatellite markers used for fine-mapping of the critical region in Families DF44 (B) and TR77 (C). Along the x-axis, cM are given from the telomere of the p-arm to the telomere of the q-arm of chromosome 6. Additional family members, who were not available for the genome scan, were included in the fine-mapping study in both families. D: Ideogram of chromosome 6 and detailed presentation of the critical region identified in the families DF44 and TR77 in comparison with the published *DFNB66* and *DFNB67* locus. The locations of *COL11A2* and *LHFPL5* are indicated and the combined critical region is marked with the yellow bar. [Color figure can be viewed in the online issue, which is available at www.interscience.wiley.com]**

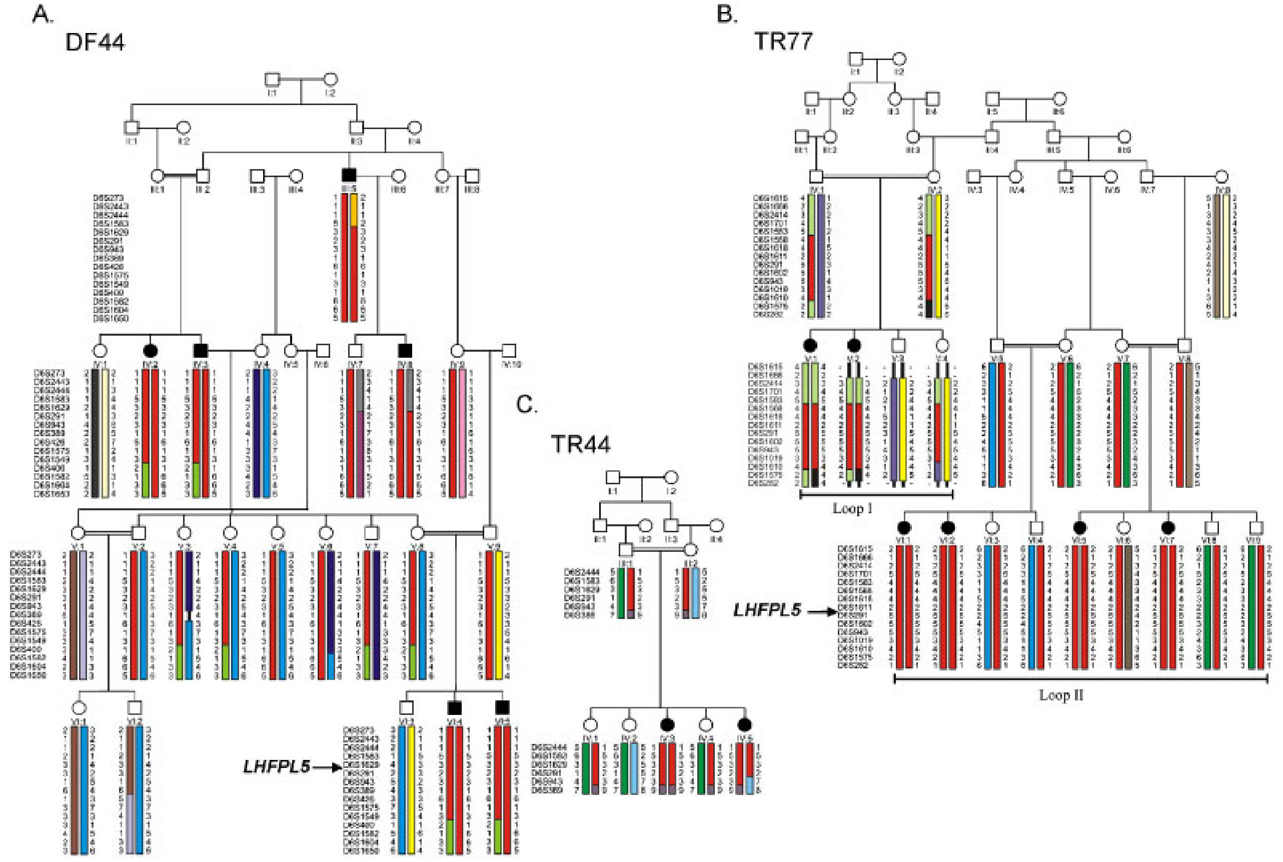

FIGURE 2. **Haplotypes in ARNSHL families linked to 6p21.3–p21.1. Markers are listed on the left of the haplotypes of Families DF44 (A), TR77 (B), and TR44 (C). The location of the *LHFPL5* gene is indicated by an arrow. The mutation-carrying haplotype is identical in Families DF44 and TR44, suggesting a founder mutation. [Color figure can be viewed in the online issue, which is available at www.interscience.wiley.com]**

A critical homozygous region of approximately 7.5 Mb was defined on chromosome 6p21.3-p21.1 between the markers *D6S1583* and *D6S1575* (Figs. 1D and 2B). A maximum two-point LOD score of 4.1 was calculated for marker *D6S1602* and a maximum multipoint LOD score of 6.12 for markers between *D6S1568* and *D6S1610* (Fig. 1C).

The critical region in both Family DF44 and Family TR77 partially overlapped with the recently described *DFNB66* locus, for which the gene has not yet been identified [Tlili et al., 2005], but it excluded *COL11A2* (MIM# 120290; see *DFNB53*, MIM# 609706) [Chen et al., 2005] by recombination events in Patients DF44-III:5 and IV:8 and TR77-V:1 and V:2 (Fig. 1D; Fig. 2A and B).

Mutation Analysis of the *LHFPL5* Gene

We considered the *LHFPL5* gene (alias *TMHS*), as a highly relevant positional candidate gene because a homozygous missense mutation in *Lhfpl5* was known to cause deafness and vestibular dysfunction in the "hurry-scurry" (*hscy*) mouse [Longo-Guess et al., 2005]. In human, the *LHFPL5* gene is comprised of four exons, of which the first three contain the protein coding sequences for a predicted four-transmembrane-spanning protein of 219 amino acids (Fig. 3D). We sequenced the three *LHFPL5* coding exons in two affected individuals from each family and identified homozygous mutations in both families. All affected members of Family DF44 carried the homozygous one base-pair deletion c.649delG in exon 2 (Fig. 3A). The nucleotide c.G649 is the last nucleotide of exon 2 followed by the invariant GT-motif of the intron 2 splice donor site. Computational analysis using the splice-site prediction program SpliceView (http://l25.itba.mi.cnr.it/~webgene/www.spliceview.html) predicted that the splice donor site of intron 2 in the mutant allele is still recognized without a decreased splice-score compared to the wild-type sequence. Therefore, the c.649delG mutation can be predicted to cause a frameshift at amino acid position 216 that introduces an extended C-terminal part of LHFPL5 with a termination codon after additional 25 erroneous amino acids (p.Glu216ArgfsX26) (Fig. 3D). None of the unaffected individuals in Family DF44 carried the c.649delG in a homozygous state and it was not detected in 170 matched control individuals. In Family TR77, the homozygous *LHFPL5* c.494C>T mutation in exon 2 was detected in all affected members (Fig. 3B). This nucleotide substitution was not observed in 170 ethnically matched control individuals. The c.494C>T mutation predicts the amino acid substitution p.Thr165Met in the second extracellular region between the transmembrane domains three and four (Fig. 3D). Residue p.Thr165 is conserved among most species and homologs with a conservation score of 7 as calculated by CONSEQ (http://conseq.bioinfo.tau.ac.il) and is located in close vicinity to the p.Cys161Phe mutation present in the *hscy* mouse (Fig. 3E) [Longo-Guess et al., 2005].

LHFPL5 Analysis in Additional Families and Patients

Sequencing of the three coding exons of *LHFPL5* was performed in 96 index patients from large Turkish ARNSHL

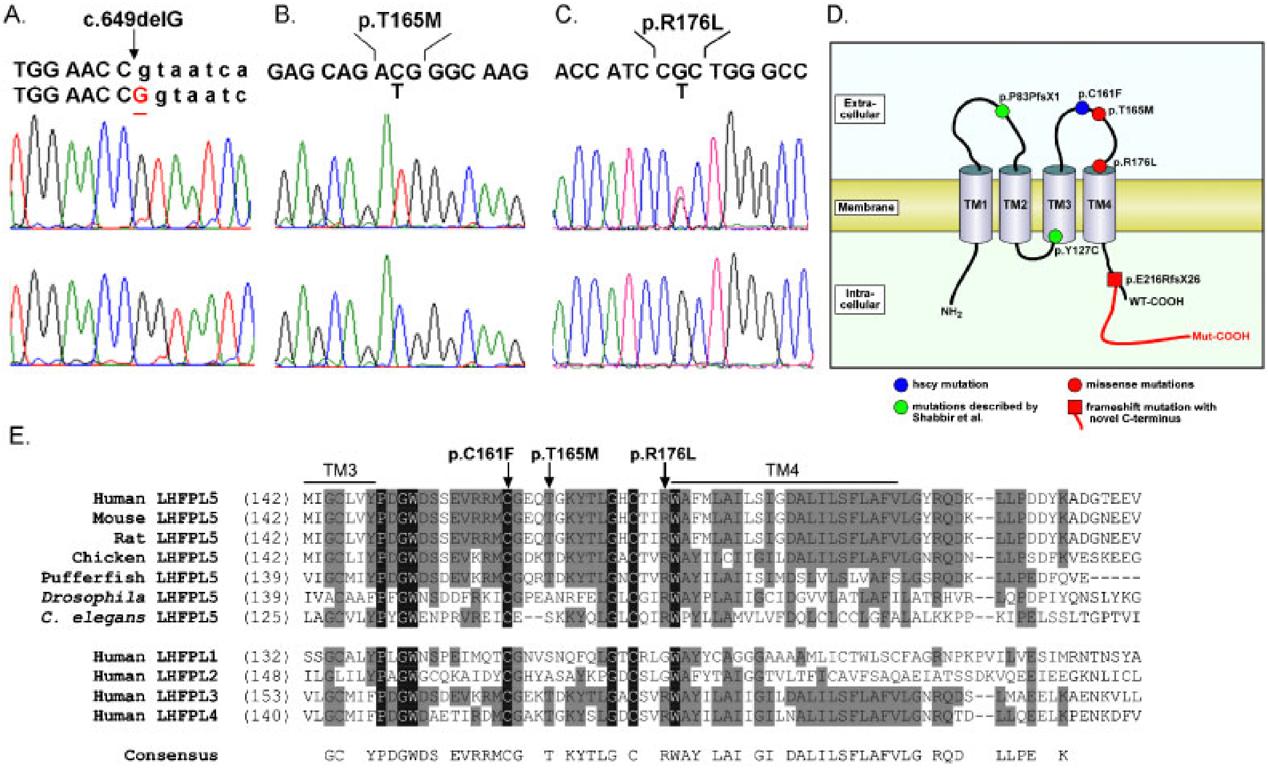
A.
c.649delG
TGG AAC C g t a a t c a
TGG AAC CG g t a a t c
B.
p.T165M
GAG CAG ACG GGC AAG
T
C.
p.R176L
ACC ATC CGC TGG GCC
T
D.
Extra-cellular
Membrane
Intra-cellular
p.P83PfsX1
p.C161F
p.T165M
p.R176L
TM1
TM2
TM3
TM4
p.Y127C
p.E216RfsX26
WT-COOH
Mut-COOH
NH2
hscy mutation
missense mutations
mutations described by Shabbir et al.
frameshift mutation with novel C-terminus
E.
p.C161F
p.T165M
p.R176L
TM3
TM4
Human LHFPL5 (142) MIGCLVYPDGWDSSEVRRMCGEQTGKYTLGHCTIRWAFMLAILSIGDALILSFLAFVLGYRQDK--LLPDDYKADGTEEV
Mouse LHFPL5 (142) MIGCLVYPDGWDSSEVRRMCGEQTGKYTLGHCTIRWAFMLAILSIGDALILSFLAFVLGYRQDK--LLPDDYKADGNEEV
Rat LHFPL5 (142) MIGCLVYPDGWDSSEVRRMCGEQTGKYTLGHCTIRWAFMLAILSIGDALILSFLAFVLGYRQDK--LLPDDYKADGNEEV
Chicken LHFPL5 (142) MIGCLIYPDGWDSSEVKRMCGDKTDKYTLGACTVRWAYILCIIGILDALILSFLAFVLGNRQDN--LLPSDFKVESKEEG
Pufferfish LHFPL5 (139) VIGCMIYPDGWDSDEVKRMCGQRTDKYTLGNCTVRWAYILAIISIMDSLVLSLVAFSLGSRQDK--LLPEDFQVE-----
Drosophila LHFPL5 (139) IVACAAFPFGWNSDDFRKICGPEANRFELGLCGIRWAYPLAIIGCIDGVVLATLAFILATRHVR--LQPDPIYQNSLYKG
C. elegans LHFPL5 (125) LAGCVLYPYGWENPRVREICE--SKKYQLGLCQIRWPYLLAMVLVFDQLCLCCLGFALALKKPP--KIPELSSLTGPTVI
Human LHFPL1 (132) SSGCALYPLGWNSPEIMQTCGNVSNQFQLGTCRLGWAYYCAGGGAAAAMLICTWLSCFAGRNPKPVILVESIMRNTNSYA
Human LHFPL2 (148) ILGLILYPAGWGCQKAIDYCGHYASAYKPGDCSLGWAFYTAIGGTVLTFICAVFSAQAEIATSSDKVQEEIEEGKNLICL
Human LHFPL3 (153) VLGCMIFPDGWDSDEVKRMCGEKTDKYTLGACSVRWAYILAIIGILDALILSFLAFVLGNRQDS--LMAEELKAENKVLL
Human LHFPL4 (140) VLGCMIFPDGWDAETIRDMCGAKTGKYSLGDCSVRWAYILAIIGILNALILSFLAFVLGNRQTD--LLQEELKPENKDFV
Consensus GC YPDGWDS EVRRMCG T KYTLG C RWAY LAI GI DALILSFLAFVLG RQD LLPE K

FIGURE 3. **Mutations identified in LHFPL5. A–C: Sequence chromatograms showing the mutations (upper sections) identified in the ARNSHL families, and the wild-type sequences (lower sections). The c.649delG (Families DF44 and TR44) and p.T165M (Family TR77) mutations are present in a homozygous state, while p.R176L was found heterozygously. DNA mutation numbering of identified mutations was given based on the cDNA sequence of the *LHFPL5* GenBank entry NM_182548.2, with +1 corresponding to the A of the ATG translation initiation codon. D: Predicted topology model of LHFPL5 with four transmembrane spanning domains (TM1 to TM4) and localization of identified mutations in the current study (red), by Shabbir et al. [2006] (green), and in the *hscy* mouse (blue). E: Alignment of part of the LHFPL5 protein sequences of several vertebrate and invertebrate species, and the human homologs LHFPL1-4. Location of predicted transmembrane domains 3 and 4 is given by the bold line above the sequences. Identical residues in all sequences are white on a black background, whereas amino acid residues that are present in six or more sequences are black on a gray background. Identified missense mutations in our families and the mouse mutation (p.C161F) are indicated with an arrow. [Color figure can be viewed in the online issue, which is available at www.interscience.wiley.com]**

families and in 90 Dutch ARNSHL patients without a mutation in *GJB2*. In the index patient of Family TR44, we again identified the c.649delG mutation and subsequent family analysis showed cosegregation of the mutation with hearing loss in the family (Fig. 2C). Both Families DF44 and TR44 originated from different cities at the East Black Sea region in Turkey and although a connection between the two families could not be established, haplotype analysis showed that the c.649delG mutation was located on the same haplotype in both families, suggesting c.649delG to be a founder mutation. In addition, the transversion c.527G>T was identified in a Dutch patient with ARNSHL in a heterozygous state predicting a substitution of leucine for the highly conserved arginine at position 176 (p.Arg176Leu) with the maximal conservation score of 9 (calculated by CONSEQ). Arg176 is predicted to be the last amino acid of the second extracellular loop between transmembrane domains three and four (Fig. 3C–E). This putative mutation was not detected in 90 Dutch control individuals. A second mutation in the known *LHFPL5* exons and adjacent intronic sequences was not detected in this patient. Since the *LHFPL5* homologs *LHFPL3* and *LHFPL4* are mainly expressed in neuronal tissue, we continued the molecular analysis and sequenced these genes in 78 index patients from Turkish ARNSHL families, but no disease-associated mutations were identified.

DISCUSSION

We provide evidence that mutations in the *LHFPL5* gene cause *ARNSHL* in humans and identified two different missense mutations and a one base-pair deletion in three consanguineous Turkish families and a sporadic Dutch patient. *LHFPL5* is the second gene in the 6p21.3-p21.1 region causing ARNSHL. A homozygous mutation in *COL11A2* was recently described in families linked to the *DFNB53* locus [Chen et al., 2005]. An additional, yet unknown ARNSHL gene might be present in this region since both genes, *COL11A2* and *LHFPL5*, were excluded by direct sequencing in the *DFNB66*-linked family [Tlili et al., 2005].

The homozygous p.Cys161Phe mutation in *Lhfpl5* was described to cause deafness and vestibular dysfunction in the "hurry-scurry" (*hscy*) mouse [Longo-Guess et al., 2005] and very recently, Shabbir et al. [2006] reported mapping of the *DFNB67* locus and identification of a homozygous deletion, c.246delC, leading to an unchanged Pro83 followed by a stop codon (p.Pro83ProfsX1), and missense mutation (p.Tyr127Cys) in *LHFPL5* (referred as *TMHS*) in two families from Pakistan. In both families, affected individuals presented with bilateral profound hearing loss without vestibular dysfunction. Therefore, no obvious phenotypic difference to our families exists.

LHFPL5 belongs to the family of tetraspan proteins with four transmembrane domains and two connecting extracellular loops (Fig. 3D). Although the specific function of LHFPL5 is not yet understood, it is intriguing to mention that mutations in various other genes encoding tetraspan proteins have been described in syndromic and nonsyndromic forms of hearing loss (e.g., *GJB2*; *GJB3*, MIM# 600101; *CLDN14*, MIM# 605608; *USH3A*, MIM# 276901) [Kelsell et al., 1997; Xia et al., 1998; Joensuu et al., 2001; Wilcox et al., 2001; Adato et al., 2002]. Immunohistochemical studies suggested that LHFPL5 is specifically expressed in stereocilia of inner and outer hair cells of the mouse during stereocilia formation, suggesting an important role in hair bundle morphogenesis [Longo-Guess et al., 2005; Shabbir et al., 2006]. As a consequence of p.Cys161Phe, homozygous *hscy* mice did not express LHFPL5 protein in the inner ear, although mRNA was still detected. Impairment of translation or rapid degradation of the mutated protein due to modifications or mislocalization was discussed as the underlying mechanism.

We identified the c.649delG (p.Glu216ArgfsX26) mutation on the same haplotype in two Turkish families from the East Black Sea region. Although both families originated from different cities, a shared founder carrying this mutation is likely. It will be interesting to test the frequency of c.649delG in an extended cohort of ARNSHL patients from this region in Turkey. It is unlikely that c.649delG changes the efficiency of the nearby located splice donor site of intron 2 leading to an aberrant splice product. In a preliminary experiment, we amplified and sequenced *LHFPL5* mRNA isolated from lymphocytes of a heterozygous carrier of the mutation and interestingly, could not detect the mutant allele (data not shown). This result gives a first hint that the deletion might cause mRNA decay, which would lead to complete loss of *LHFPL5* transcript and protein in a homozygous patient. In addition. the c.246delC mutation reported by Shabbir et al. [2006] predicts a truncation of the LHFPL5 protein at position 84. Even if the mRNA is not decayed, the truncated protein would lack three of its four transmembrane domains (Fig. 3D) and this would most likely cause loss-of-function.

The p.Thr165Met and p.Arg176Leu mutations are both located in the second extracellular loop of LHFPL5 in close vicinity to the mutation found in the *hscy* mouse (Fig. 3D). Whether the human *LHFPL5* mutations cause an analogy to the suggested effect of p.Cys161Phe in *hscy* mice [Longo-Guess et al., 2005], complete loss of LHFPL5 protein due to, for example, consequences for the solubility or structural properties of LHFPL5, remains to be elucidated.

Interestingly, we did not observe vestibular dysfunction in the patients of the presented families as could be expected from the phenotype present in *hscy* mice. A different expression pattern of *LHFPL5* in humans or additional compensating mechanisms in the vestibular system might explain the phenotypic difference. Such a difference in vestibular phenotype has been described for several other genes causing hearing loss in both human and mouse (e.g., *DFNB31/Whrn* [Holme et al., 2002; Mburu et al., 2003]).

We did not detect a second *LHFPL5* mutation in the Dutch ARNSHL patient carrying the heterozygous p.Cys161Phe mutation that she inherited from the normal hearing father. Clinically, the patient presented with a profound congenital sensorineural hearing loss. We cannot exclude a second mutation in a regulatory domain or intronic sequence of *LHFPL5*. Also, digenic inheritance might be present in this patient as it has been described in other ARNSHL patients. A mutation in *GJB2* was excluded.

Since the *LHFPL5* homologs *LHFPL3* and *LHFPL4* are mainly expressed in neuronal tissues, these genes were tested for involvement in the pathogenesis of ARNSHL. No disease-causing mutations were detected in 78 index patients from Turkish ARNSHL families, excluding mutations in these genes as a common cause for ARNSHL in the Turkish population.

In conclusion, we provide further evidence that mutations in *LHFPL5* (alias *TMHS*) cause ARNSHL without vestibular dysfunction. Although further experimental support is needed, loss of LHFPL5 function seems to be a plausible underlying mechanism.

ACKNOWLEDGMENTS

We thank all family members that participated in this study, and M. Langen, N. Sahin, E. Kandemir, Ö. Kücüköner, Y. Cinel-Boz, and Y. Ofluoglu for excellent technical assistance. This work was supported in part by the Turkish Academy of Sciences, in the framework of the Young Scientist Award Program, BW/TUBA-GEBIP/2002-1-20 (to B. W.); the European Commission FP6 Integrated Project EUROHEAR, LSHG-CT-20054-512063 (to C.W.R.J.C., C.K., H.K., and B.W.); Research Fund of Istanbul University, project number: T-1255/01112001 (to A.U.); the Karadeniz Technical University Research Fund 2002.114.001.3 (to A. K.); and the German Federal Ministry of Science and Education through the National Genome Research Network (to G.N., C.B., and P.N.).

REFERENCES

Abecasis GR, Cherny SS, Cookson WO, Cardon LR. 2001. GRR: graphical representation of relationship errors. Bioinformatics 17:742–743.

Abecasis GR, Cherny SS, Cookson WO, Cardon LR. 2002. Merlin—rapid analysis of dense genetic maps using sparse gene flow trees. Nat Genet 30:97–101.

Adato A, Vreugde S, Joensuu T, Avidan N, Hamalainen R, Belenkiy O, Olender T, Bonne-Tamir B, Ben-Asher E, Espinos C, Millan JM, Lehesjoki A-E, Flannery JG, Avraham KB, Pietrokovski S, Sankila E-M, Beckmann JS, Lancet D. 2002. *USH3A* transcripts encode clarin-1, a four-transmembrane-domain protein with a possible role in sensory synapses. Eur J Hum Genet 10:339–350.

Chen W, Kahrizi K, Meyer NC, Riazalhosseini Y, Van Camp G, Najmabadi H, Smith RJ. 2005. Mutation of *COL11A2* causes autosomal recessive non-syndromic hearing loss at the DFNB53 locus. J Med Genet 42:e61.

Holme RH, Kiernan BW, Brown SD, Steel KP. 2002. Elongation of hair cell stereocilia is defective in the mouse mutant whirler. J Comp Neurol 450:94–102.

Joensuu T, Hamalainen R, Yuan B, Johnson C, Tegelberg S, Gasparini P, Zelante L, Pirvola U, Pakarinen L, Lehesjoki AE, de la Chapelle A, Sankila EM. 2001. Mutations in a novel gene with transmembrane domains underlie Usher syndrome type 3. Am J Hum Genet 69:673–684.

Kelsell DP, Dunlop J, Stevens HP, Lench NJ, Liang JN, Parry G, Mueller RF, Leigh IM. 1997. Connexin 26 mutations in hereditary non-syndromic sensorineural deafness. Nature 387: 80–83.

Kruglyak L, Daly MJ, Reeve-Daly MP, Lander ES. 1996. Parametric and nonparametric linkage analysis: a unified multipoint approach. Am J Hum Genet 58:1347–1363.

Longo-Guess CM, Gagnon LH, Cook SA, Wu J, Zheng QY, Johnson KR. 2005. A missense mutation in the previously undescribed gene Tmhs underlies deafness in hurry-scurry (*hscy*) mice. Proc Natl Acad Sci USA 102:7894–7899.

Mburu P, Mustapha M, Varela A, Weil D, El Amraoui A, Holme RH, Rump A, Hardisty RE, Blanchard S, Coimbra RS, Perfettini I, Parkinson N, Mallon AM, Glenister P, Rogers MJ, Paige AJ, Moir L, Clay J, Rosenthal A, Liu XZ, Blanco G, Steel KP, Petit C, Brown SD. 2003. Defects in whirlin, a PDZ domain molecule involved in stereocilia elongation, cause deafness in the whirler mouse and families with DFNB31. Nat Genet 34: 421–428.

Mehl AL, Thomson V. 1998. Newborn hearing screening: the great omission. Pediatrics 101:e4.

Mehl AL, Thomson V. 2002. The Colorado newborn hearing screening project, 1992-1999: on the threshold of effective population-based universal newborn hearing screening. Pediatrics 109:e7.

Morton NE. 1991. Genetic epidemiology of hearing impairment. Ann NY Acad Sci 630:16–31.

O'Connell JR, Weeks DE. 1998. PedCheck: a program for identification of genotype incompatibilities in linkage analysis. Am J Hum Genet 63:259–266.

Shabbir MI, Ahmed ZM, Khan SY, Riazuddin S, Waryah M, Khan SN, Camps RD, Ghosh M, Kabra M, Belyantseva IA, Friedman TB, Riazuddin S. 2006. Mutations of human *TMHS* cause recessively inherited nonsyndromic hearing loss. J Med Genet (DOI:10.1136/jmg.2005.039834).

Sobel E, Lange K. 1996. Descent graphs in pedigree analysis: applications to haplotyping, location scores, and marker-sharing statistics. Am J Hum Genet 58:1323–1337.

Strauch K, Fimmers R, Kurz T, Deichmann KA, Wienker TF, Baur MP. 2000. Parametric and nonparametric multipoint linkage analysis with imprinting and two-locus-trait models: application to mite sensitization. Am J Hum Genet 66:1945–1957.

Tlili A, Mannikko M, Charfedine I, Lahmar I, Benzina Z, Ben Amor M, Driss N, Ala-Kokko L, Drira M, Masmoudi S, Ayadi H. 2005. A novel autosomal recessive non-syndromic deafness locus, DFNB66, maps to chromosome 6p21.2-22.3 in a large Tunisian consanguineous family. Hum Hered 60:123–128.

Wilcox ER, Burton QL, Naz S, Riazuddin S, Smith TN, Ploplis B, Belyantseva I, Ben-Yosef T, Liburd NA, Morell RJ, Kachar B, Wu DK, Griffith AJ, Riazuddin S, Friedman TB. 2001. Mutations in the gene encoding tight junction claudin-14 cause autosomal recessive deafness DFNB29. Cell 12:165–172.

Woods CG, Valente EM, Bond J, Roberts E. 2004. A new method for autozygosity mapping using single nucleotide polymorphisms (SNPs) and EXCLUDEAR. J Med Genet 41:e101.

Xia JH, Liu CY, Tang BS, Pan Q, Huang L, Dai HP, Zhang BR, Xie W, Hu DX, Zheng D, Shi XL, Wang DA, Xia K, Yu KP, Liao XD, Feng Y, Yang YF, Xiao JY, Xie DH, Huang JZ. 1998. Mutations in the gene encoding gap junction protein beta-3 associated with autosomal dominant hearing impairment. Nat Genet 20:370–373.

Downloaded from thorax.bmjjournals.com on 7 March 2006

BTNL2 gene variant and sarcoidosis

Y Li, B Wollnik, S Pabst, M Lennarz, E Rohmann, A Gillissen, H Vetter and C Grohé

Thorax 2006;61;273-274
doi:10.1136/thx.2005.056564

Updated information and services can be found at:
http://thorax.bmjjournals.com/cgi/content/full/61/3/273

These include:

References This article cites 5 articles, 3 of which can be accessed free at:
http://thorax.bmjjournals.com/cgi/content/full/61/3/273#BIBL

Rapid responses You can respond to this article at:
http://thorax.bmjjournals.com/cgi/eletter-submit/61/3/273

Email alerting service Receive free email alerts when new articles cite this article - sign up in the box at the top right corner of the article

Topic collections Articles on similar topics can be found in the following collections

Genetics (3690 articles)
Diffuse parenchymal lung disease (75 articles)

Notes

To order reprints of this article go to:
http://www.bmjjournals.com/cgi/reprintform

To subscribe to *Thorax* go to:
http://www.bmjjournals.com/subscriptions/

Downloaded from thorax.bmjjournals.com on 7 March 2006

Table 1 Baseline biochemistry and peak cortisol levels following insulin induced hypoglycaemia in two female adult patients taking inhaled/intranasal corticosteroids

	Patient 1	Patient 2
08.00 cortisol (200–600 nmol/l)	169/198	113/198
08.00 ACTH (<12 pmol/l)	4.5	2.8/2.9
Insulin-like growth factor-1 (0.4–1.6 U/ml)	0.54	0.89/0.79
Free thyroxine (10–21 pmol/l)	11	15.9/15.6*
Thyroid stimulating hormone (0.3–4 mIU/l)	0.77	1.77/1.95*
Prolactin (50–370 mIU/l)	224	111/87
Luteinising hormone (IU/l)†	11.3	26.4/18.4
Follicular stimulating hormone (IU/l)‡	6.5	50.1/42.7
α-subunit (IU/l)§	0.41	Not done
Anti-microsomal antibodies	Negative	Positive
Dehydrepiandrosterone (µmol/l)¶	<1.0	<1.0
Results of insulin tolerance test		
Baseline cortisol (200–600 nmol/l)	160	159
Minimum blood glucose (<2.2 mmol/l)	1.9	1.6
30 minute cortisol (nmol/l)	327	343
60 minute cortisol (nmol/l)	450	492
90 minute cortisol (nmol/l)	313	388
120 minute cortisol (nmol/l)	227	282
Peak growth hormone (>13 mU/l)	40.3	4.9

Normal ranges and units are in brackets. ''Normal'' peak cortisol level following hypoglycaemia >550 nmol/l. When more than one value is quoted, the tests were performed on different days.
*On thyroxine.
†Reference range (RR): females – premenopausal 2.5–130 IU/l, postmenopausal >15 IU/l, males 1.5–14 IU/l.
‡RR: females – premenopausal 1.6–33 IU/l, postmenopausal >16 IU/l, males 0.9–8.1 IU/l.
§RR: males and females – premenopausal 0.05–0.4 IU/l, postmenopausal 0.37–1.15 IU/l.
¶RR: females – premenopausal 2.2–9.1 µmol/l, postmenopausal 0.3–1.7 µmol/l, males 5.3–9 µmol/l.

disorders and ischaemic heart disease, the ITT is a safe test when performed in experienced centres.[3] Indeed, a review of >6500 ITTs reported that only seven patients (0.1%) experienced an adverse event, all of which reversed following intravenous glucose.[6] To our knowledge, only two studies have used the ITT to investigate the HPA axis in asthmatic children treated with inhaled fluticasone. The first reported an inadequate response to insulin-induced hypoglycaemia in three children taking 1000–2250 µg/day.[7] In the second study, nine of 18 subjects treated with 250–750 µg/day for up to 16 weeks exhibited evidence of adrenal suppression which recovered following cessation of treatment.[1]

Finally, as hypopituitarism of probable autoimmune aetiology has been reported in patients with celiac disease,[8] the possibility that autoimmune hypophysitis contributed to the patients' symptoms and pituitary deficiency cannot be definitively excluded.

In summary, this report suggests that inhaled (together with intranasal) fluticasone may suppress the HPA axis in adults and that symptomatic adrenal insufficiency may develop, particularly if dosing is variable and intermittent. These cases illustrate that clinical symptoms may alert the physician to the possibility of adrenal suppression which can then be confirmed using basal and/or stimulated tests of HPA function in selected patients. Further investigation to determine the prevalence of these effects in adult patients is warranted.

J R Greenfield, K Samaras
Department of Endocrinology, St Vincent's Hospital, and Garvan Institute of Medical Research, Sydney, Australia

Correspondence to: A/Prof K Samaras, Diabetes and Obesity Research Program, Garvan Institute of Medical Research, 384 Victoria Street, Darlinghurst 2010, Australia; K.samaras@garvan.org.au

doi: 10.1136/thx.2005.049643

References

1. **Mahachoklertwattana P**, Sudkronrayudh K, Direkwattanachai C, *et al*. Decreased cortisol response to insulin induced hypoglycaemia in asthmatics treated with inhaled fluticasone propionate. *Arch Dis Child* 2004;**89**:1055–8.
2. **Todd GRG**, Acerini CL, Ross-Russell R, *et al*. Survey of adrenal crisis associated with inhaled corticosteroids in the United Kingdom. *Arch Dis Child* 2002;**87**:457–61.
3. **Greenfield JR**, Samaras K. Evaluation of pituitary function in the fatigued patient: a review of 59 cases. *Eur J Endocrinol* 2006;**154**:147–57.
4. **Lipworth BJ**. Systemic adverse effects of inhaled corticosteroid therapy: A systematic review and meta-analysis. *Arch Intern Med* 1999;**159**:941–55.
5. **Casale TB**, Nelson HS, Stricker WE, *et al*. Suppression of hypothalamic-pituitary-adrenal axis activity with inhaled flunisolide and fluticasone propionate in adult asthma patients. *Ann Allergy Asthma Immunol* 2001;**87**:379–85.
6. **Fish HR**, Chernow B, O'Brian JT. Endocrine and neurophysiologic responses of the pituitary to insulin-induced hypoglycemia: a review. *Metabolism* 1986;**35**:763–80.
7. **Todd G**, Dunlop K, McNaboe J, *et al*. Growth and adrenal suppression in asthmatic children treated with high-dose fluticasone propionate. *Lancet* 1996;**348**:27–9.
8. **Collin P**, Kaukinen K, Valimaki M, *et al*. Endocrinological disorders and celiac disease. *Endocrinol Rev* 2002;**23**:464–83.

BTNL2 gene variant and sarcoidosis

Sarcoidosis is an inflammatory granulomatous disorder that primarily affects the lungs and lymph nodes. Other organs such as the brain, eyes, heart, and skin can also be affected. The disease is characterised by non-caseating granulomas and an exaggerated cellular immune response caused by increased inflammatory activity.[1] The course of the disease is acute and mild in approximately 20% of all patients. In most patients a chronic stage develops which can lead to lung fibrosis. Although the exact pathogenesis of sarcoidosis remains unclear, familial clustering of the disease and the increased risk of relatives to develop sarcoidosis suggest that there might be a genetic predisposition to develop the disease.[2]

A significant association was recently reported in Germany between sarcoidosis and a frequent single nucleotide polymorphism (SNP) in the *BTNL2* gene, rs2076530.[3] *BTNL2* is a member of the immunoglobulin gene family and is related to *CD80* and *CD86* co-stimulatory receptors, although its exact function is unknown.[4] *BTNL2* is located on chromosome 6p21.3 in close proximity to the *HLA* gene cluster. rs2076530 is located at position 1 of the donor splice site in intron 5 and the associated A allele causes the usage of an alternative donor site leading to a 4 bp deletion at the mRNA level, frameshift, and premature truncation at the protein level.[3] The rs2076530 SNP alone was also associated with sarcoidosis in a case-control study of white American subjects.[4] No replication of the *BTNL2* rs2076530 susceptibility to sarcoidosis has yet been studied in an independent German case-control study. We therefore performed a case-control association study in 210 patients with sarcoidosis and 202 controls. Written informed consent was given by each participant and the study was approved by the ethics committee of Bonn University School of Medicine.

The diagnosis of sarcoidosis was based on evidence of non-caseating epitheloid cell granuloma in biopsy specimens and chest radiographic abnormalities. Different stages were defined as previously described.[5] A chronic course was defined as disease over at least 2 years or at least two episodes in a lifetime. Acute sarcoidosis was defined as one episode of acute sarcoidosis which had totally resolved at the date of the examination. None of the individuals in the control group (healthy white German subjects of mean age 38.32 (15.53) years) had a history of lung disease or showed any symptoms of lung or other disease by chest radiography or laboratory blood tests. Genotyping of rs207653 was performed using the Taqman technique with a commercially available assay (Applied Biosystems, Germany). SPSS Version 12 was used for statistical analysis. The genotype distributions in the cohort were in accordance with the Hardy-Weinberg equilibrium.

The A allele frequency of rs2076530 was significantly increased in sarcoidosis patients compared with controls (A = 0.6929, G = 0.3071 in cases; A = 0.6188, G = 0.3812 in controls). It was significantly associated with an increased risk of sarcoidosis in co-dominant and dominant models (OR 2.31 (95% CI 1.27 to 4.23); $p<0.006$, table 1), but not in a recessive model ($p = 0.276$). The calculated population attributable risk (PAR) for AA homozygotes and AG heterozygotes was 34.6%. Our results were in accordance with the reported association between *BTNL2* and sarcoidosis and replicated the finding that A allele carriers of rs2076530 have a more than twofold increased risk of developing sarcoidosis compared with GG homozygotes in the German population.

We also examined whether this increased risk is present in both chronic and acute forms of sarcoidosis. Interestingly, we found that the chronic form—but not the acute form—was significantly associated with the A allele in co-dominant and dominant models (OR 2.87

Downloaded from thorax.bmjjournals.com on 7 March 2006

Table 1 Statistical analysis of the case-control study

	Co-dominant				Dominant (AA/AG *v* GG)				Recessive (AA *v* AG/GG)			
	AA	AG	GG	p value	AA/AG	GG	OR (95% CI)	p value	AA	GG/AG	OR (95% CI)	p value
Controls	84 (41%)	82 (41%)	36 (18%)		166	36			84	116		
Cases	99 (47%)	93 (44%)	18 (9%)	**0.021**	192	18	**2.31 (1.27 to 4.23)**	**0.006**	99	111	1.25 (0.85 to 1.85)	0.276
Acute	30 (42%)	32 (45%)	9 (13%)	0.576	62	9	1.49 (0.68 to 3.28)	0.358	30	41	0.99 (0.57 to 1.71)	0.97
Chronic	59 (52%)	47 (41%)	8 (7%)	**0.021**	106	8	**2.87 (1.29 to 6.42)**	**0.007**	59	55	0.67 (0.43 to 1.07)	0.095

Significant associations are shown in bold.

(95% CI 1.29 to 6.42), $p<0.0069$; table 1) with a PAR for AA homozygotes and AG heterozygotes of 50%.

This study underlines the importance of the association of *BTNL2* rs2076530 variant with the susceptibility to develop sarcoidosis in a German population. Furthermore, our data suggest that susceptibility is preferentially towards the chronic form of the disease.

Y Li, B Wollnik
Center for Molecular Medicine Cologne (CMMC) and Institute of Human Genetics, University of Cologne, Germany

S Pabst, M Lennarz
Medizinische Universitäts-Poliklinik, Rheinische-Friedrich-Wilhelms Universität Bonn, Germany

E Rohmann
Center for Molecular Medicine Cologne (CMMC) and Institute of Human Genetics, University of Cologne, Germany

A Gillissen
Städtisches Klinikum St Georg, Leipzig, Germany

H Vetter, C Grohé
Medizinische Universitäts-Poliklinik, Rheinische-Friedrich-Wilhelms Universität Bonn, Germany

Correspondence to: Professor Dr med C Grohé, Medizinische Universitäts-Poliklinik, Wilhelmstr, 35-37, D-53111 Bonn, Germany; c.grohe@uni-bonn.de

doi: 10.1136/thx.2005.056564

Competing interests: none.

References

1 **Newman LS**, Rose CS, Maier LA. Sarcoidosis. *N Engl J Med* 1997;**336**:1224–34.
2 **Rybicki BA**, Iannuzzi MC, Frederick MM, *et al.* ACCESS Research Group. Familial aggregation of sarcoidosis. A case-control etiologic study of sarcoidosis (ACCESS). *Am J Respir Crit Care Med* 2001;**164**:2085–91.
3 **Valentonyte R**, Hampe J, Huse K, *et al.* Sarcoidosis is associated with a truncating splice site mutation in BTNL2. *Nat Genet* 2005;**37**:357–64.
4 **Rybicki BA**, Walewski JL, Maliarik MJ, *et al.* ACCESS Research Group. The BTNL2 gene and sarcoidosis susceptibility in African Americans and Whites. *Am J Hum Genet* 2005;**77**:491–9.
5 **Costabel U**, Hunninghake GW. Statement on sarcoidosis. Joint Statement of the American Thoracic Society (ATS), the European Respiratory Society (ERS) and the World Association of Sarcoidosis and Other Granulomatous Disorders (WASOG) adopted by the ATS Board of Directors and by the ERS Executive Committee. *Am J Respir Crit Care Med* 1999;**160**:736–55.

Asthma and allergies in Germany

We read the study by Zöllner and colleagues published recently in *Thorax* about the levelling off of asthma and allergies among children in Germany between 1992 and 2001.[1] We have published a study looking at the same issue and using a similar protocol (ISAAC)[2] to assess the symptoms, diagnosis, and severity of asthma and allergies in more than 15 000 children aged 6–7 and 13–14 years between 1995 and 2000 in Münster, Germany.[3] We found a tendency towards an increase in current symptoms of asthma and allergies in both age groups, but more so among girls.[3]

Indices of diagnosis either remained the same or increased in parallel with the increase in symptoms, arguing against a change in diagnostic behaviour as an explanation for our results. Indices of severity also showed a homogenous increase in the 5 year study period, pointing towards an increase in the overall burden of asthma and allergies within the society.[3]

Regrettably, these results, coming from Germany, were not considered in either the discussion of Zöllner's report or in the affirmative title that no increase in asthma and allergies occurred in Germany in the 1990s. Even more regrettable is the fact that when our study was alluded to in the discussion and conclusion of the paper by Zöllner *et al*, it was cited—contrary to our results—as one of the studies showing a decrease or levelling off of asthma and allergies among children.[1]

W Maziak, U Keil
Institute of Epidemiology and Social Medicine, University Clinic of Muenster, Muenster, Germany; maziak@net.sy

References

1 **Zöllner IK**, Weiland SK, Piechotowski I, *et al.* No increase in the prevalence of asthma, allergies, and atopic sensitisation among children in Germany: 1992–2001. *Thorax* 2005;**60**:545–8.
2 **Asher MI**, Keil U, Anderson HR, *et al.* International Study of Asthma and Allergies in Childhood (ISAAC): rationale and methods. *Eur Respir J* 1995;**8**:483–91.
3 **Maziak W**, Behrens T, Brasky TM, *et al.* Are asthma and allergies in children and adolescents increasing? Results from ISAAC phase I and phase III surveys in Münster, Germany. *Allergy* 2003;**58**:572–9.

Authors' reply

Unfortunately, the paper by Maziak *et al*[1] published in *Allergy* was listed as reference number 18 instead of number 21 in the reference list of our paper.[2] We apologise for any misunderstanding which may have arisen from this error. A correction is published below.

In the paper by Maziak *et al*[1] the prevalences in 1994/5 and 1999/2000 are compared. As we know from our own studies, trend analyses based on (only) two time points may be difficult and should be interpreted with caution. Indeed, in their investigation Maziak *et al* did not find a significant increase in the lifetime prevalence of asthma and hay fever, except in one subgroup. The effect found in 13–14 year old girls could also be due to a former underdiagnosis of asthma in girls, as discussed in their paper.

Since our results are based on six cross sectional surveys, we consider the title and the conclusion—that we did not see an increase in asthma and allergies from 1992 to 2001—to be appropriate.

I Zöllner
Department of Epidemiology and Health Reporting, Baden-Wuerttemberg State Health Office, Wiederholdstr 15, D-70174 Stuttgart, Germany; Iris.Zoellner@rps.bwl.de

Reference

1 **Maziak W**, Behrens T, Brasky TM, *et al.* Are asthma and allergies in children and adolescents increasing? Results from ISAAC phase I and phase III surveys in Münster, Germany. *Allergy* 2003;**58**:572–9.
2 **Zöllner IK**, Weiland SK, Piechotowski, *et al.* No increase in the prevalence of asthma allergics, and atopic sensitisation among children in Germany: 1992–2001. *Thorax* 2005;**60**:545–8.

CORRECTIONS

doi: 10.1136/thx.2005.029561corr1

In the paper entitled "No increase in the prevalence of asthma, allergies, and atopic sensitisation among children in Germany: 1992–2001" by I K Zöllner *et al* which appeared in the July 2005 issue of *Thorax* (2005;**60**:545–8), the authors apologise for a mistake which occurred in the reference list. Reference number 18 should be number 21 and references 19–21 should be listed as 18–20.

doi: 10.1136/thx.2005.040444corr1

The paper entitled "Anticholinergics in the treatment of children and adults with acute asthma: a systematic review with meta-analysis" by G J Rodrigo and J A Castro-Rodriguez (10.1136/thx.2005.040444) has been published previously on 17 June 2005 as a *Thorax* Online First article but under the incorrect DOI (10.1136/thx.2005.047803). The publishers apologise for this error. The definitive version of the article can be found at the following citation: *Thorax* 2005;**60**:740–6.

doi: 10.1136/thx.2005.040881corr1

In the paper entitled "Hormone replacement therapy, body mass index and asthma in perimenopausal women: a cross sectional survey" by F Gómez Real *et al* published in the January 2006 issue of *Thorax* (2006;**61**:34–40), the fourth author should be **K A Franklin**, not K Franklin.

10. Appendix

Acknowledgements

Special thanks to my supervisor Bernd Wollnik. He made this PhD thesis possible and supported me always with good advice and great scientific knowledge. He inducted me into the international world of science and gave me the opportunity to enlarge my skills in foreign labs and present our findings at meetings. Furthermore, he really knows how to motivate……..

Rita Schmutzler and Thomas Wiehe, thank you for supervising my thesis and lectures during my MD/PhD program. I also thank Christian Kubisch and Peter Nürnberg for examining my thesis. Moreover, a huge thank you to Christian Kubisch and to his lab people for introducing me into the field of molecular genetics.

Many thanks to Joseph Schlessinger and Irit Lax in overseas, heads of the Yale school of medicine in the department for pharmacology. They gave me a home during my stay and the opportunity to join their great research group to implement the progress in my PhD thesis. They instructed me in many technical methods and were open minded for every scientific discussion. Special thanks in this lab to Fran, Eswar, Erin, James and Saturo. They took care of me during my stay and made everything comfortable.

Inga Ebermann, also PhD student in the Institute of Human Genetics and meanwhile a good friend, thank you for the long and sometimes cumbersome scientific discussions and for the support and fun in the daily lab routine. Special thanks also to Nadine Plume for assisting me with my project and to Yun Li for sharing his expertise. Finally, thanks to all the lab people in the LFI for the laugh and power during my PhD time.

Last but not least, I want to thank my family and the most important person at my side, Kevin Baddah. They were always there for me and supported me in all my decisions and made my PhD time enjoyable.

CURRICULUM VITAE

Personal Data

Name	Edyta
Surname	Rohmann
Date of Birth	08 March 1976
Place of Birth	Arys (Poland)
Nationality	German
Home address	Im Helltgen 15 53773 Hennef NRW, Germany
Phone	+49 177 307 460 1
Email	rohmann.e@web.de
Business address	UNIVERSITY OF COLOGNE Center for Molecular Medicine Cologne Institute of Human Genetics Kerpener Str. 34 50931 Köln NRW, Germany
Phone	+49 221 478 870 64
Email	edyta.rohmann@uk-koeln.de

Education

Oct 1999 – Apr 2004	UNIVERSITY COLOGNE, Department of Mathematics and Natural Sciences, Study of Biology with the following key classes: Developmental Biology, Biochemistry, Pharmacology Diplom: Grade 1.0 Acadamic degree: Master of Science (Dipl.- Biol.)
Aug 1996 – Aug 1999	OBERHAUSEN KOLLEG Public Institute for attainment of the general qualification for university entrance Grade: 2.0
Aug 1986 – Aug 1992	STÄDTISCHES STIFTSGYMNASIUM Xanten, NRW, Germany
Aug 1982 – Aug 1986	Elementary school in Xanten, NRW, Germany

Work Experience

Jul 2004 – Dec 2007	Interdisciplinary Postgraduate Program in Molecular Medicine (IPMM) at the Institute of Human Genetics Cologne, UNIVERSITY OF COLOGNE, Center for Molecular Medicine Cologne (CMMC), Dr. med Bernd Wollnik, CMMC-Junior Research Group V hosted by the Institute of Human Genetics, Dissertation thesis: \`Identification of the molecular basis of the lacrimo-auriculo-dento-digital-syndrome (LADD)´
Nov 2005 – Jan 2006	Within the dissertation habitation at the Yale University School of Medicine, Department of Pharmacology, New Haven, US Prof. Dr. Joseph Schlessinger
May 2003 – Apr 2004	Diplom´s thesis with the UNIVERSITY COLOGNE, Institute of Legal Medicine, DNA- Department, Topic: \`Establishment of Y- and X- chromosomal short tandem repeats for forensic investigation and descent examination in consideration of population genetics´
Feb 2002 – Apr 2002	Traineeship, University of Cologne, Institute of Legal Medicine, DNA- Department
May 2000 – Aug 2002	Temporary job, physician assistant, specialization in neurology

Okt 2001	Traineeship, Zoo Duisburg, Section for whales and dolphins
Aug 1995 – Jul 1996	Job as physician assistant, specialization in orthopedics
Aug 1992 – Jul 1995	Job training for physician assistant, specialization in orthopedics

Scientific Awards

Participant and young scientist representative of the University of Cologne at the Meeting of Nobel Laureates in Medicine/ Physiology in Lindau, 2007

The Nature Genetics publication received the shared Medical faculty prize 2006 for the best publication of the Medical Faculty at the University Cologne in 2006.

Publications

Lew E, Bae JH, **Rohmann E**, Wollnik B, and Schlessinger J; Structural basis for reduced FGFR2 activity in LADD syndrome: Implications for FGFR Autoinhibition and Activation; Proc Natl Acad Sci U S A. (2007): Dec. 104 (50): 19802-19807.

Kaplan Y, Vargel I, Kansu T, Akin B, **Rohmann E**, Kamaci S, Uz E, Ozcelik T, Wollnik B, Akarsu NA: Novel p.R229G Missense Mutation in the FRMD7 Gene Causes X-Linked Idiopathic Congenital Nystagmus Linked to Xq26-q27. Br J Ophthalmol. (2007): Oct 25; [Epub ahead of print]

Pabst S, Wollnik B, **Rohmann E**, Hintz Y, Grohé C: A novel stop mutation truncating critical regions of the cardiac transcription factor NKX2.5 in a large family with autosomal-dominant inherited congenital heart disease. Clin Res Cardiol. (2007); Sep 25; [Epub ahead of print]

Shams I, **Rohmann E**, Eswarakumar VP, Lew E, Yuzawa S, Wollnik B, Schlessinger J, Irit L: LADD syndrome is caused by reduced activity of the FGF10-FGF receptor 2 signaling pathway. Mol Cell Biol. (2007); 27: 6903-6912.

Rohmann E, Brunner H, Kayserili K, Uyguner O, Nürnberg G, Lew E, Dobbie A, Eswarakumar V, Uzumcu A, Ulubil-Emeroglu M, Leroy J, Li Y, Becker C, Lehnerdt K, Cremers C, Yüksel-Apak M, Nürnberg P, Kubisch C, Schlessinger J, Bokhoven H, Wollnik B; Mutations in different components of FGF signaling in LADD syndrome; Nat Genetics (2006): Apr. 38 (4): 414-7

Kalay E, Li Y, Uzumcu A, Uyguner O, Collin R, Caylan R, Ulubil-Emeroglu M, Kersten F, Hafiz G, van Wijk E, Kayserili H, **Rohmann E**, Wagenstaller J, Hoefsloot L, Strom T, Nürnberg G, Baserer N, Hollander A, Cremers F, Cremers C, Becker C, Brunner H, Nürnberg P, Karaguzel A, Basaran S, Kubisch C, Kremer H, Wollnik B ; Mutations in the lipoma HMGIC fusion partner-like 5 (LHFPL5) Gene Cause Autosomal Recessive Nonsyndromic Hearing Loss ; Human Mutation (2006): 27(7), 633-639

Li Y, Wollnik B, Pabst S, Lennarz M, **Rohmann E**, Gillissen A, Vetter H, Grohe C ; BTNL2 gene variant and sarcoidosis ; Thorax (2006): 61, 273-274

Congresses

Rohmann E., Lax I., Lew E.D., Eswarakumar V.P., Brunner H.G., Li Y., Kayserili H., Schlessinger J., Wollnik B. Oral Presentation: LADD syndrome is caused by mutations that reduce the tyrosine kinase activity of FGFR2. 18th Annual Meeting of The German Society of Human Genetics March 7 –10, 2007, Bonn.

Rohmann E., Lax I., Lew E.D., Eswarakumar V.P., Brunner H.G., Li Y., Kayserili H., Schlessinger J., Wollnik B. Oral Presentation: LADD syndrome is caused by mutations that reduce the tyrosine kinase activity of FGFR2. 56th Annual Meeting of The American Society of Human Genetics, October 9 –13, 2006, New Orleans.

Wollnik B., Brunner H.G., Kayserili H., Uyguner O., Nürnberg G., Lew E.D., Dobbie A., Eswarakumar V.P., Uzumcu A., Ulubil-Emeroglu M., Leroy J.G., Li Y., Becker C., Lehnerdt K., Cremers C.W., Yuksel-Apak M., Nürnberg P., Kubisch C., Schlessinger J., van Bokhoven H., **Rohmann E.** Oral Presentation: Mutations in different components of FGF-signaling in LADD syndrome. 17th Annual Meeting of the German Society of Human Genetics, March 8 –11, 2006, Heidelberg.

Wollnik B., Brunner H.G., Kayserili H., Uyguner O., Nürnberg G., Lew E.D., Dobbie A., Eswarakumar V.P., Uzumcu A., Ulubil-Emeroglu M., Leroy J.G., Li Y., Becker C., Lehnerdt K., Cremers C.W., Yuksel-Apak M., Nürnberg P., Kubisch C., Schlessinger J., van Bokhoven H., **Rohmann E.** Oral Presentation: Mutations in different components of FGF-signaling in LADD syndrome. 38th European Human Genetics Conference, May 9 –12, 2006, Amsterdam.

Köln, den 27.02.2008

Erklärung II

Ich versichere, dass ich die von mir vorgelegte Dissertation selbständig angefertigt, die benutzten Quellen und Hilfsmittel vollständig angegeben und die Stellen der Arbeit - einschließlich Tabellen, Karten, und Abbildungen - , die anderen Werken im Wortlaut oder dem Sinn nach entnommen sind, in jedem Einzelfall als Entlehnung kenntlich gemacht habe; dass diese Dissertation noch keiner anderen Fakultät oder Universität zur Prüfung vorgelegen hat; dass sie – abgesehen von unten angegebenen Teilpublikationen – noch nicht veröffentlicht worden ist sowie, dass ich eine solche Veröffentlichung vor Abschluss des Promotionsverfahrens nicht vornehmen werde.
Die Bestimmungen dieser Promotionsordnung sind mir bekannt. Die von mir vorgelegte Dissertation ist von Dr. med. Bernd Wollnik betreut worden.

Teilpublikationen:

Lew E, Bae JH, **Rohmann E**, Wollnik B, and Schlessinger J; Structural basis for reduced FGFR2 activity in LADD syndrome: Implications for FGFR Autoinhibition and Activation; Proc Natl Acad Sci U S A. (2007): Dec. 104 (50): 19802-19807.

Kaplan Y, Vargel I, Kansu T, Akin B, **Rohmann E**, Kamaci S, Uz E, Ozcelik T, Wollnik B, Akarsu NA: Novel p.R229G Missense Mutation in the FRMD7 Gene Causes X-Linked Idiopathic Congenital Nystagmus Linked to Xq26-q27. Br J Ophthalmol. (2007): Oct 25; [Epub ahead of print]

Pabst S, Wollnik B, **Rohmann E**, Hintz Y, Grohé C: A novel stop mutation truncating critical regions of the cardiac transcription factor NKX2.5 in a large family with autosomal-dominant inherited congenital heart disease. Clin Res Cardiol. (2007); Sep 25; [Epub ahead of print]

Shams I, **Rohmann E**, Eswarakumar VP, Lew E, Yuzawa S, Wollnik B, Schlessinger J, Irit L: LADD syndrome is caused by reduced activity of the FGF10-FGF receptor 2 signaling pathway. Mol Cell Biol. (2007); 27: 6903-6912.

Rohmann E, Brunner H, Kayserili K, Uyguner O, Nürnberg G, Lew E, Dobbie A, Eswarakumar V, Uzumcu A, Ulubil-Emeroglu M, Leroy J, Li Y, Becker C, Lehnerdt K, Cremers C, Yüksel-Apak M, Nürnberg P, Kubisch C, Schlessinger J, Bokhoven H, Wollnik B; Mutations in different components of FGF signaling in LADD syndrome; Nat Genetics (2006): Apr. 38 (4): 414-7

Kalay E, Li Y, Uzumcu A, Uyguner O, Collin R, Caylan R, Ulubil-Emeroglu M, Kersten F, Hafiz G, van Wijk E, Kayserili H, **Rohmann E**, Wagenstaller J, Hoefsloot L, Strom T, Nürnberg G, Baserer N, Hollander A, Cremers F, Cremers C, Becker C, Brunner H, Nürnberg P, Karaguzel A, Basaran S, Kubisch C, Kremer H, Wollnik B ; Mutations in the lipoma HMGIC fusion partner-like 5 (LHFPL5) Gene Cause Autosomal Recessive Nonsyndromic Hearing Loss ; Human Mutation (2006): 27(7), 633-639

Li Y, Wollnik B, Pabst S, Lennarz M, **Rohmann E**, Gillissen A, Vetter H, Grohe C ; BTNL2 gene variant and sarcoidosis ; Thorax (2006): 61, 273-274

Ich versichere, dass ich alle Angaben wahrheitsgemäß nach bestem Wissen und Gewissen gemacht habe und verpflichte mich, jedmögliche, die obigen Angaben betreffenden Veränderungen, dem Promotionsausschuss unverzüglich mitzuteilen.

Köln, den 27.02.2008 ....
Ort, Datum Unterschrift